The Dissertation Committee for Shawn Curtis Griffiths Certifies that this is the approved version of the following dissertation:

Issues Related to Site Property Variability and Shear Strength in Site Response Analysis

Committee:

Brady R. Cox, Supervisor

Ellen M. Rathje, Co-Supervisor

Kenneth H. Stokoe II

Clark R. Wilson

Wassim M. Ghannoum

Issues Related to Site Property Variability and Shear Strength in Site Response Analysis

by

Shawn Curtis Griffiths, BS; MSCE

Dissertation

Presented to the Faculty of the Graduate School of

The University of Texas at Austin

in Partial Fulfillment

of the Requirements

for the Degree of

Doctor of Philosophy

The University of Texas at Austin

August 2015

Dedication

To my sweetheart wife, who, as my friend and fellow adventurer has earned every bit of this degree with me.

Acknowledgements

The faculty members who have helped me along my path include, Dr. Norman Dennis, Dr. Micah Hale, Dr. Jim Bay, Dr. Ken Stokoe and many others. They have each been a great personal help to me in both my academic and non-academic pursuits. The graduate students I have had the pleasure of working with are not only much smarter than me, but have become friends whom I look forward to working with in the future. Parents and siblings have bolstered my resolve during seemingly overwhelming odds and moments of self-doubt. I am grateful for Dr. Ellen Rathje who voluntarily showed interest, contributed thoughtful incites and provided valuable feedback, throughout all of my research at Texas. Working with her has been a great pleasure. I have worked with Dr. Brady Cox for the past six years. I am, and will be, forever grateful that he cared enough to cut me back, smooth the rough edges, and help me pursue my goals. Finally, because family is the most important, I want to acknowledge my wife, who, by my side endured, and enjoyed the adventures of graduate school.

Issues Related to Site Property Variability and Shear Strength in Site Response Analysis

Shawn Curtis Griffiths, Ph.D.

The University of Texas at Austin, 2015

Supervisor: Brady R. Cox

Co-Supervisor: Ellen M. Rathje

Nonlinear site response analyses are generally preferred over equivalent linear analyses for soft soil sites subjected to high-intensity input ground motions. However, both nonlinear and equivalent linear analyses often result in large induced shear strains (3-10%) at soft sites, and these large strains may generate unusual characteristics in the predicted surface ground motions. One source of the overestimated shear strains may be attributed to unrealistically low shear strengths implied by commonly used modulus reduction curves. Therefore, modulus reduction and damping curves can be modified at shear strains greater than 0.1% to provide a more realistic soil model for site response. However, even after these modifications, nonlinear and equivalent linear site response analyses still may generate unusual surface acceleration time histories and Fourier amplitude spectra at soft soil sites when subjected to high-intensity input ground motions. As part of this work, equivalent linear and nonlinear 1D site response analyses for the well-known Treasure Island site demonstrate the challenges associated with accurately modeling large shear strains, and subsequent surface response, at soft soil sites.

Accounting for the uncertainties associated with the shear wave velocity profile is an important part of a properly executed site response analyses. Surface wave data from

Grenoble, France and Mirandola, Italy have been used to determine shear wave velocity (Vs) profiles from inversion of surface wave data. Furthermore, Vs profiles from inversion have been used to determine boundary, median and statistically-based randomly generated profiles. The theoretical dispersion curves from the inversion analyses as well as the boundary, median and randomly generated Vs profiles are compared with experimentally measured surface wave data. It is found that the median theoretical dispersion curve provides a satisfactory fit to the experimental data, but the boundary-type theoretical dispersion curves do not. Randomly generated profiles result in some theoretical dispersion curves that fit the experimental data, and many that do not. Site response analyses revealed that the greater variability in the response spectra and amplification factors were determined from the randomly generated Vs profiles than the inversion or boundary Vs profiles.

Table of Contents

List of Tables

List of Figures

Chapter 1:

Introduction

1.1 PROBLEM STATEMENT

One dimensional equivalent linear site response analyses are frequently used to model the influence of local soil conditions on surface ground shaking. Important sub-surface information for these analyses include; shear wave velocity, soil layer thickness, input ground motions, and dynamic soil properties. When soft soils are subject to high intensity motions large shear strains (i.e. 0.1-3%) may be predicted. These large shear strains are beyond the maximum shear strains measured in the laboratory and may result in unrealistic predicted surface ground motions.

Accounting for the uncertainties in site response analyses is becoming increasingly important, especially for probabilistic hazard design analyses. Uncertainty is inherent in experimentally measured surface wave dispersion data, and may be used to ensure that shear wave velocity profiles are within measured uncertainty bounds. Due to the non-unique, ill-posed and mixed determined nature of inversion, many theoretical soil models may match the experimental dispersion data equally well. Current methods used to account for uncertainty in Vs profiles include bounding-type and randomly generated Vs profiles. These bounding-type and randomly generated profiles are rarely, if ever, compared with the experimental dispersion data. Furthermore, when these profiles are used in site response analyses, the effect on the predicted surface ground motions as compared with the profiles from inversion has not been well quantified.

1.2 SCOPE OF RESEARCH

The main outcomes for this research include; 1) investigating how modifying the dynamic soil properties influence the predicted surface response of soft soils subject to high-intensity motions, 2) determine how the theoretical dispersion curves of the Vs profiles determined from inversion, bounding-type, and randomly generated methods compare with the experimentally measured dispersion data and, 3) determine how Vs profiles determined from inversion, bounding-type, and randomly generated methods affect the predicted site response results. Each of these outcomes will be determined by performing one dimensional, linear elastic, equivalent linear or nonlinear site response analyses.

1.3 ORGANIZATION OF DISSERTATION

This dissertation is organized into three chapters. Each chapter is a self-contained journal article that includes a literature review, research findings, and conclusions. Chapter 2 presents site response analyses for the Treasure Island site using both equivalent linear and nonlinear methods. This soft soil site subject to high-intensity motions results in large predicted shear strains, which approach values associated with shear failure. Chapter 2 investigates how to modify the dynamic soil properties at high shear strains and what effect these modifications have on the predicted surface response.

Chapter 3 explores the validity of a number of different methods that can be used to account for Vs uncertainty in site response. The validity of various Vs profiles are evaluated using a surface wave dispersion approach and, hence, the Vs models considered have been developed primarily from surface wave testing. Specifically, the Vs profiles investigated are categorized into three groups: (1) Vs profiles determined directly from surface wave inversion, (2) simple statistical Vs profiles (including

bounding-type, median, and other percentile Vs profiles), and (3) statistically-based, randomly-generated Vs profiles. These three approaches are discussed for surface wave data collected at two international blind-study sites. The validity of each approach is evaluated in a quantitative manner using the experimentally-measured dispersion data as a reference.

Chapter 4 uses the Vs profiles determined in Chapter 3 to perform linear elastic and equivalent linear site response analyses. The variability in the predicted surface response from each of the three groups are quantitatively compared with one another. A relationship between the dispersion misfit and the root-mean-squared-difference in the response spectra is explored. Additionally a subset of the randomly generated Vs profiles made up of only Vs profiles that have theoretical dispersion curves that match the experimentally measured dispersion data are investigated. Chapter 5 includes a brief conclusion.

Chapter 2:

Modeling Large Shear Strains in Site Response Analyses of Soft Soils

Shawn C. Griffiths [a], Brady R. Cox [a]*, Ellen M. Rathje [a]

[a] Department of Civil, Architectural and Environmental Engineering, The University of Texas, 301 E Dean Keeton Stop C1792, Austin, TX, USA 78712
* Corresponding author. Tel.: 512 471 9162, *Email address:* brcox@utexas.edu

Abstract

Nonlinear site response analyses are generally preferred over equivalent linear analyses for soft soil sites subjected to high-intensity input ground motions. However, both nonlinear and equivalent linear analyses often result in large induced shear strains (3-10%) at soft sites, and these large strains may generate unusual characteristics in the predicted surface ground motions. One source of the overestimated shear strains may be attributed to unrealistically low shear strengths implied by commonly used modulus reduction curves. Therefore, modulus reduction and damping curves can be modified at shear strains greater than 0.1% to provide a more realistic soil model for site response. However, even after these modifications, nonlinear and equivalent linear site response analyses still may generate unusual surface acceleration time histories and Fourier amplitude spectra at soft soil sites when subjected to high-intensity input ground motions. In this study, we use equivalent linear and nonlinear 1D site response analyses for the well-known Treasure Island site to demonstrate challenges associated with accurately modeling large shear strains, and subsequent surface response, at soft soil sites.

keywords: Dynamic soil properties, Nonlinear site response analysis, Equivalent linear site response analysis, Soft soils, Earthquake

2.1. INTRODUCTION

One dimensional (1D) site response analyses are typically utilized to predict the amplification and/or attenuation of seismic ground motions by modeling the propagation of shear waves as they travel from bedrock to the ground surface. These analyses help to quantify the effects of local soil conditions on shaking intensities, and ultimately yield surface time histories and response spectra necessary for structural and geotechnical design. When 1D site response analyses are conducted for soft soil sites subjected to high-intensity input ground motions, large shear strains (3-10%) typically are predicted within the soil column. These large shear strains exceed the range where dynamic soil properties (i.e., shear modulus, G, and damping ratio, D) have been determined most reliably and often approach values that are associated with shear failure of the soil. For example, the normalized shear modulus reduction (G/G_{max}) and damping relationships published by Darendeli [1] were based on limited data at shear strains greater than 0.1% and no data at shear strains greater than 0.6%, as shown in Figure 2.1. Similar maximum shear strain levels exist in the databases used by others to develop dynamic soil property relationships, including Seed and Idriss [2], Hardin and Drenevich [3], and the Electric Power Research Institute (EPRI) [4]. Even the dataset for soft, fine-grained soils compiled by Vucetic and Dobry [5] only contains measurements of G/G_{max} and damping up to shear strains of approximately 1.0%. The lack of dynamic soil data at large shear strains necessitates the extrapolation of dynamic soil properties to values beyond their initial published bounds. These extrapolations may yield implied shear strengths that are either too high or too low relative to the estimated, or measured, static shear strength of the soil. To address this issue, Stewart and Kwok [6] and Hashash et al. [7] have proposed methods for modifying the G/G_{max} curves at large shear strains to more realistically represent the soil shear strength. These modifications can be used to produce G/G_{max} curves that more realistically represent the static shear strength of the soil at shear strains greater than 1.0%. In turn, site response analyses conducted with these modified

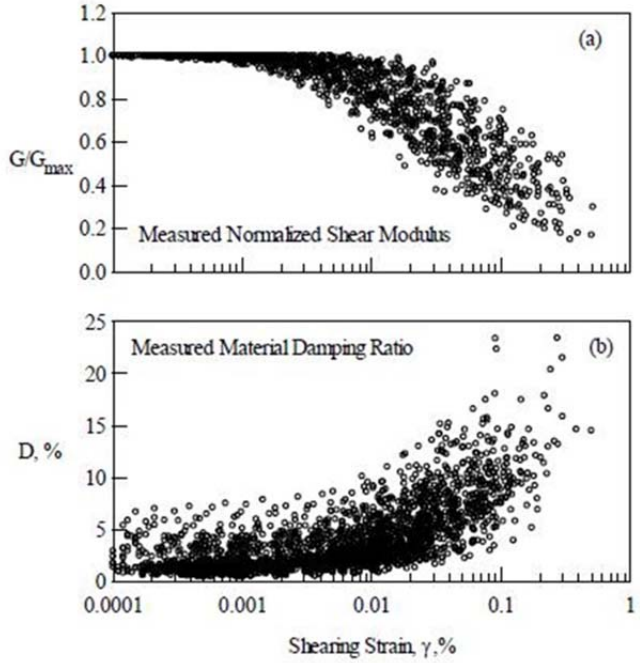

Figure 2.1. Modulus reduction and damping data from Darendeli [1].

G/G_{max} curves are believed to produce more reliable estimates of shear strain and ground shaking for soft soil sites subjected to high-intensity input ground motions.

This paper describes 1D site response analyses conducted for the Treasure Island site in California. These analyses are used to: (1) investigate the problems encountered with modeling high intensity input ground motions at soft soil sites, (2) explore the influence of modifications to the large strain dynamic soil properties on the induced shear strains and predicted surface motions, and (3) critically evaluate the surface ground motions predicted from both nonlinear (NL) and equivalent linear (EQL) analyses before and after modifying the dynamic soil properties. Based upon previous observations and soil characteristics, the Treasure Island site is likely to exhibit liquefaction during strong earthquake events. While it is recognized that nonlinear effective stress site response analyses using a pore water pressure generation model could be used to analyze the coupled site amplification and liquefaction responses, the focus of this study was to investigate/compare the dynamic response results from EQL and NL analyses in a

manner as similar as possible. Hence, the added complexities/uncertainties associated with nonlinear effective stress analyses and pore water pressure generation models have not been included for any of the analyses presented.

2.2. MODIFICATION OF DYNAMIC SOIL PROPERTIES AT LARGE SHEAR STRAINS

Dynamic site response analyses at soft soil sites may require estimates of shear modulus (G) and damping ratio (D) over a shear strain range spanning four orders of magnitude (i.e., $<10^{-3}$% to 10%). The variation of these dynamic properties with strain are defined using a G/G_{max} curve (where G_{max} is the maximum shear modulus at small strains) and a damping curve. While static soil properties such as shear strength are routinely measured at shear strains well above 1.0%, dynamic soil property curves commonly are measured up to only moderate shear strains (i.e., 0.3% to 1.0%). Theoretically dynamic and static testing methodologies should be able to be combined to model the entire stress-strain behavior of the soil, but this has proven difficult in practice because static tests optimized to obtain shear strength estimates are not good at obtaining accurate shear modulus measurements at smaller strains, and vice-versa. Thus, the commonly utilized G/G_{max} curves obtained from dynamic testing have historically been extrapolated to larger shear strains without any consideration for the shear strength implied by the large strain portion of the curve.

The shear stress (τ) as a function of shear strain (γ) can be obtained from a normalized G/G_{max} curve, the in-situ Vs, and the soil mass density (ρ) according to:

$$\tau = \gamma \cdot G = \gamma \cdot \left(G / G_{\max} \right) \cdot V_S^{\,2} \cdot \rho \qquad \text{Eq. 2.1}$$

When this relationship is extrapolated to large shear strains, a shear strength is implied at strains where failure is typically defined in static testing (i.e., 3-5%). This implied shear strength may or may not be realistic relative to expected soil behavior.

Examples of G/G_{max} curves that have been extrapolated to 10% shear strain are presented in Figure 2.2. The following properties/parameters are assumed for this sandy soil layer: an effective friction angle of 33°, a shear wave velocity (Vs) of 150 m/s, an over consolidation ratio (OCR) of 1.0, a coefficient of uniformity (C_u) of 3.0, a vertical effective stress (σ'_{vo}) of 58.4 kPa, and a K_o value of 0.5. This information was used to develop appropriate G/G_{max} curves using four common relationships. Here, each relationship has been extrapolated beyond its approximately 0.3%-1% data limits to a shear strain of 10%. The G/G_{max} curves of Seed and Idriss [2] and EPRI [4] were simply extrapolated to larger strains along a hyperbolic trend, while the Darendeli [1] and Menq [8] relationships are defined by equations that can be easily extrapolated to shear strains of 10%, even though they are not constrained by data at such large shear strains.

Figure 2.2b shows the shear stress versus shear strain curves implied by each extrapolated G/G_{max} relationship according to Eq. 2.1. Also shown is the estimated Mohr-Coulomb shear strength of 38 kPa, which was calculated using the vertical effective stress and the effective friction angle of 33° of the soil. These commonly used G/G_{max} relationships imply shear strengths, at approximately 3% shear strain, which range from 15 - 40 kPa. In this case, only the extended G/G_{max} curve of Menq [8] provides a realistic estimate of the static shear strength relative to the friction angle and the shear strength implied from the G/G_{max} relationship published by Darendeli [1] is only 55% of the Mohr-Coulomb estimate of shear strength. Chui et al. [9] documented a similar trend when comparing measured shear strengths with the shear strengths implied from the G/G_{max} relationship of Darendeli [1] at shallow depths. However, it must be stressed that the curves have been extended approximately two orders of magnitude beyond the maximum shear strains in the database as shown in Figure 2.1, so this is not unexpected. When G/G_{max} curves do not accurately represent the static shear strength at large shear strains, the G/G_{max} curves can be modified to better-represent the measured or estimated shear strengths according to procedures developed by Stewart and Kwok [6] and Hashash et al. [7].

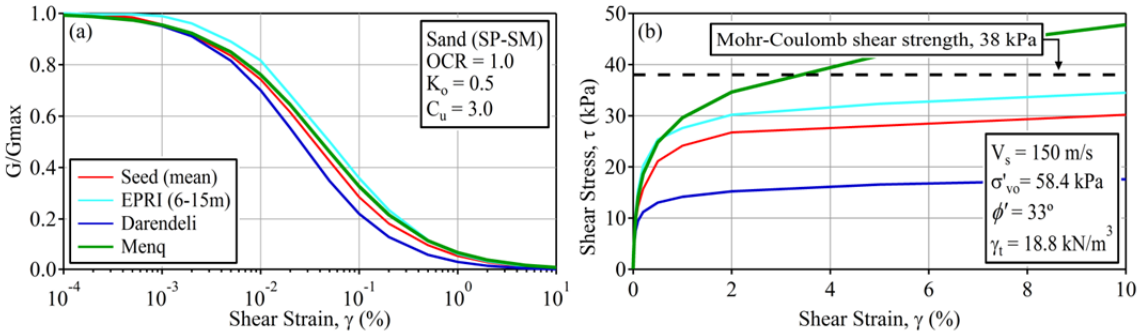

Figure 2.2. (a) Modulus reduction curves for a sandy soil from Seed and Idriss [2], EPRI [4], Darendeli [1] and Menq [8], each of which has been extended to 10% shear strain from the published maximum shear strains of 0.3% to 1.0% in their databases and (b) associated shear stress implied by the modulus reduction curves in comparison with the Mohr-Coulomb shear strength.

Stewart and Kwok [6] developed a procedure that can be used to match the standard G/G_{max} curve at small shear strains, while gradually increasing the G/G_{max} at larger shear strains such that the target strength is reached. This procedure provides a systematic way to modify the G/G_{max} curve to obtain a realistic strength estimate; however, it does not modify the nonlinear hysteric stress-strain curve. Therefore, no changes are made to the damping curve, and this approach cannot be used to determine the nonlinear stress-strain model parameters for NL analyses.

The procedure proposed by Hashash et al. [7] explicitly identifies nonlinear stress-strain parameters that fit the target modulus reduction and damping curves. This procedure takes advantage of the modulus reduction and damping curve fitting procedure (MRDF), developed by Phillips and Hashash [10], which matches the target G/G_{max} curve over the entire strain range without large overestimation of the D curve. The MRDF curve fitting procedure modifies the hysteretic loading and unloading rules using a strain-dependent reduction factor to better model the cyclic response at large shear strains while maintaining a relatively simple expression. Prior to the development of the MRDF curve fitting procedure, slight adjustments in the G/G_{max} curve would cause a large overestimation of the D curve in NL analyses.

The Hashash et al. [7] procedure is illustrated in Figure 2.3 using the same sandy soil shown in Figure 2.2. The initial target G/G_{max} curve (Figure 2.3a), prior to modification to account for shear strength, is based on the relationship published by Darendeli [1]. After the initial target G/G_{max} curve is obtained, it is manually adjusted at shear strains greater than 0.1% so that the shear stresses better approximate the target static shear strength at a shear strain between 3% and 5% (Figure 3b). The manually adjusted G/G_{max} curve, along with the original damping curve, are then used as target curves to determine stress-strain model parameters generated using the MRDF curve fitting procedure, as implemented in the site response program DEEPSOIL [11]. The process of manual adjustment and MRDF curve fitting is repeated until the MRDF stress-strain model parameters represent the target G/G_{max} curve, as well as the corresponding shear stress-shear strain curve that match the static shear strength at the desired shear strain. The final MRDF fit to the manually adjusted G/G_{max} curve is termed the strength corrected G/G_{max} curve. It is important to note that seemingly small adjustments in the G/G_{max} curve can translate into large differences in the implied shear strength (Figures 2.3a and 2.3b).

Modification can also be made to the damping curve at large strains where little damping data are available (Figure 2.1). Unlike the case for G/G_{max}, there is no target damping at large strains derived from strength testing or other means. One alternative is to cap the large strain damping at 15% (Figure 2.3c) because few damping values greater than 15% have been measured (Figure 2.1). This approach also avoids over damping and it has been utilized in other studies, including Chiu et al. [9].

Within the site response program DEEPSOIL [11], the MRDF curve fitting procedure includes two different options for calculating the damping parameters: (1) MRDF-Darendeli, which allows the damping curve to decrease below some maximum value at large shear strains, and (2) MRDF-UIUC, which does not allow the damping value to decrease at large shear strains. The MRDF-UIUC model was used in this work, and was even flexible enough to handle modified versions of damping curves that were

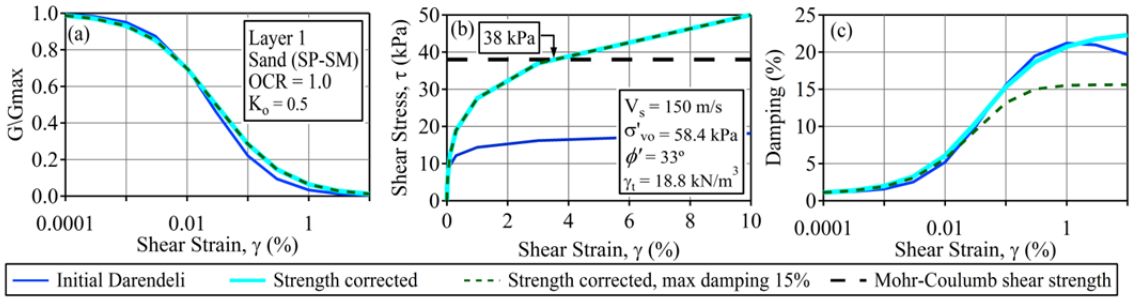

Figure 2.3. Dynamic soil properties for a sandy soil: (a) initial G/G_{max} curve from Darendeli [1] with strength corrected G/G_{max} curves, (b) corresponding implied shear strength for each of the G/G_{max} curves and, (c) damping curves from the MRDF UIUC curve fitting procedure with and without damping capped at 15%.

capped at 15%. The ability of the MRDF model to replicate the target damping curve of Darendeli [1] at small shear strains and follow a smooth transition to a maximum damping value of 15% at larger shear strains (Figure 3c) demonstrates the versatility of the MRDF curve fitting method.

2.3. Site Description and Input Ground Motions

Treasure Island (TI) was chosen as the site for this study due to the well documented site investigations, the presence of soft soils, and the high-intensity design ground motions resulting from its proximity to multiple faults capable of large magnitude earthquakes. In short, the TI site represents a typical soft soil site that could pose a challenge to those attempting to accurately perform 1D site response analyses for seismic design.

2.3.1. Site Description

Treasure Island is a 400 acre, man-made island in San Francisco Bay, located between San Francisco and Oakland, California. The shear wave velocity (Vs) profile and other soil data used for this study were obtained from Dickenson [12] and Pass [13], and are summarized in Figure 2.4. The site consists of a soft silty sand (SP-SM) layer

from the surface to a depth of 13 m, beneath which Young San Francisco Bay Mud (CH) continues to a depth of 29 m. These layers overlie a stiffer 12 m thick silty sand layer (SP-SM) and a layer of Old Bay Clay (CL), which extends from 41 m to 91 m with a well graded sandy layer (SW) inclusion between 76 m and 81 m. The soil profile was divided into nine major layers, as shown in Figure 2.4. These major layers were further divided into sublayers which were all assigned the same dynamic soil properties as the main layer. The sublayer thicknesses were chosen so that numeric filtering below 50 Hz would not be problematic during site response analyses. Input ground motions were applied to the Franciscan sandstone bedrock, with a Vs = 1220 m/s at a depth of 98 m.

2.3.2. Ground Motion Selection

A bedrock (Site Class B) uniform hazard spectrum (UHS) [14] was used to select input motions for the analyses. The UHS was developed from the 2008 United States Geological Survey (USGS) national seismic hazard maps using a probability of exceedance of 2% in 50 years [15]. Deaggregations for the TI site were performed using the USGS 2008 interactive deaggregation tool [16], which indicates that the seismic hazard for periods ranging from 0.1 to 5 s is dominated by earthquake events with mean magnitudes between 7.0 and 7.7 at distances between 13 and 20 km. Using these magnitude and distance ranges as a guide, a set of 162 possible earthquake time histories were identified from the PEER Strong Motion Database [17]. SigmaSpectra [18,19] was used to select and scale five input ground motions from the assembled set that had spectral shapes similar to the UHS and minimized the sum of squared error across the entire UHS.

The five selected ground motions are presented in Figure 2.5, which includes the median of the scaled ground motions and the target UHS. These motions were scaled by factors ranging from 5 to 14. The use of such high scaling factors is required due to the high seismic intensity expected at the site for the 2% in 50 year motion. Because similar site response results were obtained from each of the input ground motions, subsequent

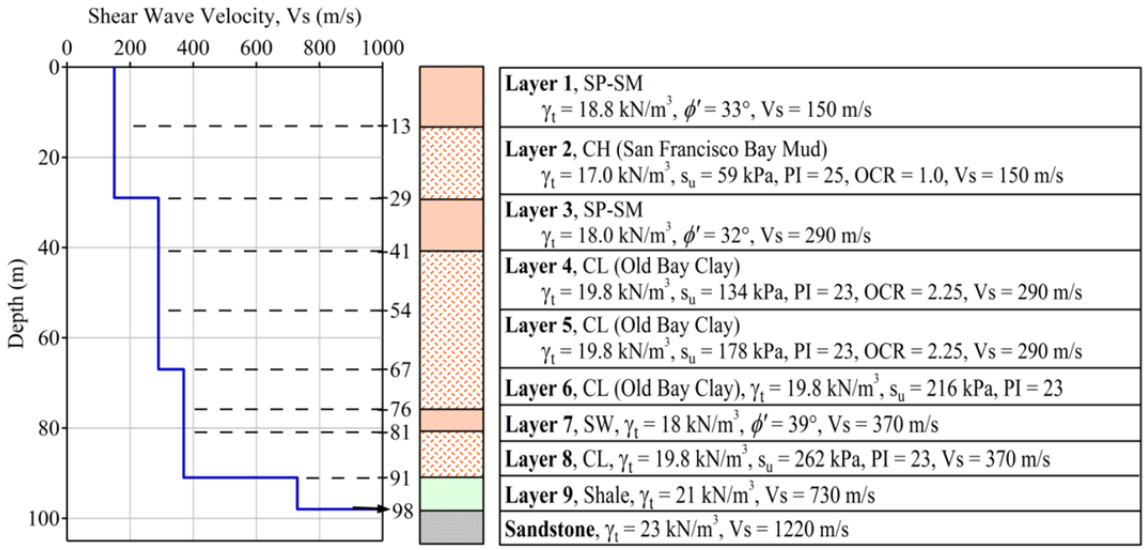

Figure 2.4. Shear wave velocity, soil type, and main soil layers for Treasure Island, using data derived from Dickenson [12] and Pass [13]).

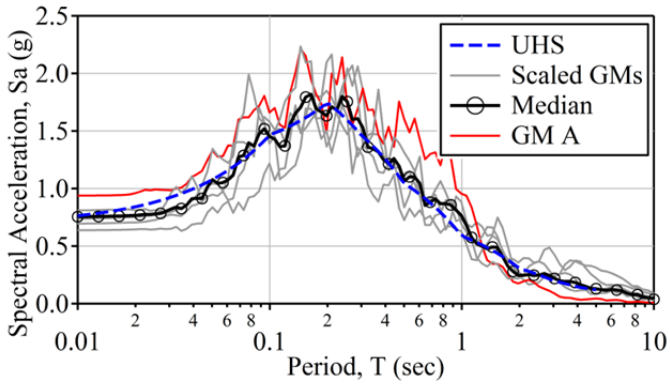

Figure 2.5. Uniform hazard spectrum (2% in 50-year probability of exceedance) for the TI site with five scaled input ground motions.

site response comparisons throughout this paper utilize only one of the five input motions, which is identified as ground motion A (GM A). This motion was recorded at the Wonderland station during the 1994 Northridge earthquake (M = 6.7, R = 15 km, RSN 1011).

2.4. SITE RESPONSE RESULTS

The computer program DEEPSOIL v 5.1[11] was used to perform both the EQL and NL site response analyses presented in the subsequent sections. Identical soil models in terms of the shear wave velocity profile and nonlinear shear modulus reduction and damping curves were used for each type of analysis. The NL analyses were performed as total stress analyses, with the nonlinear stress-strain response represented by the modified Kondner-Zelasko (MKZ) hyperbolic-type model. As noted earlier, the MRDF curve fitting procedure, which utilizes modified Masing rules with a strain-dependent reduction factor [10], was used to model the unload/reload stress-strain response and obtain a better fit to damping curves at large strain. The NL analysis did not incorporate the effects of cyclic degradation or pore pressure generation.

2.4.1. Site Response Analyses using Initial Soil Properties

The initial analyses presented in this section utilized input GM A, the Vs profile in Figure 2.4, and dynamic soil properties from the Darendeli [1] relationship extended to 10% shear strain without any consideration for shear strength or a cap on damping. For illustration, the modulus reduction and damping curves for Layer 1 are shown in Figure 2.3. The acceleration response spectrum of input motion GM A and the associated surface response spectra for the EQL and NL analyses are presented in Figure 2.6. At most periods the EQL analysis predicts a greater surface response spectrum than the NL analysis, with the largest difference occurring at a period of about 1.0 s, where the EQL spectral acceleration is 0.67 g and the NL spectral acceleration is 0.34 g. Generally speaking, the surface spectra exhibit significant deamplification relative to the input motion at periods less than 2.0 s, with amplification predicted at longer periods. Most notably, the surface response spectra for all analyses are essentially flat at periods less than 2.0 s, which is not characteristic of typical acceleration response spectra from recorded surface motions at soft soil sites.

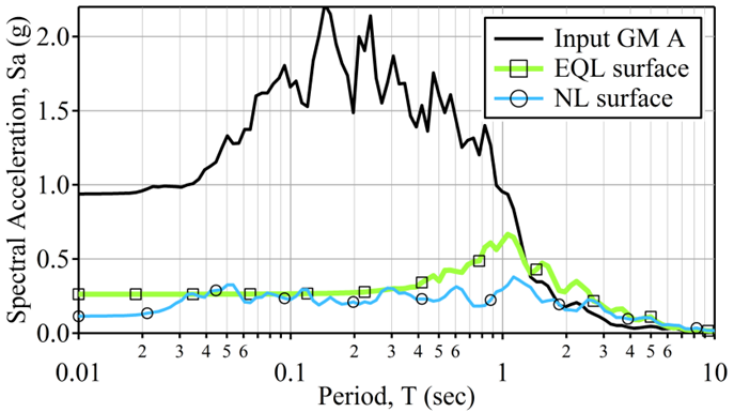

Figure 2.6. Input acceleration response spectrum along with EQL and NL surface response spectra obtained using the initial dynamic soil properties from Darendeli [1] at the TI site.

The maximum shear strains generated from the initial analyses using input motion GM A are presented in Figure 2.7. The NL and EQL shear strains are similar over most depths, with maximum shear strains greater than 2.0% predicted at depths near 10 and 30 m. Nearly every depth has predicted maximum shear strains greater than 0.1% to 0.2%, which is the threshold above which the results from EQL and NL analyses often begin to diverge and the results from EQL analyses become questionable [20, 21]. At these strain levels, the large damping values used in the EQL analyses result in significant overdamping of high frequencies, which tends to result in significant deamplification and a very flat response spectrum at short periods. Because NL analyses model the fully nonlinear stress-strain response over time during earthquake shaking, this overdamping is believed to be minimized. Interestingly, however, the response spectrum from NL analysis in Figure 2.6 is also very flat at short periods.

The input acceleration-time history, GM A, and predicted surface time histories from the initial NL and EQL analyses are presented in Figure 2.8. The peak ground acceleration (PGA) for the input motion is 0.93 g, while the surface PGA is 0.11 g and 0.26 g for the NL and EQL analyses, respectively. The NL time history visually includes

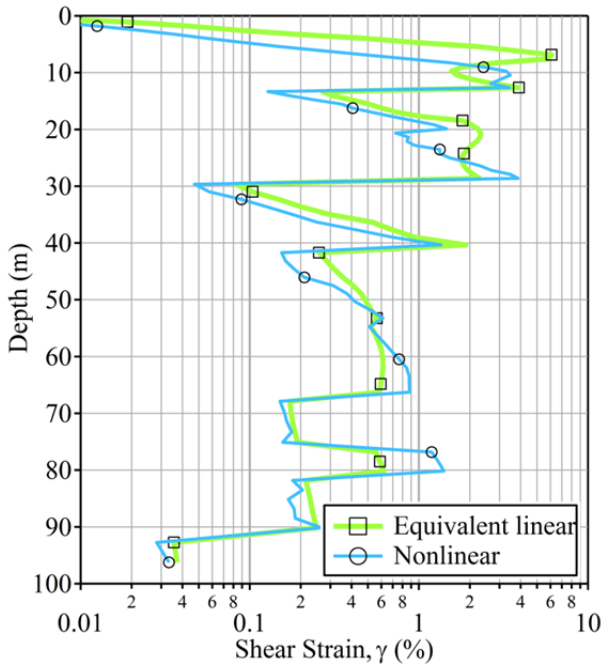

Figure 2.7. Maximum predicted shear strains from NL and EQL analyses using the initial dynamic soil properties at the TI site

more high frequency content than the EQL time history, which demonstrates that the high frequencies are less attenuated in the NL analysis despite the fact that the high frequency spectral accelerations from NL analysis are smaller than for EQL analysis. Nonetheless, the predicted NL time history contains some unexpected characteristics, such as vertical jumps in acceleration (e.g., at t = 5.0 s) that are followed by high frequency motion and time periods of near constant acceleration (e.g., t = 12.5 s). The EQL time history does not display these characteristics, but it contains almost no high frequencies.

The frequency content for each of the acceleration time histories was investigated further by examining the Fourier amplitude spectra (FAS), which were smoothed using a log-based triangular window (Figure 2.9). The EQL and NL motions show amplification of frequencies less than about 0.6 to 0.8 Hz relative to the input motion, and deamplification at higher frequencies. However, the shapes of the FAS of the EQL and NL motions diverge significantly at frequencies greater than about 1.5 Hz. The EQL

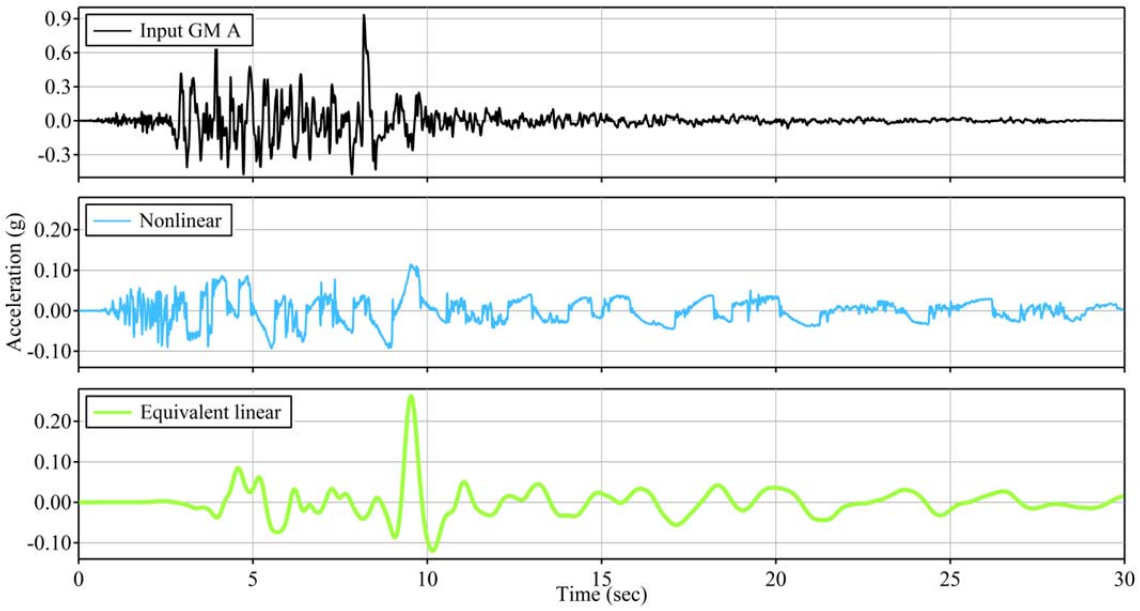

Figure 2.8. Input acceleration time history along with surface acceleration time histories for the NL and EQL analyses using the initial dynamic soil properties at the TI site.

FAS decreases in amplitude very quickly, while the NL FAS displays a relatively flat slope that is uncharacteristic of earthquake motions. Furthermore, the NL FAS merges with the input FAS at frequencies greater than 30 Hz, which is not expected due to the anticipated loss of high frequency energy due to the response of this soft soil site.

The flat response spectra at short periods and the unusual characteristics in the time histories are indications that the initial site response analyses are not producing reliable results for the large shear strains induced in the soil. As a first effort to remedy these problems, the site response analyses were repeated after modifying the dynamic soil properties according to the descriptions outlined in Section 2.2.

2.4.2. Site Response Analyses using Modified Dynamic Soil Properties

The layers that require modification of their dynamic properties are those that experience the largest shear strains. Given the induced shear strains shown in Figure 2.7, layers 1 and 2 experience the largest shear strains and require modification. However,

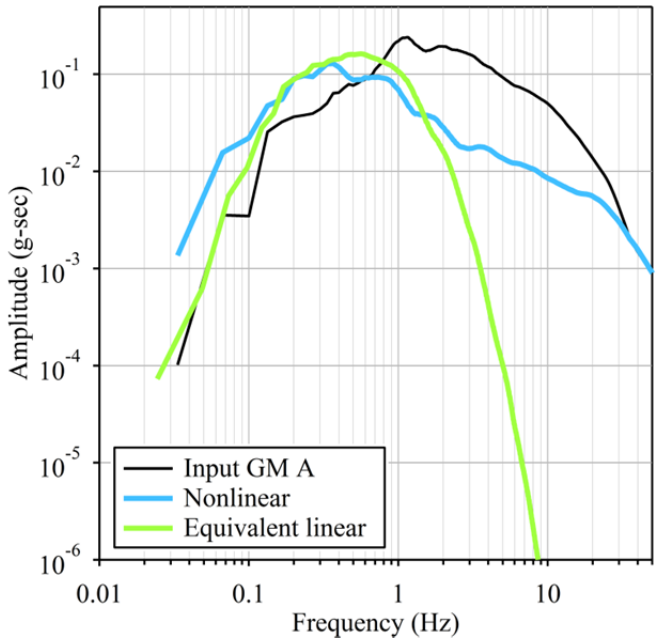

Figure 2.9. Fourier amplitude spectra for the input motion and the surface motions from NL and EQL analyses using the initial dynamic soil properties at the TI site.

modifying the properties in these layers may simply move the location of largest shear strains to other layers. Therefore, analyses were performed in which the dynamic properties in all layers were modified. The modifications considered include; 1) modifying the G/G_{max} curve to be consistent with a specified shear strength, and 2) capping the damping curve at 15%.

The surface response spectra from NL and EQL analyses after making modifications to different layers in the sub-surface profile are presented in Figure 2.10. Modifying only the modulus reduction curves for layers 1 and 2 to represent an appropriate strength generates a significant increase in the surface response spectra. This increase is larger for the EQL analysis than for the NL analysis. Modifying the modulus reduction curve and capping the damping curve at 15% for layers 1 and 2 further increases the surface response spectra, but the effect is incrementally much smaller than for the modification of G/G_{max} curve only. Finally, modifying the modulus reduction and damping curves for all layers generates another modest increase in the surface response

spectra. At most periods and for both the NL and EQL analyses, the spectral accelerations for the case where the modulus and damping were modified in all layers are nearly double those from the initial case. While these spectra still exhibit relatively flat spectral shapes at periods less than 0.2 s, the spectral shapes are improved relative to the initial scenario, with larger spectral accelerations and pronounced peaks at periods greater than 0.2 s. These characteristics are particularly prominent for the EQL analyses, and in fact, the EQL analysis predicts significantly larger motions than the NL analysis over most periods. The results in Figure 2.10 show that strength correcting the modulus curves in layers where shear strains exceed 1% is very important, and should be done at all soft soil sites. Nonetheless, modifying the modulus reduction and damping curves for all layers is viewed as most appropriate.

Shear strains predicted for the initial case and the fully-modified case (i.e. strength corrected G/G_{max} and capped D in all layers) are compared in Figure 2.11, alongside the Vs profile and soil type. The top two layers of the soil profile exhibit the largest shear strains for both the initial and fully-modified cases. For the NL analyses, the predicted maximum shear strain at a depth of 12 m was increased from 3.5% to 5% after fully-modifying the dynamic soil properties. The opposite trend occurred at a depth of 28 m, where the fully-modified analyses predicted a maximum shear strain of 2% versus 4% for the initial analyses. In contrast, the EQL analyses predict only a slight reduction in maximum shear strains in the top two layers when the fully-modified properties are used. As these results show, modifications to the dynamic soil properties have the potential to increase or decrease predicted shear strains along the depth of the soil profile because: (1) stiffer layers generally strain less, (2) increases in stiffness may transfer greater seismic energy into overlying layers, resulting in larger shear strains, and (3) stiffening of soil layers may result in greater impedance contrasts which will reflect more seismic energy back down into underlying layers.

Figure 2.12 shows the surface time histories from the analyses with the initial and fully-modified properties. The increased shear stiffness associated with the

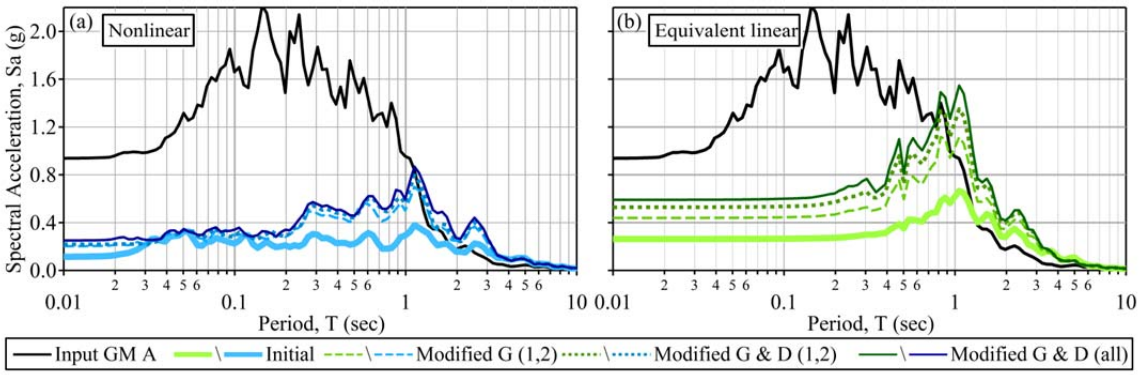

Figure 2.10. Response spectra for all considered G/G_{max} and D scenarios for both the (a) nonlinear and (b) equivalent linear analyses at the TI site.

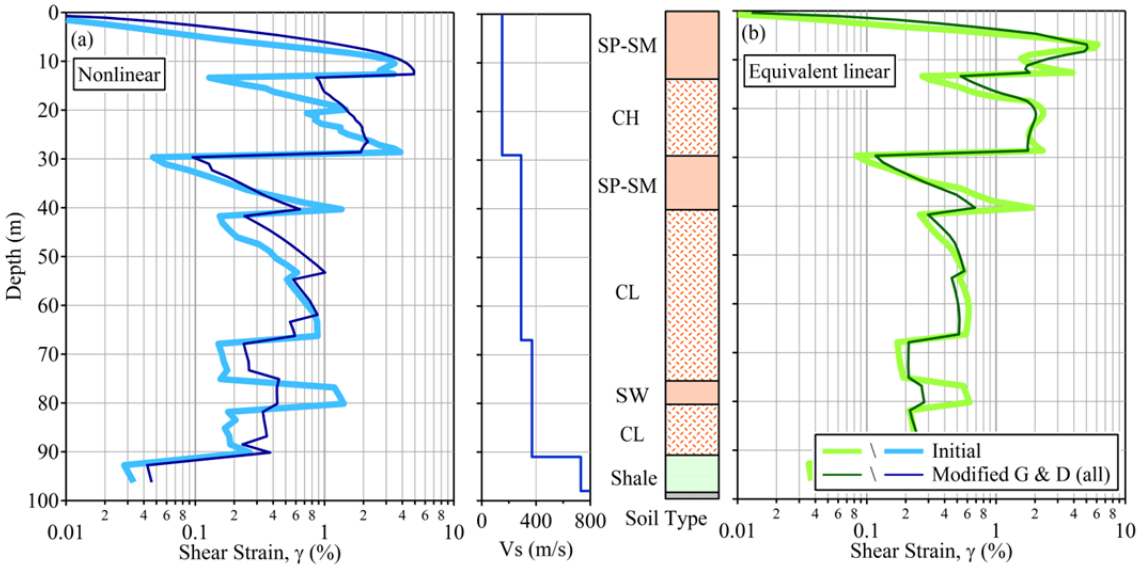

Figure 2.11. Maximum predicted shear strain profiles for the initial and fully modified G/G_{max} and D scenarios for the (a) nonlinear and (b) equivalent linear analyses, with the shear wave velocity profile and soil type for the TI site.

fully-modified cases yielded increased amplitudes and more high frequency content of the surface time histories for both NL and EQL analyses. The fully-modified NL time history still displays some near vertical jumps, as well as some near constant

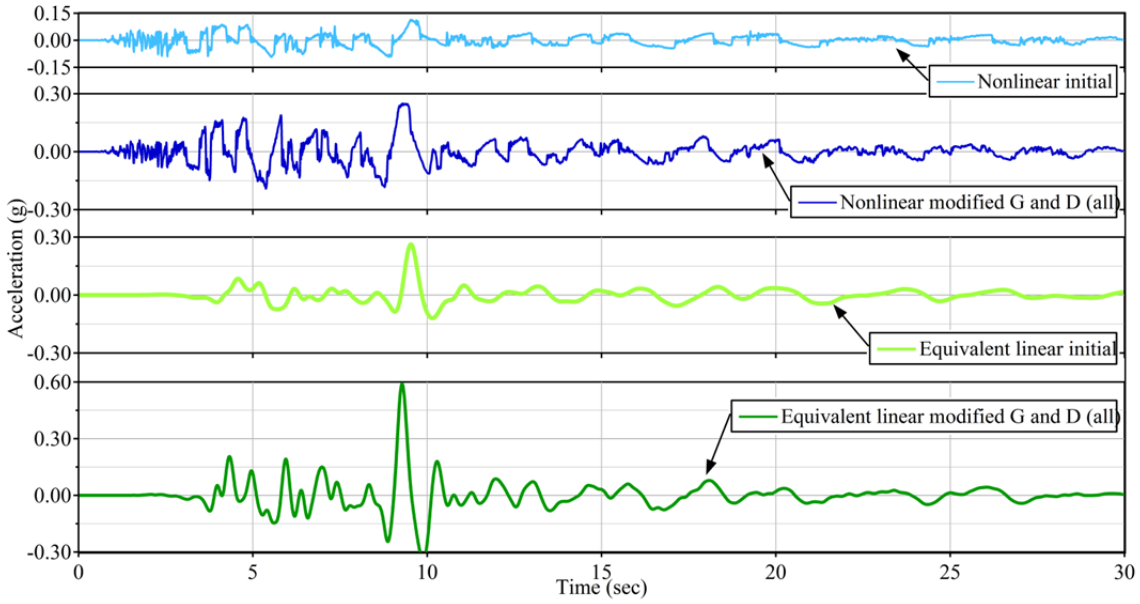

Figure 2.12. Predicted surface acceleration time histories of the initial and fully-modified cases for NL and EQL analyses for the TI site.

accelerations (i.e. t = 12.5 s), but these characteristics are less severe than for the initial analysis. A better idea of the frequency content of the computed surface motions can be obtained by examination of the FAS (Figure 2.13). At frequencies greater than about 0.3 Hz, the fully-modified cases have larger amplitudes than the initial cases for both the NL and EQL analyses. Nonetheless, the FAS for the fully-modified NL analysis still exhibits a flat, almost log-linear decrease in amplitude at frequencies greater than 0.5 Hz. As noted above, this is an uncharacteristic spectral shape not observed in actual recorded ground motions.

2.5. Comparisons with Large Intensity Motions Recorded at Soft Soil Sites

As a means to qualitatively assess the results of the NL and EQL site response analyses presented above, the expected frequency content of large intensity surface motions at soft soil sites has been investigated using high intensity recorded motions from two soil sites from the Kik-net network in Japan. The selected sites are KSRH 10 and IBRH 11, which have average shear wave velocities in the top 30 m (Vs_{30}) of 212

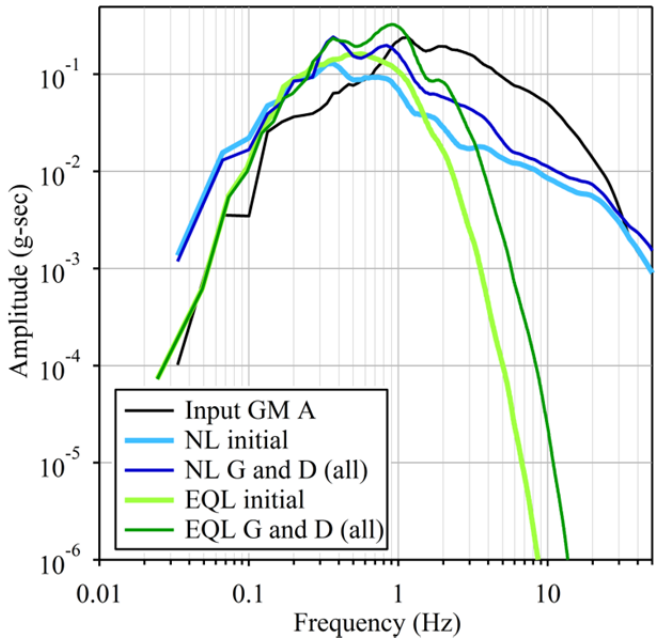

Figure 2.13. Fourier amplitude spectra of the initial and fully-modified cases for the NL and EQL analyses at the TI site.

m/s and 242 m/s, respectively. These values are larger than the Vs_{30} of 152 m/s for the TI site, but the two Kik-net sites have minimum shear wave velocities that are similar to TI, The surface and downhole time histories recorded at the KSRH 10 site during the M = 8.0 Tokachi-oki earthquake have PGAs of 0.49 g and 0.09 g, respectively. At the IBRH 11 site the surface and downhole PGAs are 0.82 g and 0.25 g, respectively, recorded during the M = 9.0 Tohoku earthquake. The recorded downhole and surface PGAs reveal the considerable soil amplification experienced at each site. Although deamplification was predicted by the EQL and NL analyses of the TI site, the induced strains computed from site response analyses for the KSRH 10 and IBRH 11 sites during these events are 0.2% and 3.7%, respectively, which are within the range predicted by the analyses of the TI site. These levels of induced strains, along with the soft soils (i.e., Vs less than 200 m/s) present at these sites, are consistent with the TI analyses and justify the comparison of the Kik-net surface recordings with the surface motions predicted by EQL and NL site response analyses at the TI site.

Thirty second intervals of the high intensity surface time histories recorded at the two Kik-net sites are presented in Figure 2.14, along with the surface time histories resulting from the fully-modified EQL and NL site response analyses at TI. A qualitative comparison reveals that neither of the high intensity Kik-net time histories portray the unique characteristics observed in the acceleration time histories from the NL analyses. Furthermore, both recorded time histories have more high-frequency content than the predicted time histories, particularly when compared with the lack of high frequencies in the motions from the EQL analysis.

FAS from each of the four time histories are shown in Figure 2.15. Both of the FAS from the Kik-net recordings display a sharp decrease in amplitude at frequencies greater than 10 Hz. A similar decrease is observed in the FAS from the EQL analysis, but it occurs at a much lower frequency (i.e., about 2-3 Hz). The sharp decrease in Fourier amplitude present in the Kik-net data is typical of recorded surface time histories and is often modeled using the spectral decay parameter known as kappa (κ) [22]. The decay of the acceleration FAS with frequency is described with an exponential function, $\exp(-\pi \cdot \kappa \cdot f)$, where larger values of kappa correspond to less high frequency motion. Kilb et al. [23] reported kappa values that ranged from 0.005 s to 0.1 s, while Campbell [24] reported that rock motions in Western North America commonly yield kappa values around 0.04 s. Generally, kappa increases as the shear wave velocity of the subsurface materials decrease and the depth of sediments increase [25, 26]. Included in Figure 2.15 is the theoretical decay of the FAS at high frequencies given kappa values of 0.03 s and 0.1 s. These values bracket the observed spectral decay in the Kik-net motions and the larger value (κ = 0.1 s) generally represents an upper bound from observed ground motions [25]. In contrast, the FAS from the EQL analysis displays significantly more decay, with a corresponding value of kappa equal to 0.3 s. This value of kappa was estimated from the slope of log (FAS) vs. frequency (Figure 2.15b) using the method of Anderson and Hough [22]. This large value of kappa indicates that the EQL approach is overdamping the high frequency response. The high frequency decay in the FAS from

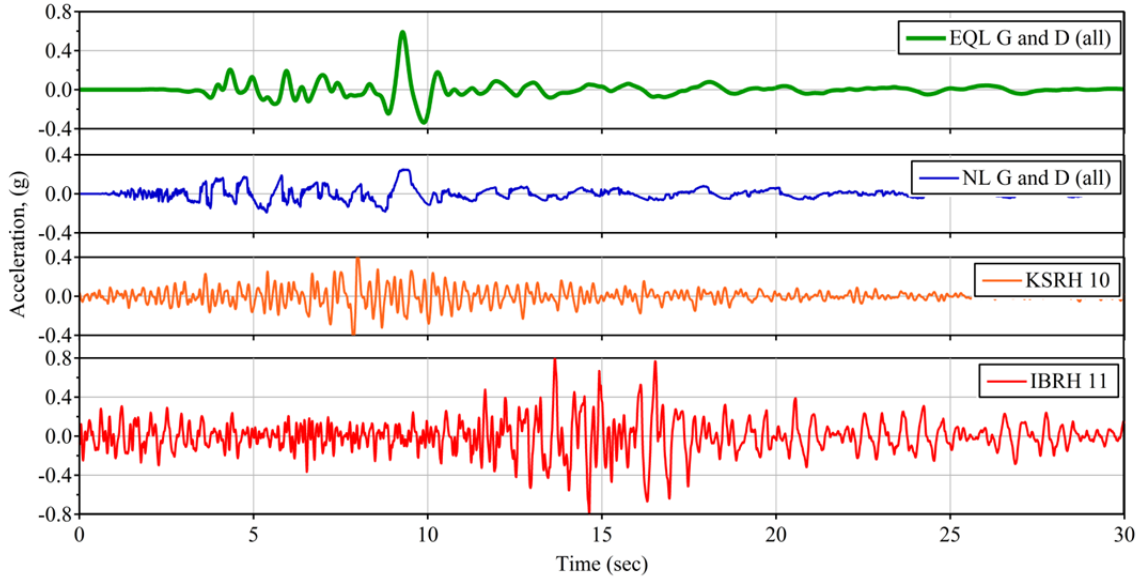

Figure 2.14. Acceleration time histories for the EQL and NL fully-modified site response analyses at the TI site along with recorded time histories from two Kik-net sites.

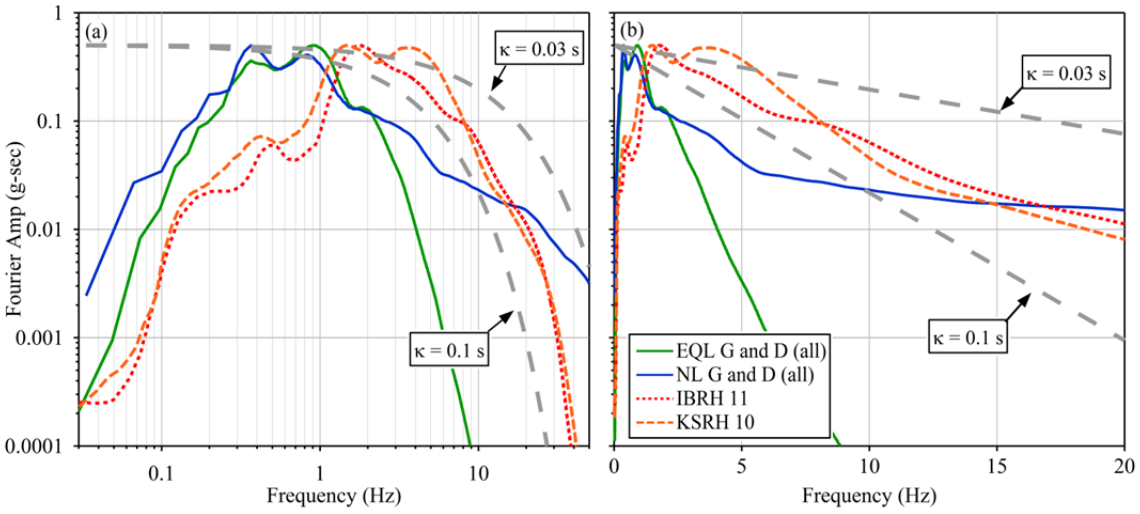

Figure 2.15. Fourier amplitude spectra for the NL and EQL fully-modified analyses at the TI site along with FAS from surface time histories recorded at soft soil sites with high intensity motions from the Kik-net database and the expected shapes of FAS using κ values of 0.03 and 0.1 s.

the NL analysis does not fit the kappa model. In fact, when plotted as log FAS vs. frequency (Figure 2.15b) the FAS from NL analysis is not linear and a value of kappa cannot be determined.

The results in Figure 2.14 and 2.15 demonstrate that unresolved issues remain when performing site response analyses at soft soil sites for high intensity motions. Although incorporating the shear strength of the soil in the modulus reduction and damping curves can improve the computed surface response for these cases, the high frequency components of motion still remain questionable. EQL analysis tends to overdamp the high frequencies and produce unrealistically large kappa values compared with those associated with recorded motions at soft soil sites. NL analysis produces motions with larger components of high frequency motion, but the spectral shape at high frequencies is not consistent with seismological theory and the computed surface acceleration-time histories contain some unrealistic characteristics. Additional research is needed to improve the prediction of site response using either EQL or NL analysis at soft sites for high intensity input motions. This research should focus specifically on the spectral shape of the FAS at high frequencies predicted by site response analysis, as well as the time domain characteristics.

2.6. CONCLUSIONS

Nonlinear and equivalent linear site response analyses often result in large induced shear strains (3-10%) at soft soil sites subject to high-intensity input ground motions. However, dynamic soil properties typically used in these site response analyses were generally developed from minimal data at shear strains greater than 0.1-0.3%. Therefore, modulus reduction and damping curves must be extended with care, such that they provide realistic estimates of soil strength, stiffness, and damping at large shear strains. In this study, 1D site response analyses have been performed at Treasure Island, a well-known soft soil site near several major active faults, to demonstrate challenges

associated with accurately modeling large shear strains and developing realistic surface ground motions.

The Treasure Island analyses were performed using input ground motions scaled to a target UHS, which was developed using a 2% probability of exceedance in 50 years. Both EQL and NL site response analyses, with identical shear wave velocity profiles and nonlinear shear modulus reduction and damping curves, were performed using the computer program DEEPSOIL [11]. G/G_{max} curves at large shear strains were strength corrected to better match the estimated static shear strength of the soil according to the method proposed by Hashash et al. [7]. Additionally, damping at large shear strains was capped at 15%. Modifying G/G_{max} in the layers with the greatest predicted shear strains had a more significant impact on the amplitude and shape of the surface time histories and response spectra than any further modifications to G/G_{max} or D. Nonetheless, modifications to the modulus reduction and damping curves for all layers within a soft soil model should be investigated to ensure that realistic shear strengths are modeled and excessive damping values are not utilized.

Even after fully-modifying dynamic soil properties in all layers, the site response results at Treasure Island qualitatively appear to be uncharacteristic relative to typical high-intensity surface ground motions recorded at soft soil sites. This is true for both EQL and NL analyses. Specifically, the spectral shapes of surface ground motions predicted by EQL analyses appear to have unrealistically high kappa values, while those predicted by NL analyses do not resemble any typical kappa relationship. Therefore, future work should focus on improvements to current of EQL and NL site response models to better predict the high frequency characteristics of earthquake shaking for soft soil sites subject to high intensity input motions and to preserve realistic acceleration time histories.

Although it is commonly believed that NL site response analyses provide more realistic estimates of site response at large strains, and in particular predict larger amplification at short periods, this study shows that predicted short period amplification

from EQL analyses can be larger than from NL analyses. In fact, EQL analyses actually produced spectral accelerations that were approximately twice as large as the NL values across all periods at the Treasure Island site. Therefore, until the issues associated with modeling large shear strains are resolved, caution should be exercised in simply assuming that NL analyses will provide the most conservative estimates of site response at soft soil sites.

2.7. ACKNOWLEDGEMENTS

No financial support was received for the work presented in this paper.

2.8. REFERENCES

[1] Darendeli, M. (2001). "Development of a New Family of Normalized Modulus Reduction and Material Damping Curves," Ph.D. Dissertation, University of Texas at Austin. Austin, TX.

[2] Seed, H. and Idriss, I. (1970). "Soil Moduli and Damping Factors for Dynamic Response Analyses," *Report No. EERC-70-10*, Earthquake Engineering Research Center, University of California, Berkeley, CA.

[3] Hardin, B.O., and Drnevich, V.P. (1972). "Shear Modulus and Damping in Soils: Measurement and Parameter Effects". Journal of the Soil Mechanics and Foundations Division, Proceedings of the American Society of Civil Engineers, Vol. 98, No. SM6, pp. 603-624.

[4] Electric Power Research Institute, EPRI (1993). "Guidelines for Determining Design Basis Ground Motions". Report No. EPRI TR-102293, Palo Alto, CA.

[5] Vucetic, M., and Dobry, R. (1991). "Effect of Soil Plasticity on Cyclic Response". Journal of Geotechnical Engineering, Vol. 117, No. 1, pp. 89-107.

[6] Stewart, J.P., and Kwok, A.O.L. (2008). "Nonlinear Seismic Ground Response Analysis: Code Usage Protocols and Verification against Vertical Array Data." Proc., ASCE conference of Geotechnical Earthquake Engineering and Soil Dynamics IV, Geotechnical Special Publication 181, ASCE, Sacramento, CA.

[7] Hashash, Y.M.A., Phillips, C., and Groholski., D.R. (2010). "Recent Advances in Non-linear Site Response Analysis." Proc., 5th International Conf. on Recent Advances in Geotechnical Earthquake Engineering and Soil Dynamics, NEES, San Diego, CA.

[8] Menq, F. Y. (2003) "Dynamic Properties of Sandy and Gravelly Soils," Ph.D. Dissertation, University of Texas at Austin. Austin, TX.

[9] Chiu, P., Pradel, D.E., Kwok, A.O., Stewart, J.P. (2008). "Seismic Response Analyses for the Silicon Valley Rapid Transit Project." Proc., ASCE conference of Geotechnical Earthquake Engineering and Soil Dynamics IV, Geotechnical Special Publication 181, ASCE, Sacramento, CA.

[10] Phillips, C., and Hashash, Y.M.A. (2009). "Damping Formulation for Non-linear Site Response Analyses." Soil Dynamics and Earthquake Engineering. Vol., 29, pp. 1143-1158.

[11] Hashash, Y.M.A., Groholski, D.R., Phillips, C.A., Park, D, and Musgrove, M. (2012) "DEEPSOIL 5.1, User Manual and Tutorial." pp. 107.

[12] Dickenson, S.E. (1994). "Dynamic Response of Soft and Deep Cohesive Soils During the Loma Prieta Earthquake of October 14, 1989". Ph.D. thesis, University of California, Berkeley, p. 331.

[13] Pass, D.E. (1994). "Soil Characterization of the Deep Accelerometer Site at Treasure Island, SanFrancisco, California". M.S. thesis, University of New Hampshire, Durham, NH.

[14] American Society of Civil Engineers (2010). "Minimum Design Loads for Buildings and Other Structures". ASCE Standard ASCE/SEI 7-10, American Society of Civil Engineers, Reston, Virgina.

[15] United States Geological Survey (USGS), (2008). "National Seismic Hazard Maps: Documentation," USGS Open File Report 2008-1128.

[16] United Sates Geological Survey (USGS), (2008). 2008 Interactive Deaggregations, <http://geohazards.usgs.gov/deaggint/2008/>, (Jan 9, 2013).

[17] Pacific Earthquake Engineering Research Center, PEER (2011). "Users Manual for the PEER Ground Motions Database Web Application" The Peer Center, University of California, Berkeley, CA. http://peer.berkeley.edu/peer_ground_motion_database/site.

[18] Kottke, A. and Rathje, E. (2013) "SigmaSpectra," <http://nees.org/resources/sigmaspectra>.

[19] Kottke, A. and Rathje, E.M. (2008). "A Semi-Automated Procedure for Selection and Scaling of Recorded Earthquake Motions for Dynamic Analysis" Earthquake Spectra, Earthquake Engineering Research Institute, Vol. ,24, No. 4, pp. 911-932.

[20] Matasovic, N. and Hashash, Y. (2012) "Practices and Procedures for Site-Specific Evaluations of Earthquake Ground Motions" National Cooperative Highway Research Program, Synthesis 428, a Synthesis of Highway Practice, Transportation Research Board, Washington, D.C.

[21] Kaklamanos, J., Bradley, B.A., Thompson, E.M., and Baise, L.G. (2013) "Critical Parameters Affecting Bias and Variability in Site-Response Analyses Using Kik-net Downhole Array Data". Bulletin of the Seismological Society of America, Vol. 103, No. 3. pp. 1733-1749.

[22] Anderson, J.G., and Hough, S.E. (1984). "A Model for the Shape of the Fourier Amplitude Spectrum of Acceleration at High Frequencies." Bulletin of the Seismological Society of America. Vol., 74, No. 5, pp. 1969-1993.

[23] Kilb, D., Biasi, G., Anderson, J., Brune, J., Peng, Z., and Vernon, F. (2012). "A Comparison of the Spectral Parameter Kappa from Small and Moderate Earthquakes Using Southern California ANZA Seismic Network Data." Bulletin of the Seismological Society of America. Vol., 102, No. 1, pp. 284-300.

[24] Campbell, K.W. (2003). "Prediction of Strong Ground Motion Using the Hybrid Empirical Method and Its Use in the Development of the Ground-Motion (Attenuation) Relations in Eastern North America". Bulletin of the Seismological Society of America, Vol., 93, No. 3, pp. 1012-1033.

[25]Van Houtte, C., Drouet, S., and Cotton, G. (2011) "Analysis of the Origins of κ (Kappa) to Compute Hard Rock to Rock Adjustment Factors for GMPEs". Bulletin of the Seismological Society of America, Vol., 101, No. 6, pp. 2926-2941.

[26] Campbell, K.W. (2009). "Estimates of Shear-Wave Q and κ_o for Unconsolidated and Semiconsolidated Sediments in Eastern North America". Bulletin of the Seismological Society of America, Vol., 99, No. 4, pp. 2365-2392.

Chapter 3:

A Surface Wave Dispersion Approach for Evaluating Statistical Models that Account for Shear Wave Velocity Uncertainty

Shawn C. Griffiths [a], Brady R. Cox [a]*, Ellen M. Rathje [a], David P. Teague[a]

[a] Department of Civil, Architectural and Environmental Engineering, The University of Texas, 301 E Dean Keeton Stop C1792, Austin, TX, USA 78712
* Corresponding author. Tel.: 512 471 9162, *Email address:* brcox@utexas.edu

Abstract

A number of strategies exist to account for the epistemic uncertainty and aleatory variability in shear-wave velocity profiles used in site response analyses. Epistemic uncertainty may be accounted for by using median and bounding-type profiles while aleatory variability may be accounted for by using randomization or Monte Carlo procedures. How the profiles from these procedures compare with the experimentally measured surface wave dispersion data is rarely, if ever, considered. The following paper details the surface wave data collection, dispersion procedure and inversion procedure from sites in Mirandola, Italy and Grenoble, France. Additionally, theoretical dispersion curves from the; median, bounding-type and statistically-based randomly-generated profiles for each site were compared with the experimentally measured dispersion data. It is found that the median theoretical dispersion curve provides a satisfactory fit to the experimental data, but the boundary-type theoretical dispersion curves do not. Randomly generated profiles results in some theoretical dispersion curves that fit the experimental data, and many that do not. The authors recommend computing the theoretical dispersion curves of the candidate profiles, and comparing it with the measured dispersion data prior to using the candidate profiles in site response analyses.

3.1. INTRODUCTION

Site response simulations using equivalent linear and nonlinear analyses show that the shear wave velocity (Vs) profile has a large influence on the amplitude and frequency content of predicted surface ground motions (e.g., Bazurro and Cornell 2004, Rathje et al.

2010, Barani et al. 2013). Hence, the development of appropriate Vs profiles for use in site response analyses is of paramount importance. While standard engineering design codes stress the importance of accounting for uncertainty in Vs when performing site-specific site response analyses (e.g., ASCE 2010, AASHTO 2011), no firm guidelines are provided regarding the appropriate methods that should be used to realistically account for this important effect. Matasovic and Hashash (2012) summarized survey responses from thirty state Departments of Transportation (DOT) regarding their practices and procedures for site response analysis. Of the survey responses, 33% indicated using a median Vs profile with upper and lower bound Vs profiles, 23% indicated not directly accounting for Vs uncertainty, and 13% indicated using a range of Vs profiles or randomization models, such as Monte Carlo simulations or the Toro (1995) Vs randomization model. While the results of this survey are based on only 30 responses, they give a glimpse into the two most common methods currently utilized for accounting for Vs uncertainty in site response analysis: (1) bounding-type profiles developed from a single reference Vs profile by arbitrarily increasing and decreasing the reference Vs profile by a constant factor such as +/- 20% to 30%, and (2) statistical-type profiles developed directly from either a large number of individual Vs profiles measured across a site and/or indirectly from Monte Carlo/randomization models. Either way, the resulting Vs profiles are often used blindly to account for Vs uncertainty in site response and are rarely evaluated in a quantitative manner in order to judge if they realistically represent potential subsurface stiffness/layering conditions.

This paper explores the validity of a number of different methods that can be used to account for Vs uncertainty in site response using a surface wave dispersion approach to help judge if a given Vs profile matches the experimentally measured "site signature". Specifically, the Vs profiles investigated are categorized into three groups: (1) Vs profiles determined directly from surface wave inversion, (2) simple statistical Vs profiles (including bounding-type, median, and other percentile Vs profiles), and (3) statistically-based, randomly-generated Vs profiles developed through a procedure such as that

proposed by Toro (1995). These three approaches are discussed below for surface wave data collected at two international blind-study sites. The validity of each approach is evaluated in a quantitative manner using the experimentally-measured dispersion data as a reference. A companion paper investigates the effects of using each approach to account for Vs uncertainty in site response.

3.2. SHEAR WAVE VELOCITY PROFILE UNCERTAINTY

Vs profiles can be measured in-situ using invasive or non-invasive techniques. In either case, there is uncertainty associated with the final Vs profile(s), which contributes to uncertainty in the site response predictions. According to EPRI (2012), two different types of uncertainty influence site response estimates: (1) aleatory variability and (2) epistemic uncertainty. In terms of Vs, aleatory variability results from the inherent variability/randomness associated with the subsurface layering and stiffness across the footprint of the site. Thus, aleatory variability is linked to the horizontal and vertical spatial variability of Vs. If limited Vs data exists spatially, it is hard to realistically quantify aleatory variability and assumptions must be made. Epistemic uncertainty results from data uncertainty and/or a lack of scientific knowledge. Thus, even for a single location, epistemic uncertainty in Vs exists due to factors such as vertical sampling interval and method of data analysis/interpretation. Currently, epistemic uncertainty in Vs is rarely quantified by those performing either invasive or non-invasive testing. Rather, a single, deterministic Vs profile is typically provided for a single testing location without consideration of data uncertainty. This results in the need to make assumptions about the epistemic uncertainty in Vs.

Both epistemic uncertainty and aleatory variability in Vs are typically accounted for in probabilistic site response analyses for critical projects such as nuclear facilities. Epistemic uncertainty is accounted for by developing a mean, or base-case, Vs profile along with alternative upper- and lower-bound Vs profiles, which represent relatively stiffer and softer perturbations of the base-case profile, respectively. These are akin to

the bounding-type Vs profiles discussed above, which are often generated for standard, less rigorous site response analyses by arbitrarily increasing and decreasing the reference Vs profile by a constant factor such as +/- 20% to 30%. Aleatory variability in Vs is accounted for in site response analyses via a randomization process about the base-case, upper- and lower-bound Vs profiles. This is most commonly performed using the Toro (1995) Vs randomization model. If abundant Vs data is available at a site, the statistical parameters needed to constrain epistemic uncertainty and aleatory variability can be obtained. Otherwise, conservative estimates must be made.

3.2.1. Invasive Methods of Shear Wave Velocity Measurement

The most common invasive techniques for obtaining Vs measurements are downhole (including seismic CPT), crosshole, and P-S suspension logging. While considered more reliable than non-invasive techniques, invasive methods require at least one borehole, which can render them cost prohibitive for determining multiple Vs profiles spatially across a large site and/or for obtaining Vs data at depths greater than 30 - 60 m. Regardless, invasive methods typically yield only a single Vs profile for a single borehole (or a set of boreholes in the case of crosshole testing). While epistemic uncertainties associated with travel time picks and the various methods used to determine a layered velocity model are present in borehole methods, they are rarely, if ever, quantified and passed on for subsequent use in site response.

When only a single Vs profile is available for a site, bounding-type profiles are often used as a means to account for epistemic Vs uncertainty. As discussed above, in many projects these bounding profiles are typically derived by increasing and decreasing the single Vs profile by +/- 20% to 30%, as indicated in Figure 3.1a. For projects with a sufficient budget, spatial/aleatory variability in the thickness and Vs of soil and rock layers across the site can be estimated by drilling multiple boreholes (Figure 3.1b) and conducting invasive tests in each one. The Vs profiles scattered across the site may then

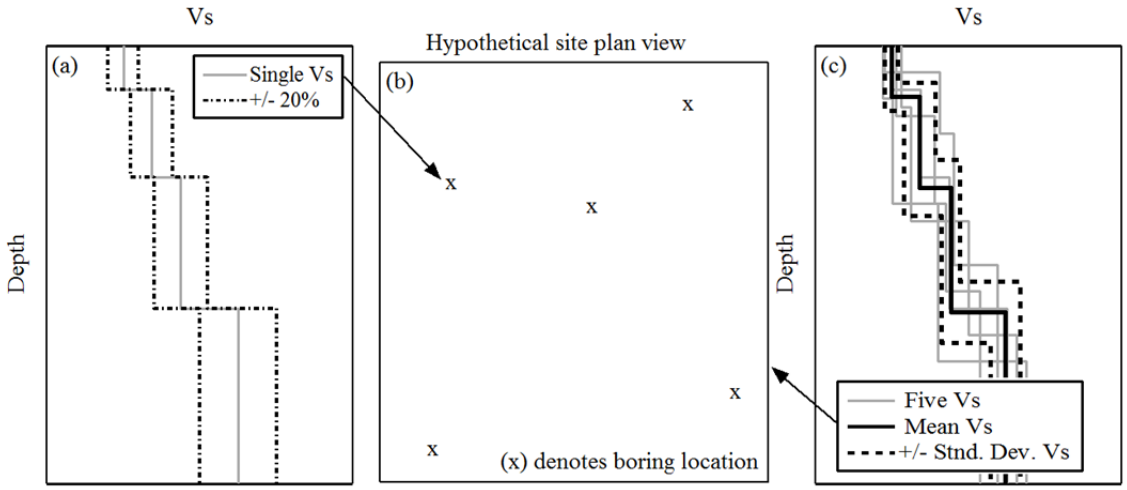

Figure 3.1. Schematic detailing potential methods for accounting for Vs uncertainty associated with invasive methods: a) a single Vs profile using a single borehole with +/- 20% bounding-type Vs profiles, b) a hypothetical site showing possible locations of five borings and, c) five Vs profiles from each of the five borings used to determine simple statistical Vs profiles such as the mean and +/- one standard deviation.

be used to calculate simple statistical profiles, such as the mean profile and +/- one standard deviation profiles, as presented in Figure 3.1c. Alternatively, these profiles can also be used to guide development of statistically-based, randomly-generated Vs profiles through a procedure such as that proposed by Toro (1995). While common on critical projects, collecting a large number spatially distributed Vs profiles is rarely utilized for routine engineering applications due to the high costs associated with drilling and performing invasive tests in multiple boreholes.

3.2.2. Non-Invasive Methods of Shear Wave Velocity Measurement

Non-invasive techniques, such as surface wave testing, can provide a cost effective means to develop deep Vs profiles for many engineering applications (Foti et al. 2014). Surface wave testing has grown significantly in popularity over the past 25 years (e.g., Socco et al. 2010, Foti et al. 2011). Although there are numerous techniques to

collect and analyze surface wave data, all generally consist of the following three steps; (1) field data acquisition, (2) dispersion processing, and (3) shear wave velocity inversion (Stokoe et al. 1994, Foti et al. 2011, Cox et al. 2014). Uncertainties are associated with each step of this generalized process and some basic background information is required to understand how these uncertainties can be quantified.

Data acquisition involves measuring wavefields with strong surface wave content using arrays of receivers. Wavefields can be actively-generated at the ground surface (e.g., using a drop weight or dynamic shaker) or passively-generated from cultural noise/ambient vibrations or seismic microtremors. Active sources generally generate higher frequency surface waves, which provide spatial resolution close to the surface. Conversely, passive sources usually produce lower frequency surface waves, allowing sampling to greater depths (Garofalo et al. 2016a). Combining active and passive methods, as suggested by Rix et al. (2002) and Foti et al. (2009), is advantageous as the combination of high and low frequency surface waves allows for both near-surface resolution and greater depth of investigation. Presently, most surface wave testing is based on Rayleigh waves, however, Love waves can also be analyzed (Fah et al. 2006). Figure 3.2a presents a schematic of a typical experimental surface wave setup utilizing both a linear array of receivers for active-source testing and a circular array of receivers for passive-source testing. Typical linear array lengths vary from 25 m to 100 m, while typical circular array apertures vary from 50 m to 1,000 m, depending on the desired depth of investigation and the footprint of the site.

Dispersion processing involves deriving a relationship between surface wave phase velocity and frequency from the experimentally measured data. A number of strategies are available to extract the experimental dispersion data from active- and passive-source measurements (e.g., Aki 1957, Capon 1969, Stokoe et al. 1994, Park et al. 1998, Zywicki 1999). Despite the large number of procedures available, and the even greater number of researchers and practitioners using slight variations of these

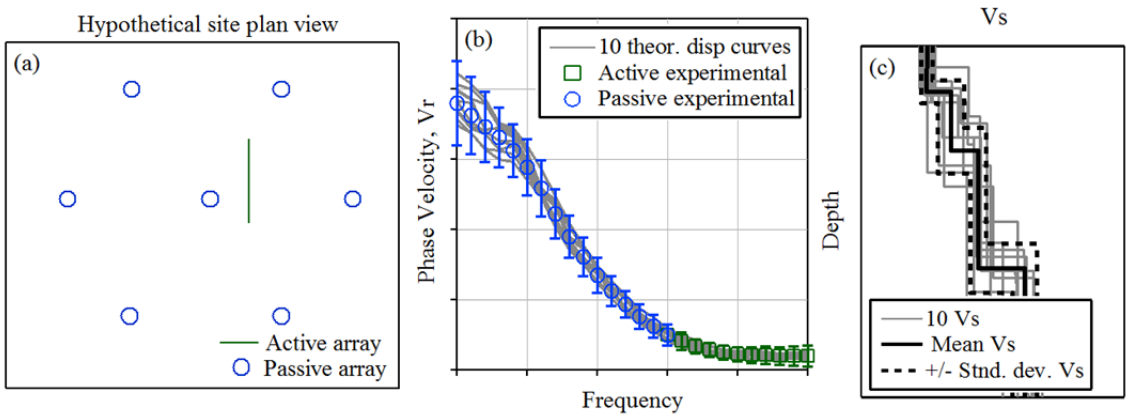

Figure 3.2. Schematic detailing potential methods for accounting for Vs uncertainty associated with surface wave methods: a) a hypothetical site showing typical layout of active and passive receiver arrays, b) experimental active and passive dispersion data with 10 theoretical dispersion curves that fit within the uncertainty bounds of the experimental data, and c) 10 corresponding Vs profiles that fit the experimental dispersion data.

procedures, similarities in the experimental dispersion data obtained from multiple analysts at a single site are often

evident (Cournou et al. 2006). In fact, two recent blind-analysis studies published by Cox et al. (2014) and Garofalo et al. (2016a) compared experimental dispersion curves obtained from a number of individual teams who analyzed common experimental data sets collected at sites ranging from deep, soft soils to shallow, stiff rock. These studies found that the coefficient of variation (COV) for dispersion data was generally less than 5-10% over the most commonly measured frequency bands. This result provides strong evidence that the experimental dispersion data from a site can be derived robustly by different analysts using a wide variety of processing methods with minimal uncertainty. Therefore, the experimental dispersion data measured at a site may be considered as a robust "site signature", which includes important information about how seismic waves propagate across the site. Figure 3.2b shows a schematic of an experimental dispersion curve with associated uncertainty (+/- one standard deviation) from combined active and passive surface wave measurements. In contrast to invasive methods, non-invasive

surface wave methods "sample" soil over a broad spatial area, varying from tens to hundreds of meters laterally across a site, depending on the aperture of the array and the desired depth of investigation. Due to the large spatial sampling, experimental surface wave data inherently includes information on aleatory/lateral variability. Thus, the experimental dispersion data, with its associated uncertainties, likely already contains important information concerning variability of wave propagation across a large footprint. Higher frequency data is typically derived from smaller arrays that sample less material spatially, while lower frequency data is typically derived from larger arrays that sample more material spatially. Thus, the uncertainties associated with higher frequency data are typically less than those associated with lower frequency data.

After the experimental dispersion data and associated uncertainties have been determined, inversion analyses are employed to develop one or more suitable Vs profiles for the site. The inversion process consists of finding one or more layered earth models whose theoretical dispersion curve(s) suitably match the experimentally determined data. The layered earth models are comprised of thickness, Vs, compression wave velocity (Vp) or Poisson's ratio, and the mass density for each layer. Numerous inversion techniques are available (e.g., Rothman 1985, Herrmann 1987, Yamanaka and Ishada 1996, Lai 1998, Xia et al. 1999, Socco and Boiero 2008, Wathelet 2008, Molnar et al. 2010, Maraschini and Foti 2010), but the direct determination of a single, unique Vs profile from an experimental dispersion curve is generally not possible, regardless of which technique is used, due to the nonlinear, ill-posed, and mixed determined nature of the inverse problem (Foti et al. 2014). However, it is possible to obtain a number of different Vs profiles that satisfactorily fit the experimental dispersion data (Foti et al. 2009, Wood et al. 2014). Figure 3.2c shows 10 hypothetical Vs profiles whose theoretical dispersion data fit the experimental data in Figure 3.2b. For the purposes of illustration, this hypothetical example uses only 10 layered earth models. In practice, the number of layered earth models searched in an inversion can range from hundreds to millions, depending on the number of inversion parameters (i.e., number of layers and

ranges for their corresponding thicknesses, Vp, Vs, and mass density) and the complexity of the experimental dispersion data (i.e., higher and effective modes, significant data uncertainty, etc.).

The non-unique nature of surface wave inversion is perhaps the biggest criticism of these methods. However, assuming the analyst has performed a rigorous inversion and has given due diligence to exploring different models, a non-unique answer may not be a deficiency because multiple realistic Vs profiles are needed to account for Vs uncertainty in site response. Therefore, one must simply decide which Vs profiles to use in subsequent site response analyses and how to realistically quantify the associated uncertainty. As noted above, the uncertainty present in the experimental surface wave data is the result of both epistemic uncertainty and aleatory variability. While the subsequent inversion uncertainty is strictly epistemic, it is influenced by the aleatory variability contained in the experimental data. Thus, it would be very challenging to uncouple these two sources of uncertainty/variability in the final Vs profiles obtained from surface wave testing.

3.3. SURFACE WAVE DATA COLLECTION AND PROCESSING AT CASE STUDY SITES

A suite of invasive and non-invasive geophysical testing was conducted at three sites in Europe for the InterPacific (Intercomparison of methods for site parameter and velocity profile characterization) project (Garofalo et al. 2016a and Garofalo et a. 2016b). The three sites investigated for the InterPacific project were located in Mirandola, Italy; Grenoble, France; and Cadarache, France. The geologic conditions at these three sites can be broadly defined as soft-soil, stiff-soil, and hard-rock, respectively. The objective of the InterPacific project is to assess the reliability of invasive and non-invasive seismic site characterization methods in various soil/rock conditions. The invasive methods used at the sites were downhole, crosshole, and P-S suspension logging. Non-invasive testing consisted primarily of active- and passive-source surface wave testing. Blind analyses of the invasive and non-invasive data from multiple researchers/practitioners in a number of

different countries was used to quantify the uncertainty/variability expected in both data collection and processing at all three sites. Although many teams analyzed the invasive and non-invasive data collected at these sites, only the surface wave data analyzed by the authors for the Mirandola and Grenoble sites are discussed here. However, a reference crosshole Vs profile from each site is presented to validate the Vs profiles obtained from surface wave testing.

A detailed description of the active and passive surface wave data collected at the InterPacific sites is provided in Garofalo et al. (2016a). A general synopsis is provided here. Rayleigh wave active-source data were acquired using two 48-channel arrays with spacings between successive vertical 4.5-Hz geophones of between 1 m and 2 m. For the Mirandola site, active-source Love wave data were also obtained via 24 horizontal geophones spaced at 2 m. Passive-source surface wave data was collected using 3-component, intermediate-period seismometers deployed in circular arrays (ranging from 5 m to 405 m radius), triangular arrays (sides ranging from 12.5 m to 300 m), L-shaped arrays (sides 150 m long), and "large arrays" (triangular arrays sides ranging from 1,000 m to 4,000 m).

For each site, the University of Texas team used different combinations of active and passive data to develop a single surface wave dispersion curve with associated uncertainties as a function of frequency. All active-source dispersion data was analyzed using the Frequency Domain Beamformer (FDBF) method (Zywicki 1999). The dispersion data from the different linear arrays and multiple shot locations were combined using the methods described in Wood and Cox (2012) to quantify uncertainty. Ambient vibration data was analyzed using both the High Resolution Frequency-Wavenumber Transformation (HFK) and the Modified Spatial Autocorrelation (MSPAC) methods (Capon 1969, Bettig et al. 2001). The results from different arrays, different time-windows, and different processing methods were combined to develop a representative passive-source dispersion curve with associated uncertainties. Active- and passive-source dispersion curves were then combined to develop a composite Rayleigh

wave dispersion curve with error bars that represent +/- one standard deviation in phase velocity. In addition to the Rayleigh wave dispersion curve, a Love wave dispersion curve was also developed using the FDBF method and the horizontal active-source MASW data for the Mirandola site.

Horizontal-to-vertical (H/V) spectral ratios were computed for the three-component ambient vibration data at each site. The H/V curve can provide information regarding the Rayleigh wave ellipicity, which is the ratio between the horizontal and vertical axes of Rayleigh wave motion. If a wavefield consisted purely of a single Rayleigh wave, the H/V spectrum would correspond to the Rayleigh wave ellipicity (Hobiger et al. 2012). However, ambient vibrations also contain Love and body waves, which influence the H/V curve. Therefore, the H/V spectrum cannot be inverted without additional information regarding the energy content of Rayleigh, Love, and body waves. Even still, the frequency at which the H/V spectrum peaks has been shown to coincide with the first maximum in the fundamental mode Rayleigh wave ellipicity at sites containing a strong velocity contrast (Poggi and Fah 2010). Thus, while the entire H/V spectrum cannot be inverted, the peak frequency in the H/V spectrum may be used to constrain the inversion process at sites with a strong velocity contrast.

Rayleigh wave data, Love wave data (where available), and H/V peak frequency were inverted simultaneously using the Geopsy software package (www.geopsy.org). Theoretical dispersion curves (Rayleigh and Love) and Rayleigh wave ellipicity curves were generated for each trial layered earth model. The forward model calculations were originally developed by Thomson (1950) and Haskell (1953) and later modified by Dunkin (1965) and Knopoff (1964). A misfit value between the experimental data and the theoretical data was then computed for each trial layered earth model using Equation 3.1 (Wathelet 2005). For dispersion data, x_{di} corresponds to the phase velocity of the experimental data at frequency f_i, x_{ci} is the calculated phase velocity from the theoretical data at frequency f_i, σ_i is the standard deviation associated with the experimental data at frequency f_i, and n_f is the number of frequency samples considered. For ellipicity data,

x_{di} corresponds to the experimental peak frequency (based on the H/V ratio), x_{ci} corresponds to the first frequency at which the theoretical Rayleigh wave ellipicity reaches a maximum, σ_i is the uncertainty associated with the experimental peak frequency, and n_f is one.

$$\text{misfit} = \sqrt{\sum_{i=1}^{n_f} \frac{(x_{di} - x_{ci})^2}{\sigma_i^2 n_f}} \qquad \text{(Eq. 3.1)}$$

The Geopsy software averages the dispersion and ellipicity misfits in order develop a single misfit value. This value is used to assess the overall quality of fit between the experimental and theoretical data for a given trial layered earth model. A global-search neighborhood algorithm is used to explore regions of the parameter space with the lowest misfit values, thereby developing a suite of layered earth models while trying to obtain the model with the lowest possible misfit (Wathelet 2008).

More than one million layered earth models were considered during inversion of the surface wave data at each site. Of these, the 1,000 "best" models (i.e., the layered earth models with the lowest misfit values) were chosen to represent the subsurface Vs profile at each site.

3.4. Analysis of Site at Mirandola, Italy

The surface wave data chosen to develop the experimental Rayleigh wave dispersion curve at Mirandola includes all MASW arrays, all circular arrays, triangular arrays with sides less than or equal to 200 m, and the L-shaped array. A representative active-source Rayleigh wave dispersion curve with associated uncertainty was derived over the frequency range of 5 to 25 Hz. Ambient vibration HFK data was used for frequencies of 4 to 25 Hz and 0.7 to 1.3 Hz, and MSPAC data was used at frequencies ranging from 1.5 to 3.5 Hz. The choice of HFK or MSPAC data was made after visually inspecting the dispersion data and judging which was of higher quality based on a number of factors (e.g., smoothness, uncertainty bounds, bias towards high or low phase

velocity, etc.). The combined active- and passive-source Rayleigh wave dispersion curve for Mirandola is shown in Figure 3.3a, where the error bars represent +/- one standard deviation in phase velocity. The Love wave dispersion curve developed using the FDBF method with the horizontal active-source MASW data is shown in Figure 3.3b. The maximum H/V ratio from the 3-component ambient data was found to occur at 0.73 Hz with a standard deviation of 0.03 Hz. This H/V peak was used in the Geopsy inversions.

The theoretical dispersion curves corresponding to the 1,000 lowest misfit models are shown along with the experimental dispersion data in Figure 3.3. The 1,000 models fit the experimental data very well, with few theoretical dispersion data points outside of the uncertainty bounds in the experimental data. Misfit values for these 1,000 models were re-computed by the authors outside of Geopsy using Equation 3.1 without accounting for Rayleigh wave ellipicity (i.e., only based on dispersion data). The reason for re-computing misfit values was to ensure a consistent misfit calculation between models determined directly from the inversion procedure (i.e., within Geopsy) and subsequent statistical models generated outside of Geopsy. The misfit values for these 1,000 models range from 0.29 - 0.51, as indicated within the square brackets in the legend for Figure 3.3.

The Vs profiles corresponding to the 1,000 lowest misfit layered earth models and the Vs profile obtained from crosshole testing at Mirandola are presented in Figure 3.4. The 1,000 lowest misfit profiles match the crosshole Vs profile quite well, validating the surface wave results. Interestingly, the areas of the profile where the crosshole and surface wave Vs profiles diverge slightly (depths between approximately 10 m and 40 m) are also the depth ranges where the scatter in the Vs profiles obtained from inversion are the largest. The crosshole data did not extend very far into the bedrock and cannot be relied upon for determining an accurate rock velocity. However, the Vs profiles from surface wave testing indicate that the bedrock depth ranges between 110 and 120 m and the Vs of the rock varies from approximately 850 to 1,350 m/s, resulting in an impedance ratio at the bedrock interface that varies between 2.7 and 4.2. It should be noted the depth

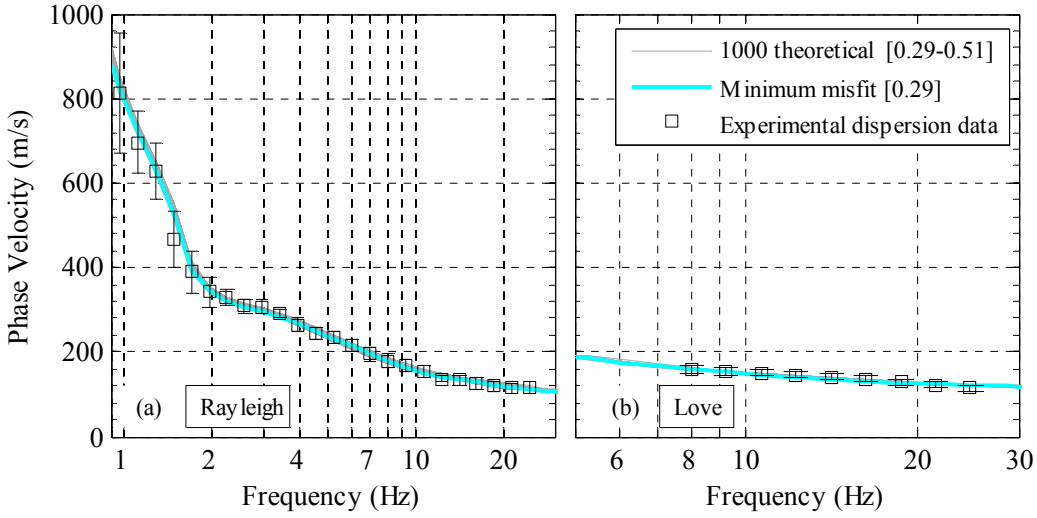

Figure 3.3. Experimental dispersion data, theoretical dispersion curves from the 1,000 lowest misfit models from surface wave inversion, and the minimum misfit theoretical dispersion curve at Mirandola, including: a) Rayleigh and b) Love wave data. Note that square brackets, [ ], indicate the misfit value(s).

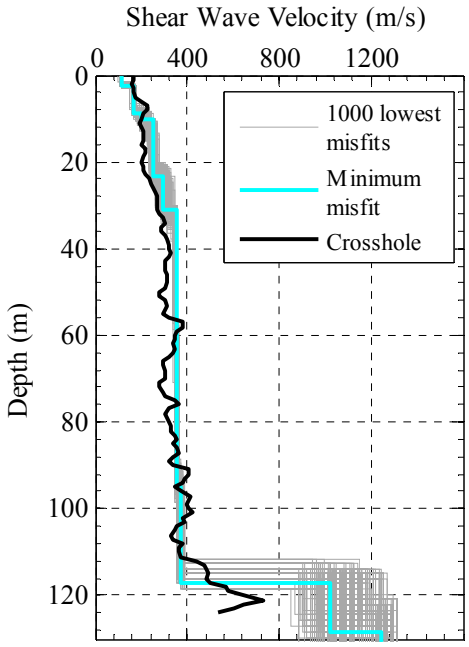

Figure 3.4. The 1,000 lowest misfit Vs profiles determined from the surface wave inversion procedure and the crosshole Vs profile at Mirandola.

to bedrock at this site is significantly less than one-half of the maximum resolved wavelength in the experimental data (roughly 700 m), which is a commonly used criteria for the maximum investigation depth (Comina et al. 2011).

3.4.1 Simple Statistical Vs Profiles

Performing individual site-response analyses on all 1,000 lowest misfit profiles would require a long computation time, especially for multiple input ground motions. Therefore, a smaller set of 50 Vs profiles was randomly sampled from the 1,000 lowest misfit profiles for further investigation. These profiles are referred to hereafter as the "50 inversion" Vs profiles. The choice of using a sample size of 50 is arbitrary, but can be justified by comparing the median Vs profile and standard deviation of the natural log of Vs (σ_{lnVs}) of both the 1,000 lowest misfit profiles and the set of 50 randomly selected Vs profiles, as presented in Figure 3.5. Because the inversion Vs profiles were each generated using the same parameter space, they each have the same number of layers. This allows for the computation of a counted-median profile by computing the median Vs value and median thickness/depth for each layer. As shown in Figure 3.5, the median Vs profile and σ_{lnVs} for the 50 randomly sampled inversion profiles are essentially indistinguishable from those of the 1,000 profiles. Therefore the choice of using 50 inversion Vs profiles is judged to be sufficient to represent all 1,000 lowest misfit Vs profiles.

As discussed above, a common method to account for epistemic uncertainty in soil properties when performing site response analyses is to use a median/base-case Vs profile along with upper- (i.e., stiffer) and lower-boundary (i.e., softer) Vs profiles. To assess the ability of these bounding-type Vs profiles to realistically account for Vs uncertainty, two sets of upper- and lower-boundary Vs profiles were generated. The first set was determined by computing the counted median of the 50 inversion Vs profiles and adjusting the Vs in each layer by +/- 20%, without changing any of the layer thicknesses. The second set was determined by computing the counted 5^{th} and 95^{th} percentile Vs

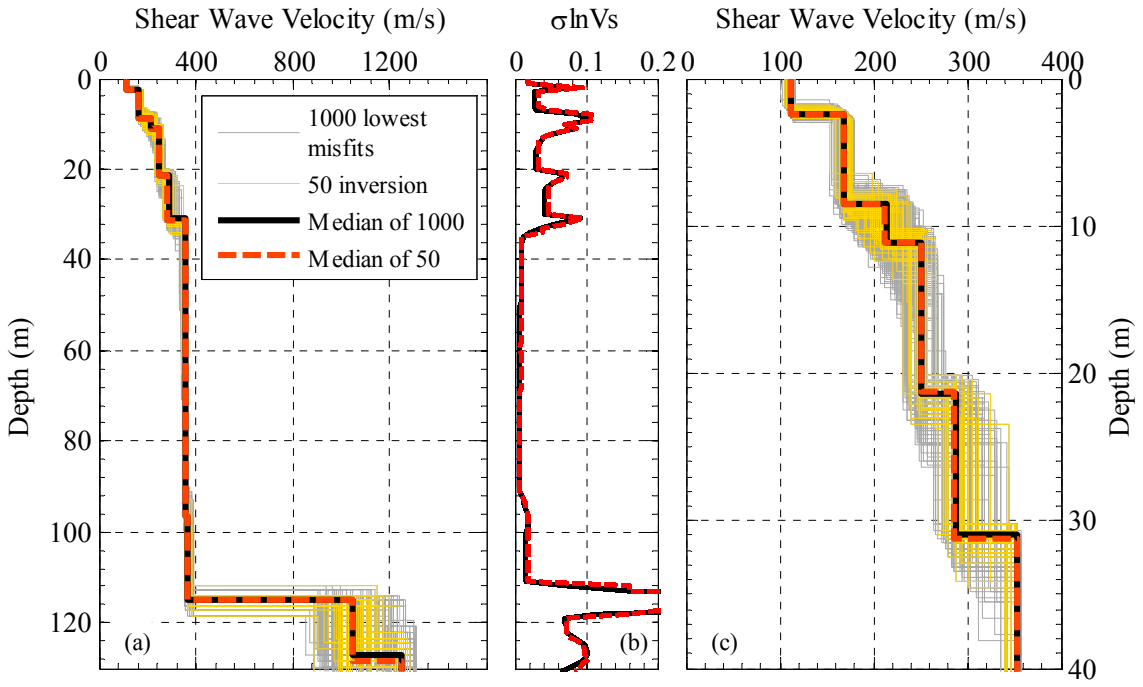

Figure 3.5. Comparisons of: a) the 1,000 lowest misfit Vs profiles from inversion with 50 randomly-selected profiles and the medians of the 1,000 and 50 profiles, b) σ_{lnVs} of the 1,000 and 50 inversion profiles, and c) zoomed view of (a), at Mirandola, Italy.

profiles from the 50 inversion Vs profiles. This was accomplished by computing the counted 5th and 95th percentile Vs for each layer as well as the counted 5th and 95th percentile depth to the bottom of each layer (termed the bottom depth). The 95th percentile Vs profile represents the combination of the 95th percentile Vs with the 5th percentile bottom depth in each layer. Similarly, the 5th percentile Vs profile was determined by combining the 5th percentile Vs with the 95th percentile bottom depth for each layer. The reason for pairing high velocities with shallow depths and low velocities with greater depths was to develop relatively stiff and soft boundary profiles that encapsulate the majority of the 50 inversion Vs profiles under consideration.

The median of the 50 inversion Vs profiles, the +/- 20% Vs profiles, and the 5th and 95th percentile Vs profiles are presented in Figure 3.6. These profiles are loosely termed “simple statistical profiles” hereafter as a way of referring to profiles that did not

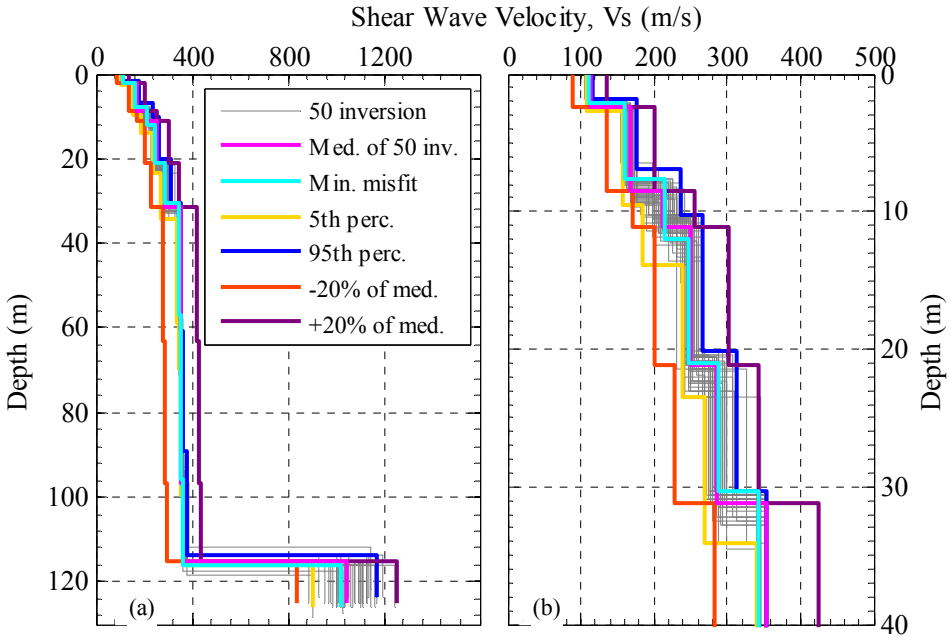

Figure 3.6. Comparisons of: a) 50 inversion Vs profiles along with the median of the 50 inversions, minimum misfit, 5th, 95th,and +/-20% Vs profiles, and b) zoomed view of (a), at Mirandola, Italy.

directly result from inversion, but rather were generated in a simplistic way from the statistics of the inversion results. The 50 inversion Vs profiles and the minimum misfit Vs profile from the 1,000 lowest misfit models are also included in Figure 3.6 for comparison purposes. For this site, the 5th and 95th percentile Vs profiles are generally bounded by the +/- 20% Vs profiles.

3.4.2 Randomly Generated Vs Profiles

As discussed above, randomization procedures can be used to develop a suite of Vs profiles that account for aleatory variability. The Vs randomization model proposed by Toro (1995), as programmed into STRATA (Kottke and Rathje, 2009) and described in Rathje et al. (2010), was used to generate a suite of 50 statistically-based, randomly-generated Vs profiles that are referred to hereafter as the "50 Toro" profiles. The procedure developed by Toro (1995) requires a baseline (i.e., initial) Vs profile and

allows the use of site-specific model parameters, predetermined default model parameters, or a combination of both. Within STRATA (Kottke and Rathje, 2009), the Toro (1995) randomization model operates on three general sets of model parameters: (1) the Vs statistical parameters, (2) the layering model parameters, and (3) the depth to bedrock parameters.

The required Vs statistical parameters include the baseline Vs profile and depth-dependent σ_{lnVs}, as well as parameters that control the inter-layer correlation coefficient between Vs. The parameters used for Mirandola were set using a combination of calculated, default, and assumed values, as indicated in Table 3.1. The median of the 50 inversion Vs profiles, which has a Vs_{30} (average Vs over the top 30 m) of 239 m/s, was used as the baseline Vs profile for the randomizations. The σ_{lnVs} values were obtained from the 50 inversion Vs profiles and are generally less than 0.1 (Figure 3.5b). These σ_{lnVs} values are substantially lower than the default values, which are dependent on site class and range from 0.25 to 0.37. The large default σ_{lnVs} values are not surprising because the Toro (1995) model is based on Vs profiles from a host of different sites within the same site class (Rathje et al., 2010). The inter-layer correlation parameters Δ, d_0, and b were each assigned the default values for sites with Vs_{30} between 180-360 m/s, which is consistent with the Vs_{30} of the median Vs profile used as a baseline. The inter-layer correlation parameters ρ_0 and ρ_{200} were assumed to be 0.8 based on previous experience.

The layering model and depth to bedrock model are used to develop a set of layers to which velocities are assigned using the Vs statistical model. The parameters for these models were all determined on a site-specific basis using the 50 inversion Vs profiles. The layering model is a non-homogenous Poisson model in which the rate of layer interfaces (λ_t), which is the inverse of the layer thickness, is a function of depth. The default layering model parameters from Toro (1995) results in λ_t decreasing with depth, which models an increase in layer thickness with depth. The inverse of the layer thicknesses of the 50 inversion Vs profiles were plotted versus depth to assess the

Table 3.1. Parameters used for the Toro (1995) randomization model for Mirandola

Inter-layer correlation		Layering model[C]		Depth of bedrock[C]	
Δ	3.9[A]	c1	2.12	mean	115 m
d_0	0[A]	c2	5.85	stnd dev.	1.1 m
b	0.344[A]	c3	-0.9		
ρ_0	0.8[B]				
ρ_{200}	0.8[B]				

A. Toro, default assuming Vs_{30} between 180-360 m/s
B. Assumed values
C. Site specific using inversion profiles

layering model parameters for Mirandola (Figure 3.7a). The model parameters c1, c2 and c3 were determined by fitting a power function through the data points. Because the number of layers is the same for each of the 50 inversion Vs profiles, the λ_t values tend to clump together over a narrow range of mid-point depths for each layer. To clarify the relationship between the Vs layering, thickness, and depth, Figure 3.7b presents the median of the 50 inversion Vs profiles and the 5th and 95th percentile Vs profiles from Mirandola with the first 5 layers numbered in both Figures 3.7a and b. Consider layer 3, for which the midpoint depth varies between 8 - 12 m and the thickness varies between about 1.1 m to 8 m. The corresponding λ_t values in Figure 3.7a all fall in a near horizontal line, depicting the narrow range in midpoint depths and the large range in thicknesses in layer 3 for the Vs profiles. The clumping of the λ_t values has not been observed when analyzing Vs profiles that have different numbers of layers (e.g., Rodriguez-Marek et al. 2014). The λ_t relationship using the Toro (1995) default parameters is also included in Figure 3.7a for comparison. At depths greater than 25 m, the Toro (1995) model fits the Mirandola site well, but at depths less than 25 m the Toro (1995) model predicts thicker layers than observed at Mirandola. The depth to bedrock was assumed to be normally distributed, and based on the 50 inversion Vs profiles it has a mean of 115 m and a standard deviation of 1.1 m. While this is a small standard

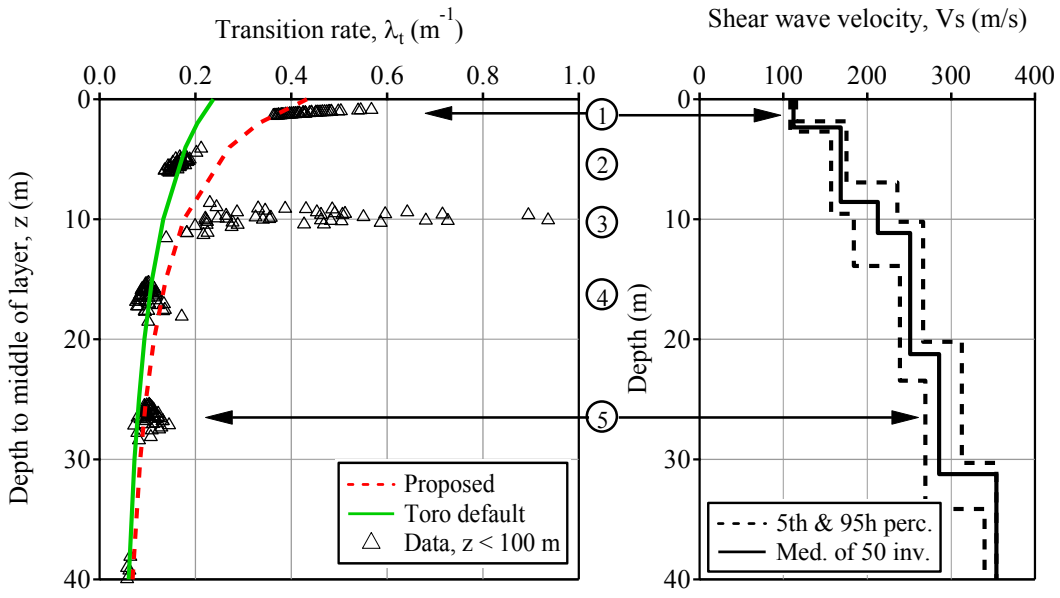

Figure 3.7. a) Layer transition rate versus layer mid depth for the 50 inversion Vs profiles at depths less than 100 m, and b) counted 5th, 95th and median of the 50 inversion Vs profiles at Mirandola.

deviation for the depth to bedrock, this range agrees well with the depth to rock indicated by the crosshole Vs profile.

The parameters in Table 1 were used to generate 60 random Vs profiles using the Toro (1995) procedure programmed into STRATA (Kottke and Rathje, 2009). These 60 Vs profiles were visually examined and the 10 profiles that appeared to be most uncharacteristic, compared with the other profiles, were discarded. The 50 remaining Toro Vs profiles generated for Mirandola are presented in Figure 3.8 along with their median, the median of the 50 inversion Vs profiles (i.e., the baseline Vs profile used in the Toro model) and the σ_{lnVs} of the Toro and inversion Vs profiles. The median Vs profiles are relatively similar, although differences are observed due to the different methods used to compute the medians. The median for the 50 Toro profiles is smooth rather than layered because it was calculated by discretizing the Vs profiles over 1 m increments prior to calculating the statistics. This was necessary because the Toro

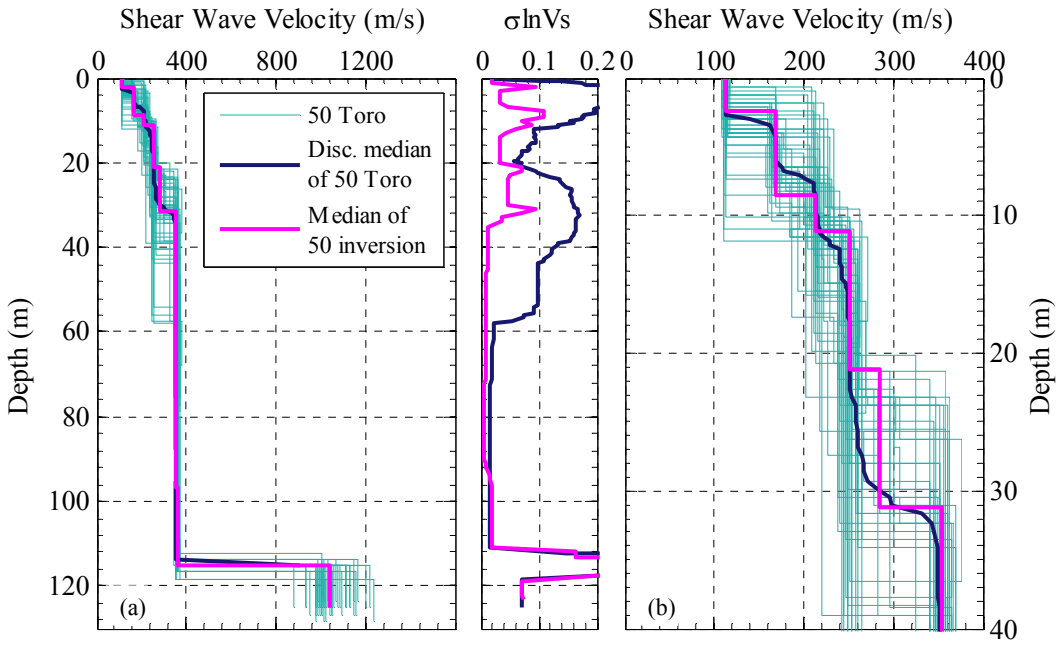

Figure 3.8. Comparisons of: a) 50 Vs profiles generated using the Toro (1995) randomization model, b) σ_{lnVs} of the 50 Toro Vs profiles, and c) zoomed view of (a) at Mirandola.

profiles, unlike the 50 inversion profiles, did not all have the same number of layers. The σ_{lnVs} values from the 50 Toro Vs profiles are reasonably close to the σ_{lnVs} values from the 50 inversion Vs profiles (Figure 3.8b), particularly at depths greater than 60 m. At shallower depths, the σ_{lnVs} values from the 50 Toro Vs profiles are approximately one to two times larger than the σ_{lnVs} values from the 50 inversion Vs profiles. This result is surprising given that the σ_{lnVs} used in the Toro (1995) model was derived from the 50 inversion Vs profiles and much smaller than the suggested default value.

3.4.3. Theoretical Dispersion Data for Vs Profiles

In total, 106 different Vs profiles were considered to represent the Vs uncertainty at Mirandola, including the 50 inversion profiles, the minimum misfit profile from inversion, the median of the 50 inversion profiles, the 5th and 95th percentile profiles, the +/- 20% of median profiles, and the 50 Toro Vs profiles. Theoretical dispersion curves

were generated for the simple statistical profiles and the 50 randomly-generated Toro Vs profiles and compared with the measured dispersion data. The theoretical dispersion curves were based on the following assumptions: (1) the mass density for each layer was assumed to be 2000 kg/m^3, except the half-space rock layer, which was assigned a density of 2300 kg/m^3, (2) the first layer in each model was assumed to be unsaturated with a Poisson's ratio of 0.33, (3) all underlying soil layers with a Vs $\leq$ 750 m/s were assumed to be saturated, thus Vp was fixed at 1500 m/s (i.e., Poison's ratio near 0.5), and (4) rock layers with Vs $\geq$ 750 m/s were assigned a Poisson's ratio of 0.33. These assumptions are consistent with those utilized during the original site inversion to obtain the 50 inversion Vs profiles.

Figure 3.9 presents the experimental dispersion data measured at Mirandola along with the theoretical dispersion data for the simple statistical Vs profiles. Misfit values for the simple statistical profiles were computed using Equation 3.1 and are included in the figure legend in square brackets. The dispersions curves from the 50 inversion Vs profiles have misfit values between 0.32 - 0.45. The median of the 50 inversion Vs profiles has a misfit value of 0.35, which is very small and reasonably close to the overall minimum misfit (0.29) obtained from the 1,000 inversion profiles. Although the median profile was developed statistically from the 50 randomly-selected inversion Vs profiles, and does not represent an actual profile from the inversion, it fits the experimental dispersion data better than many of the profiles that came directly from the inversion. In contrast, the 5th and 95th percentile Vs profiles produce theoretical dispersion curves with high misfit values of 2.41 and 1.96, respectively. These misfit values are substantially larger than any of the misfit values from the 50 inversion Vs profiles, and their theoretical dispersion curves are visibly outside of the estimated uncertainty bounds of the experimental data at frequencies between 4 – 10 Hz. The

theoretical dispersion curves associated with the -20% and +20% Vs profiles result in even poorer fits to the experimental data, with misfit values of 5.66 and 3.38, respectively. The poor misfit values for the +/- 20% profiles are easily visualized, with

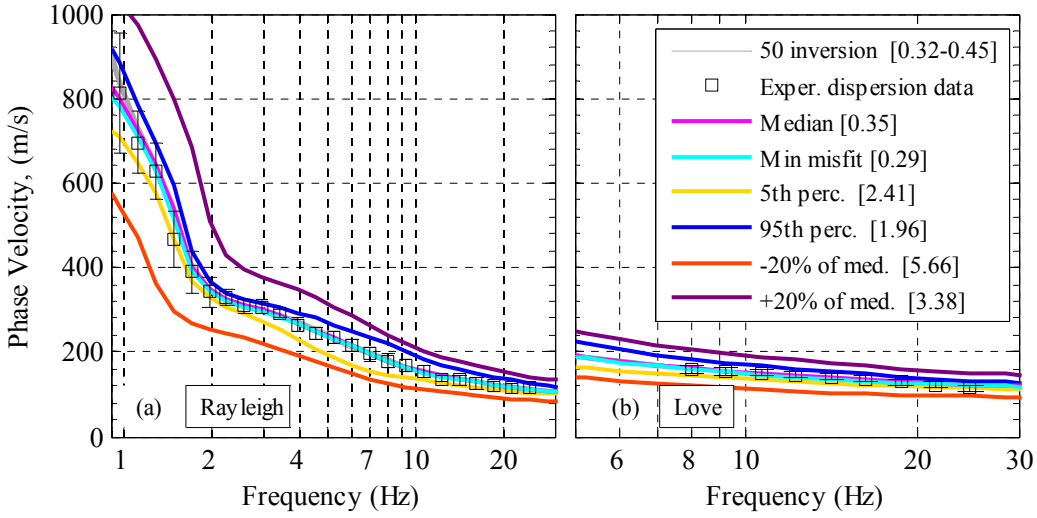

Figure 3.9. Experimental dispersion data from Mirandola and the theoretical dispersion curves from the 50 inversion Vs profiles, the minimum misfit, 5th, 95th and +/- 20% Vs profiles for a) Rayleigh wave and b) Love wave data.

theoretical dispersion curves well outside of the experimental dispersion data uncertainty bounds. Thus, in this case, the bounding-type Vs profiles developed from simple statistics do not result in a satisfactory fit of the experimental dispersion data and, therefore, do not appropriately capture the experimentally-measured site signature. As such, one must question the use of such profiles to represent the subsurface stiffness characteristics of the site.

The theoretical dispersion curves associated with the 50 Toro Vs profiles are presented with the experimental dispersion data in Figure 3.10. The misfit values for the Toro profiles range from 0.7 to 9.24. Visibly, many of the theoretical dispersion curves appear to fall within the uncertainty bounds of the experimental data, however, some of the them are extreme outliers (as evidenced by the high misfit values), particularly at frequencies greater than 3 – 4 Hz. The large range in Toro misfit values is not surprising, given the greater variability exhibited over the top 40 – 60 m in the 50 Toro Vs profiles relative to the 50 inversion Vs profiles. (refer to Figures 3.6 and 3.8). In particular, the large deviation between the Toro dispersion curves and the experimental dispersion

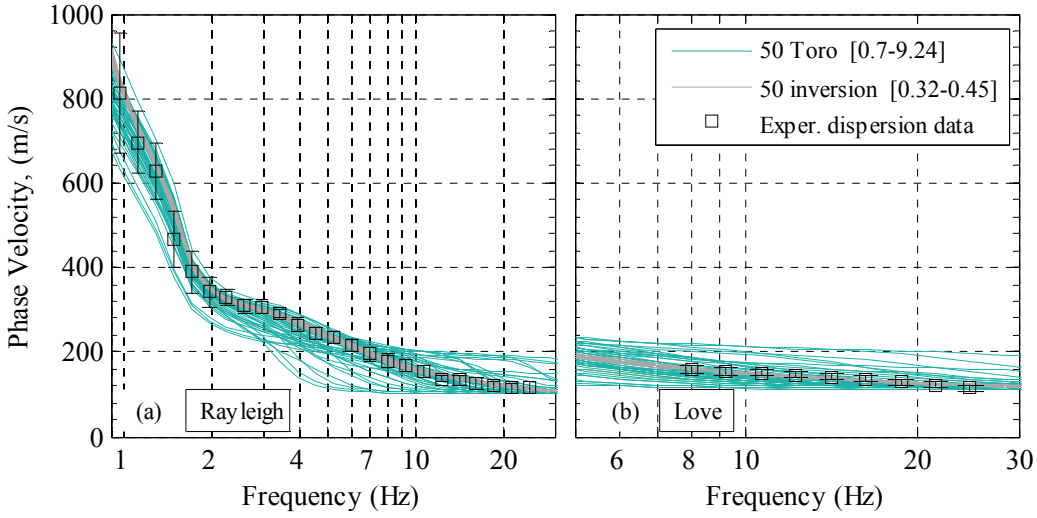

Figure 3.10. Experimental dispersion data from Mirandola and the theoretical dispersion curves from the 50 inversion Vs profiles and the 50 Toro Vs profiles for, a) Rayleigh wave and, b) Love wave data.

curves at frequencies greater than about 4 Hz is caused by the significant variability in the Toro velocity profiles within 10 m of the surface (Figure 3.8c). The thickness of the near surface layers is quite variable, with some layers as small as 1 m thick and others up to 10 m thick, and the assigned velocities are between 110 m/s and more than 200 m/s. These features are not found in the inversion profiles (Figure 3.6c) because the near surface velocities and thickness are well-constrained by the dispersion curve and its small uncertainty bounds at high frequencies. To generate a velocity profile, the Toro model generates a random set of layer thicknesses using the layering model, with no constraint on the number of layers, and then assigns velocities given the Vs randomization parameters. Monte Carlo simulations will generate realizations that are far from "average" because the unbounded statistics include these possibilities, although these realizations are less likely. Because the significant information encompassed in the dispersion data is not provided directly to the Monte Carlo simulations, but rather only the inferred statistics are provided, it is not surprising that the Toro (1995) model generates a number of velocity profiles that do not fit the dispersion data well. However,

the dispersion data could be used as a means to objectively reject unrealistic velocity profiles generated from the Toro model.

Furthermore, the Toro model produced thick near surface layers for some profiles, despite the fact that site specific layering parameters were used. This part of the Toro (1995) model could be improved to allow for better constraints on layer thickness.

To further investigate which of the 50 Toro Vs profiles provide acceptable theoretical dispersion estimates, the dispersion curves associated with the best, medium and worst misfit values from Mirandola are presented in Figure 3.11. The best, medium, and worst Toro Vs profiles were chosen by ordering the misfit values from lowest to

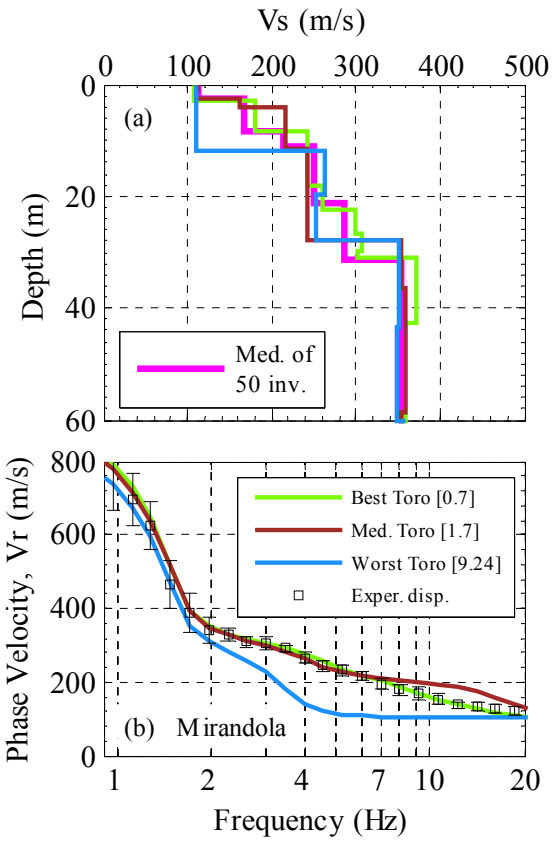

Figure 3.11. Mirandola data with, a) best, middle and worst misfit of the 50 Toro Vs profiles with b) accompanying dispersion curves and the experimental data, Grenoble data with c) best, middle and worst misfit of the 50 Toro Vs profiles with d) accompanying dispersion curves and the experimental data.

highest and then choosing the lowest (1st or best), medium (25th) and highest (50th or worst) values. The misfit value of the best Toro Vs profile (0.7) is greater than any of the misfit values corresponding to the 50 inversion Vs profiles (0.32 – 0.45). However, the best Toro Vs profile still visually fits the experimental dispersion data well and lies within the data uncertainty bounds at all frequencies. The theoretical dispersion data associated with the medium Toro Vs profile fits the dispersion data at frequencies less than 7 Hz and has a relatively high misfit value (1.7). The theoretical dispersion data associated with the worst Toro Vs profile does not match the experimental curve at frequencies greater than 2 Hz. This is the result of a soft and thick surficial layer, which appears unrealistic in light of the experimental dispersion data.

3.5. ANALYSIS OF SITE AT GRENOBLE, FRANCE

Mirandola, Italy is a fairly simple, soft, normally dispersive site without much subsurface complexity. In order to investigate a more complex site that includes velocity reversals (i.e., when an underlying layer has a lower Vs than the overlying layer), a site in Grenoble, France is considered.

The experimental Rayleigh wave dispersion curve was developed using all MASW arrays and all 2D passive-source arrays at the Grenoble site. This dispersion curve and its associated uncertainties as a function of frequency are shown in Figure 3.12. Active-source dispersion data ranged from 15 to 50 Hz. Ambient vibration HFK dispersion data was utilized at frequencies ranging from 3 to 50 Hz and MSPAC dispersion data was utilized between 0.6 and 3 Hz. Similar to Mirandola, the choice to use HFK or MSPAC processing methods over specific frequency bands was made by assessing the quality of each dispersion curve. The experimental dispersion curve flattens/decreases between approximately 3 - 15 Hz. This indicates that a low velocity layer is present at the site and/or that the experimental dispersion data is transitioning from a higher to a lower Rayleigh wave mode. Both possibilities were considered in the inversion.

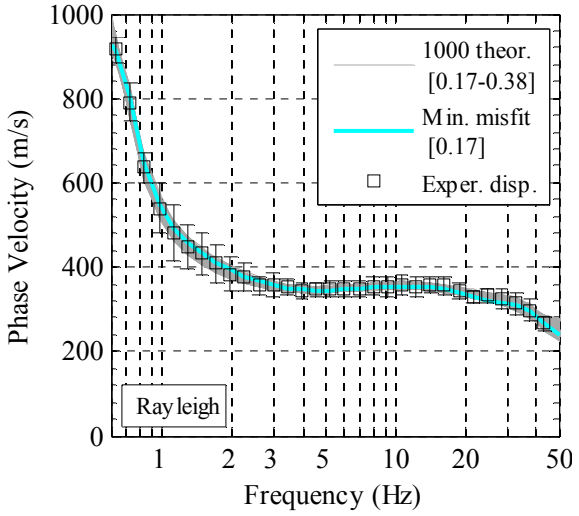

Figure 3.12. Experimental dispersion data, theoretical dispersion curves from the 1,000 lowest misfit models from the inversion, and the minimum misfit theoretical dispersion curve at Grenoble. Note that square brackets, [ ], indicate the misfit value(s).

The H/V spectrum at Grenoble exhibits weak peaks at 0.28 and 0.46 Hz. The lower frequency peak was used to constrain the theoretical Rayleigh wave ellipicity during the inversion. However, this constraint only influenced the Vs at depths ranging from 600 to 800 m, which exceeds the resolution capabilities of the largest passive-source array. Since all Vs profiles from the inversion were cut off at significantly shallower depths, this constraint had little impact on the near-surface inversion results.

The 1,000 lowest misfit models from the inversion are presented in Figure 3.12. Each of the theoretical dispersion curves lie within the measured dispersion uncertainty (+/- one standard deviation). The misfit values were re-computed outside of Geopsy and found to range from 0.17 to 0.38. All experimental dispersion data was fit with the fundamental mode. However, the influence of higher modes were investigated during the inversion and found not to produce acceptable fits to the data. In order to fit the flat/decreasing portion of the dispersion curve, a velocity reversal was investigated beginning at depths between 20 - 30 m, as shown in Figure 3.13. Compared with the

Mirandola case study, the best 1,000 Vs profiles at Grenoble visually exhibit greater variability, despite the lower misfit values.

Crosshole testing was also performed in the top 50 m at Grenoble, as shown in Figure 3.13. The 1,000 inversion Vs profiles are not able to perfectly match the abrupt, thin velocity changes measured in the crosshole data. This is not surprising considering the challenges that velocity reversals present to conventional surface wave methods (Dou and Ajo-Franklin 2014). However, it must be remembered that the Vs profiles from surface wave inversion represent average wave propagation across the extent of the receiver arrays used to record data at the site, which, in this case, varied from a minimum of approximately 50 m for the linear arrays to a maximum of over 800 m for the circular arrays. Thus, the agreement between the Vs profiles appears to be quite reasonable.

3.5.1. Simple Statistical Vs Profiles

As in the Mirandola case study presented above, a sample set of 50 randomly chosen Vs profiles at Grenoble were selected from the 1,000 lowest misfit Vs profiles determined from inversion. These 50 inversion profiles are presented in Figure 3.14. The median and σ_{lnVs} of the 1,000 and the 50 inversion Vs profiles are nearly identical at all depths, which verifies that a sample size of 50 is sufficient to represent all 1,000 Vs profiles in subsequent analyses.

The bounding-type +/- 20% Vs profiles and the 5^{th} and 95^{th} percentile Vs profiles were calculated from the statistics of the 50 inversion Vs profiles in a similar manner to the Mirandola site. These simple statistical Vs profiles are presented in Figure 3.15 along with the 50 Vs profiles from inversion and the minimum misfit Vs profile. In Figure 3.15, the Vs profiles have been terminated at depths corresponding to the first layer where a velocity of 750 m/s is exceeded. This termination criteria was selected to provide a "soft rock" reference depth for use in subsequent site response analyses (results not shown in this paper). Bedrock/half-space layers are presented in Figure 3.15 as 10-m

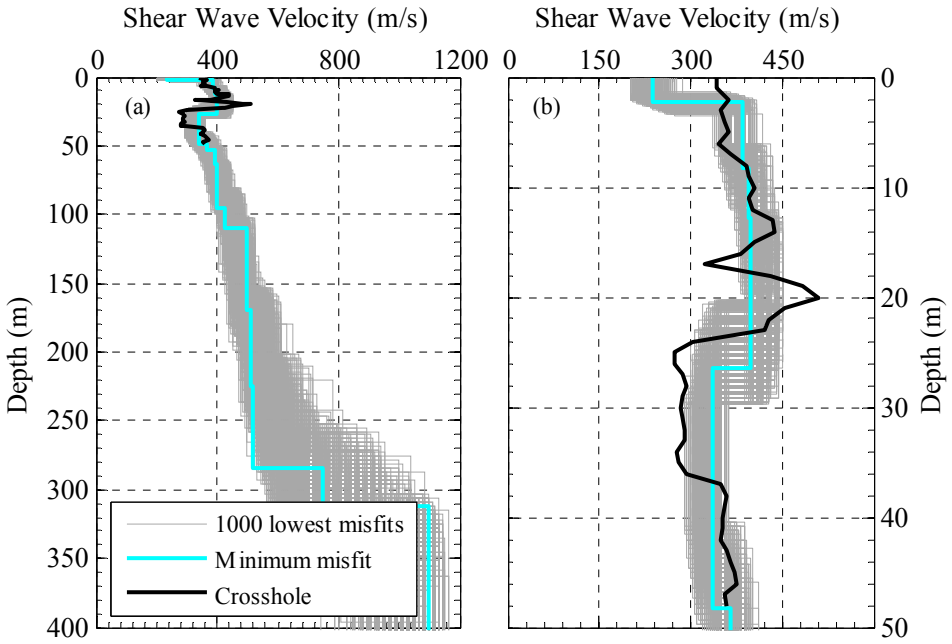

Figure 3.13. The 1,000 Vs profiles determined from the surface wave inversion procedure along with the crosshole Vs profile at Grenoble shown to depths of a) 400 m and b) 50 m.

long vertical lines. The depths to the top of the half-space for all the Vs profiles vary from about 250 to 380 m. Similar to Mirandola, the half-space depth for all profiles is significantly less than one-half of the maximum resolved wavelength from the experimental dispersion data (roughly 700 m).

3.5.2. Randomly Generated Vs Profiles

The Toro (1995) model was also used to generate 50 Vs profiles for Grenoble. The median of the 50 inversion Vs profiles was used as the baseline model, and the σ_{lnVs} values were assigned based on the 50 inversion Vs profiles. In general the σ_{lnVs} values were less than 0.1 at depths less than 250 m. The inter-layer correlation, layering model, and depth of bedrock parameters for Grenoble are presented in Table 3.2. The inter-layer correlation parameters are the same for Grenoble as Mirandola. The layering model parameters c1, c2 and c3 were determined by fitting a power function through the λ_t

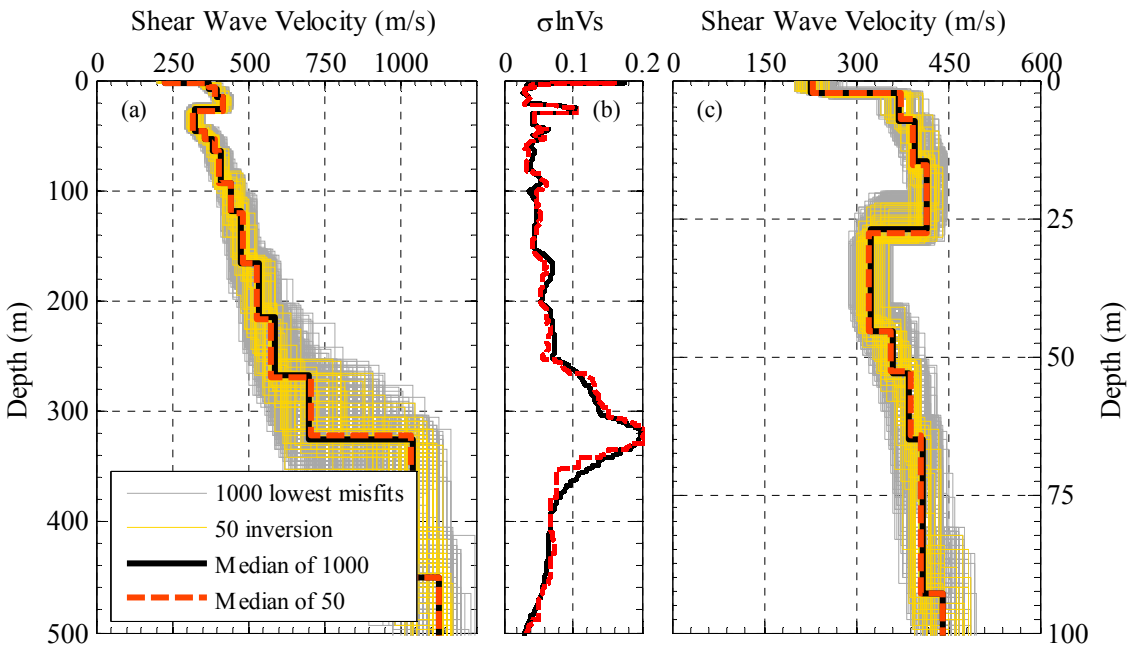

Figure 3.14. Comparisons of: a) the 1,000 lowest misfit Vs profiles from inversion with 50 randomly-selected profiles and the medians of the 1,000 and 50 profiles, b) σ_{lnVs} of the 1,000 and 50 inversion profiles, and c) zoomed view of (a) at Grenoble, France.

verses depth to the layer midpoint for the 50 inversion Vs profiles, as presented in Figure 3.16. The depth of bedrock parameters were assumed to be normally distributed, and based on the 50 inversion Vs profiles, has a mean of 320 m and a standard deviation of 26 m.

The 50 Toro Vs profiles generated for Grenoble, along with their discretized median and the median of the 50 inversion Vs profile (i.e., the baseline Vs profile used in the Toro model) are presented in Figure 3.17. At depths less than approximately 50 m, the 50 Toro Vs profiles yield σ_{lnVs} values that are nearly double the σ_{lnVs} of the 50 inversion Vs profiles, while at most other depths the σ_{lnVs} values between the 50 Toro and 50 inversion Vs profiles are similar. This greater near-surface variability in the Toro profiles was also noted for the Mirandola site and is most likely caused by significant

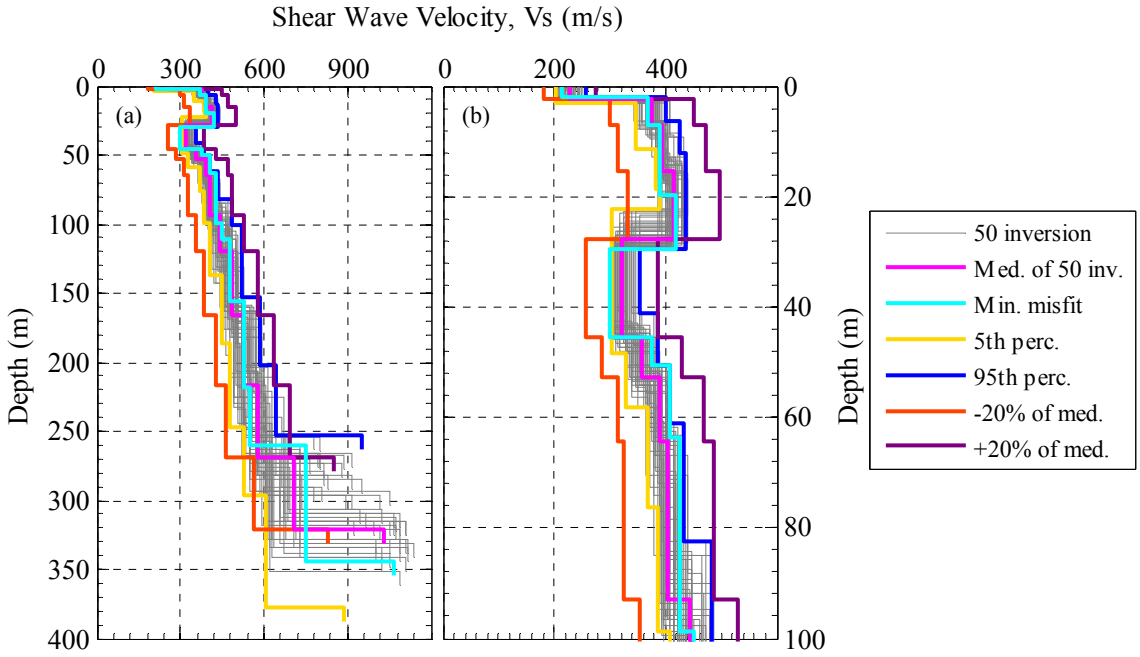

Figure 3.15. Comparison of: a) 50 inversion Vs profiles along with the median of the 50 inversion, minimum misfit, 5th, 95th,and +/-20% Vs profiles and b) zoomed view of (a), at Grenoble, France.

Table 3.2. Parameters used for the Toro (1995) randomization model for Grenoble.

Inter-layer correlation		Layering model[C]		Depth of bedrock[C]	
Δ	3.9[A]	c1	0.95	mean	320 m
d_0	0[A]	c2	10	stnd dev.	26 m
b	0.344[A]	c3	-0.62		
ρ_0	0.8[B]				
ρ_{200}	0.8[B]				

A. Toro, default assuming V_{S30} between 180-360 m/s

B. Assumed values

C. Site specific using inversion profiles

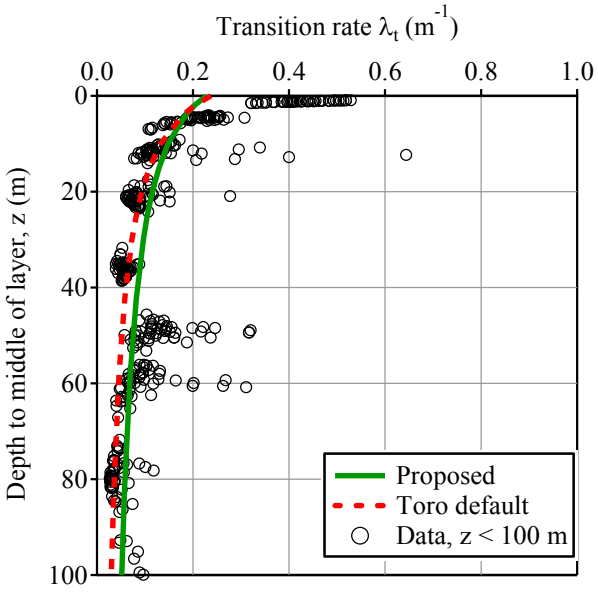

Figure 3.16. Transition rate verses layer mid depth for the 50 inversion Vs profiles at depths less than 100 m at Grenoble.

variations in the thickness of the 1st layer, despite using site-specific layering model parameters. The depth of the half-space layer in the 50 Toro Vs profiles varies between 270 m and 350 m, which is very similar to the range for the 50 inversion profiles.

3.5.3. Theoretical Dispersion Data for Vs Profiles

As with Mirandola, 106 different Vs profiles were considered at Grenoble to represent the Vs profile uncertainty. Theoretical dispersion curves were generated for each profile using the same Vp and

density assumptions described above for Mirandola. Figure 3.18 presents the experimental dispersion data measured at Grenoble along with the theoretical dispersion curves for the 50 inversion profiles and the simple-statistical profiles (Figure 3.18a) and the 50 Toro profiles (Figure 3.18b). The dispersion misfit values for all profiles are indicated in the figure legend in square brackets. The dispersion curves from the 50 inversion Vs profiles have misfit values between 0.19 - 0.33. The median of the 50 inversion Vs profiles has a misfit value of 0.27, which is within the range of the 50

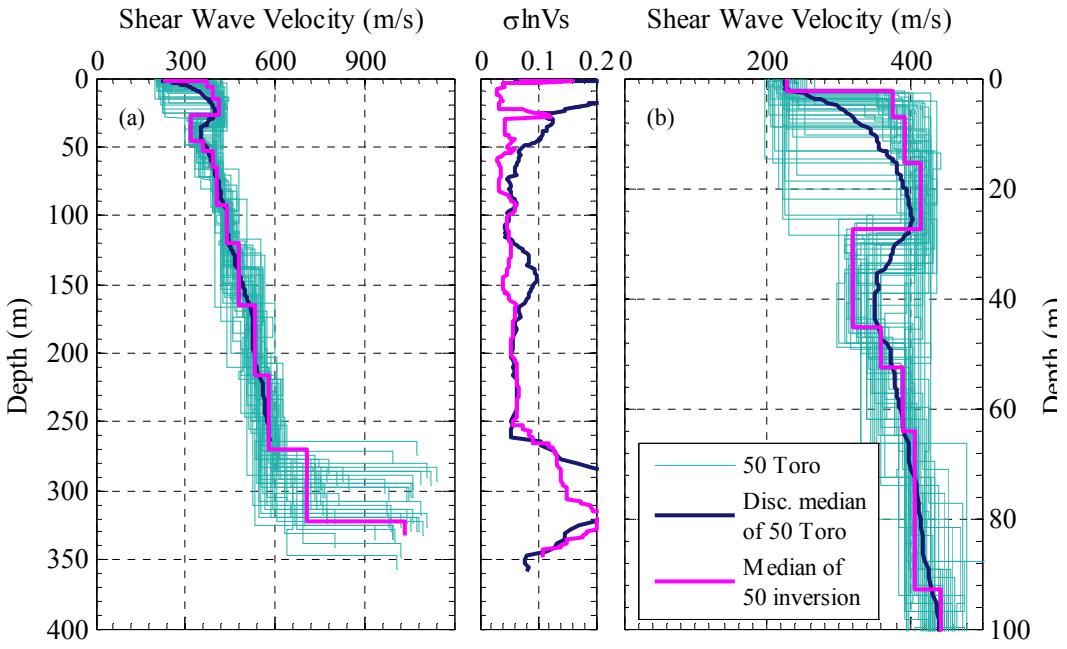

Figure 3.17. Comparisons of: a) 50 Vs profiles generated using the Toro (1995) randomization model, b) σ_{lnVs} of the 50 Toro Vs profiles, and c) zoomed view of (a) at Grenoble.

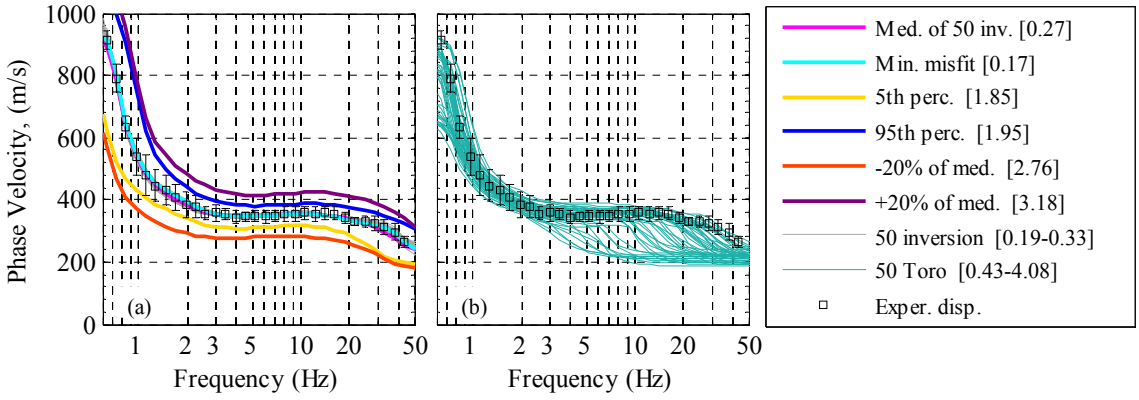

Figure 3.18. Experimental Rayleigh wave dispersion data with the a) 50 inversion, the minimum misfit, 5th, 95th and +/- 20% Vs profiles and b) 50 Toro Vs profiles at Grenoble.

inversion profiles. Like Mirandola, the median profile does not represent an actual profile resulting from the inversion, although it fits the experimental dispersion data better than a number of the profiles that came directly from the inversion. In contrast, the bounding-type 5^{th} and 95^{th} percentile Vs profiles produce theoretical dispersion curves with high misfit values of 1.85 and 1.95, respectively. These misfit values are substantially larger than any of the misfit values from the 50 inversion Vs profiles, and their theoretical dispersion curves are visibly outside of the estimated uncertainty bounds of the experimental data at nearly all frequencies. The theoretical dispersion curves associated with the -20% and +20% bounding-type Vs profiles result in even poorer fits to the experimental data, with misfit values of 3.18 and 2.76, respectively. Thus, as at Mirandola, the bounding-type Vs profiles developed from simple statistics do not result in a satisfactory fit of the experimental dispersion data and, therefore, do not appropriately capture the
experimentally-measured site signature. As such, one must question the use of such profiles to represent the subsurface stiffness of the site.

The theoretical dispersion curves associated with the 50 Toro Vs profiles are presented with the experimental dispersion data in Figure 3.18b. The misfit values for the Toro profiles range from 0.43 to 4.08. Visibly, many of the theoretical dispersion curves appear to fall within the uncertainty bounds of the experimental data, however, some of them are extreme outliers (as evidenced by the high misfit values). This is partially due to the thickness of the near surface layer, which is quite variable, ranging from 2-30 m thick with velocities between 200 - 250 m/s. Thick, soft near surface layers are evident in the dispersion curves from the low theoretical phase velocities at frequencies greater than 3 Hz. Thus, at Grenoble, a number of the randomly-generated Vs profiles developed from the Toro (1995) model do not result in a satisfactory fit to the experimental dispersion data.

The 50 Toro Vs profiles were further investigated by plotting the best, medium and worst fitting theoretical dispersion curves and corresponding Vs profiles, as shown in

Figure 3.19. The best, medium, and worst Toro Vs profiles were chosen in a similar manner to Mirandola. The best Toro Vs profile visually fit the experimental dispersion data and lies within the data uncertainty bounds at all frequencies, resulting in a satisfactory misfit value of 0.43. Conversely, the dispersion curves corresponding to the middle and worst Toro Vs profiles fail to match the experimental dispersion data at frequencies greater than 10 and 2 Hz, respectively, and below 0.9 Hz (for both profiles). The misfit values associated with the medium and worst theoretical dispersion curves are 1.5 and 4.08, respectively. Therefore, while some of the 50 Toro Vs profiles result in acceptable misfit values, many do not.

3.6. DISCUSSION AND CONCLUSIONS

Shear wave velocity profile characterization plays a critical role in site response analyses and realistic methods to account for uncertainty in Vs are needed. Efforts to robustly account for uncertainty and variability are hampered by costs associated with performing a large number of invasive tests to sufficient depths at most sites. However, the

experimental dispersion data collected from cost-effective, non-invasive surface wave techniques is robust and contains a substantial amount of information about wave propagation across a site. Thus, the experimental dispersion data is a type of site signature that can be used to help evaluate the validity of Vs profiles meant to account for epistemic uncertainty and aleatory variability. The quality of layered earth models derived from inversion of surface wave data can be quantified directly by a misfit value between the experimental and theoretical dispersion data. However, it is important to recognize that there is currently no universally-accepted way of calculating the dispersion misfit, nor is there a unique value of dispersion misfit that can be considered as "good" or "bad". For example, a misfit value of 0.9 might be "good" at one site because it visually fits the experimental data well, and/or represents the best possible fit to a complicated dataset with large dispersion variability. However, a misfit value of 0.3 might be "bad"

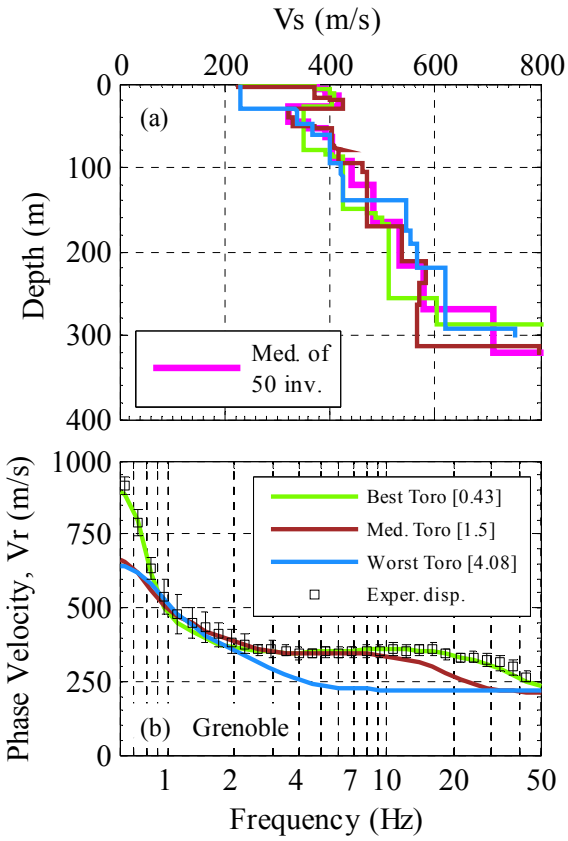

Figure 3.19. Grenoble data with a) best, middle and worst misfit of the 50 Toro Vs profiles with b) accompanying dispersion curves and the experimental data.

at another site because it does not agree with a simple dispersion dataset with small dispersion variability. Thus, misfit values from different sites cannot be compared directly with one another for a measure of the overall inversion quality from site-to-site. Nor can a universal misfit criteria be developed that allows poor layered earth models to be rejected automatically within, or across, all potential sites. Rather, the misfit values can simply be used to guide relative judgements about the quality of certain layered earth models relative to others at the same site. Hence, the discussions below are based on relative observations from the sites presented above.

At the Mirandola and Grenoble sites, the suites of Vs profiles generated directly from inversion analyses capture realistic subsurface uncertainty/variability, yet still fit the

experimental dispersion data very well. The theoretical dispersion curves associated with the median of the 50 inversion Vs profiles also fit the experimental data well at both sites. In fact, the median of the 50 inversion Vs profiles has a lower misfit than many of the profiles that came directly from the inversion analyses. Therefore, the median profile is considered as a good, simple statistical profile that can be used to reasonably represent the site stiffness. Conversely, the theoretical dispersion curves associated with the bounding-type 5^{th} and 95^{th} percentile Vs profiles and the +/- 20% Vs profiles do not fit the experimental dispersion data well at either site. As such, these Vs profiles do not appropriately capture the experimentally-measured site signature and caution should be exercised when blindly using similar bounding-type profiles to account for epistemic uncertainty. The Vs profiles derived from the Toro (1995) Vs randomization model resulted in both acceptable and unacceptable layered earth models based on dispersion misfit. Therefore, a dispersion misfit approach could be used to help select reasonable Vs profiles to account for aleatory variability at a site.

Based on the findings presented in this paper, the authors suggest several dispersion-based options for realistically accounting for Vs profile uncertainty/variability:

1) At sites where high-quality surface wave dispersion data is available, use multiple Vs profiles resulting directly from inversion in subsequent site response analyses. These profiles should all fit the experimental data and its associated uncertainties, which are inherently a combination of epistemic uncertainty and aleatory variability. If Vs randomization is still desired to further account for aleatory variability, Toro-type models or Monte Carlo simulations can be used, provided the resulting profiles are checked by comparing the theoretical dispersion curves with the experimental data. This will ensure that only profiles that fit the experimentally-measured site signature are used in subsequent analyses. Blindly using relatively stiff and soft bounding-type Vs profiles (e.g., +/- 20%) to account for epistemic uncertainty at sites where dispersion measurements are available is not appropriate and should not be done.

2) At sites where only borehole data is available, a theoretical dispersion curve could be calculated from the borehole Vs and Vp data. Realistic Uncertainty bounds could then be added to the theoretical dispersion curve in order to create a pseudo-experimental target curve. Since borehole measurements represent a point measurement and can deviate from the experimental dispersion curve obtained from surface wave methods, the uncertainty bounds may need to exceed the 5 - 10% that is often associated with surface wave data. Nonetheless, this pesuedo-experimental dispersion target curve could then form the basis for evaluating the validity of randomly generated Vs profiles meant to account for aleatory variability. If multiple boreholes are available, the data from each one could be used as a starting model for this randomization.

These are currently only suggestions for readers to consider when attempting to account for realistic Vs uncertainty in site response analyses. Additional research is needed in order to truly account for epistemic uncertainty and aleatory variability in a meaningful way. However, some current methodologies may not be appropriate and may actually result in unintended consequences when attempting to predict site response. The impact of blindly using bounding-type Vs profiles and randomly generated Vs profiles to account for uncertainty in site response is investigated in a companion paper by comparing the amplitudes and frequency contents of ground motions propagated through the Vs profiles developed in this paper.

3.7. ACKNOWLEDGMENTS

This work was supported primarily by U.S. National Science Foundation (NSF) grant CMMI-1261775. However, any opinions, findings, and conclusions or recommendations expressed in this material are those of the authors and do not necessarily reflect the views of NSF. The authors would also like to acknowledge and thank the organizing committee of the InterPacific project, which was formed under the

Research & Development Program SIGMA, funded by EDF, AEREVA, CEA, ENEL, and the CASHIMA project, funded by CEA, ILL and IITER Organization.

3.8. REFERENCES

Aki, K., (1957). "Space and time spectra of stationary stochastic waves, with special reference to microtremors". Bulletin of Earthquake Research Institute, 35, 415–457

American Association of State Highway and Transportation Officials (AASHTO). Guide Specifications for LRFD Seismic Bridge Design 2011. 2nd ed., AASHTO Washington, D.C.

American Society of Civil Engineers (ASCE). Minimum design loads for buildings and other structures, ASCE Standard ASCE/SEI 7-10, published by ASCE, Reston, Virginia.

Barani, S., Ferrari, R.D., and Ferretti, G. (2013) "Influence of Soil Modeling Uncertainties on Site Response." Earthquake Spectra, Vol. 29, No. 3, pp 705-732.

Bettig, B., Bard, P.Y., Scherbaum, F., Riepl, J., Cotton, F., Cornou, C., and Hatzfeild, D. (2001). "Analysis of dense array noise measurements using the modified spatial auto correlation method (SPAC): application to the Grenoble area." Bollettino de Geofisica Teoria e Applicata, 42(3-4), 281-304.

Bazzuro,P., and Cornell, C. (2004). "Ground Motion Amplification in Nonlinear Soil Sites with Uncertain Properties". Bulletin of the Seismological Society of America, Vol. 94, No. 6, pp. 2090 2109.

Capon, J. (1969). "High Resolution Frequency-Wavenumber Spectrum Analysis." Proceedings of the IEEE, Vol. 57, Issue 8, pp. 1408–1418.

Comina C., Foti S., Boiero D., Socco L.V. (2011). "Reliability of VS,30 Evaluation from Surface-Wave Tests." Journal of Geotechnical and Geoenvironmental Engineering, Vol. 137, pp. 579–86.

Cox, B.R., Wood, C.M. and Teague, D.P. (2014) " Synthesis of the UTexas1 Surface Wave Dataset Blind-Analysis Study: Inter-Analyst Dispersion and Shear Wave Velocity Uncertainty" Proceedings of the 2014 Geo-Congress Technical Papers, pp. 850-859.

Cornou, C., Ohrnberger, M., Boore, D.M., Kudo K., and Bard P-Y (2006). "Derivation of Structural Models from Ambient Vibration Array Tecordings: Results from an International Blind Test" In: Bard P-Y, Chaljub E, Cornou C, Cotton F, Gueguen P (eds) Third International symposium on the effects of surface geology on seismic motion, vol. 2. Grenoble, 1127–1219.

Dou, S. and Ajo-Franklin, J.B. (2014). "Full-waveform inversion of surface waves for mapping embedded low-velocity zones in permafrost." Geophysics, Vol. 79, No. 6, pp. EN107–EN124.

Dunkin J.W. (1965). "Computation of modal solutions in layered, elastic media at high frequencies." Bulletin of the Seismological Society of America, Vol. 55, pp. 335–358.

Electric Power Research Institute (EPRI) "Seismic Evaluation Guidance: Screening, Prioritization and Implementation Details (SPID) for the Resolution of Fukushima Near-Term Task Force Recommendation 2.1: Seismic" Eletric Power Research Institute, Palo Alto, CA: 2012, Report 1025287, pp. 206.

Fah, D., Stamm, G., Havenith, H.B. (2008). "Analysis of three-component ambient vibration array measurements." Geophysical Journal International, 172, 199-213.

Foti, S., Comina,C., Boiero, D., and Socco, L.V. (2009). "Non-uniqueness in surface-wave inversion and consequences on seismic site response analyses." Soil Dynamics and Earthquake Engineering, Vol. 29, pp. 982-993.

Foti, S., Lai, C., Rix, G., and Strobbia, C. (2014). "Surface Wave Methods for Near-Surface Characterization." CRC Press, Boca Raton, Florida, pp. 4.

Foti, S., Parolai, S., Albarello, D., and Picozzi, M. (2011). "Application of Surface-wave methods for seismic site characterization." Surveys in Geophysics, Vol. 32, Issue. 6, pp. 777-825.

Garofalo, F., Foti, S., Hollender, F., Bard, P.-Y., Cornou, C., Cox, B.R., Ohrnberger, M., Sicilia, D., Asten, M., Di Giulio, G., Forbriger, T., Guiller, B., Hayashi, K., Martin, A., Matsushima, S., Mercerat, D., Poggi, V., Yamanaka, H. (2016). "InterPACIFIC Project: Comparison of Invasive and Non-Invasive Methods for Seismic Site Characterization Part I: Intra-Comparison of Surface Wave Methods," Soil Dynamics and Earthquake Engineering, (submitted).

Garofalo, F., Foti, S., Hollender, F., Bard, P.-Y., Cornou, C., Cox, B.R., Dechamp, A., Ohrnberger, M., Sicilia, D., Vergniault, C. (2016). "InterPACIFIC Project: Comparison of Invasive and Non-Invasive Methods for Seismic Site Characterization Part II: Inter-Comparison Between Surface Wave and Borehole Methods," Soil Dynamics and Earthquake Engineering, (submitted).

Haskell, N. A. (1953). "The dispersion of surface waves on multilayered media." Bulletin of Seismological Society of America, Vol. 43, pp. 17–34.

Herrmann, R. B. (1987). "Surface wave inversion. Computer program in seismology." Vol. 4, Saint Louis University.

Hobiger, M., Le Bihan, N., Cornou, C., and Bard, P.Y. (2012). "Multicomponent Signal Processing for Rayleigh Wave Ellipicity Estimation." IEEE Signal Processing Magazine, pp. 29–39.

Kottke, A., and Rathje, E. (2009). "Technical Manual for Strata." Report No. 2008/10, Pacific Earthquake Engineering Research Center, Berkeley, California.

Knopoff L. (1964). "A matrix method for elastic wave problems." Bulletin of the Seismological Society of America, Vol. 54, pp. 431–438.

Kramer, S. (1996). "Geotechnical Earthquake Engineering," Prentice Hall, Upper Saddle River, New Jersey, pp. 653.

Lai, C. G. (1998). "Simultaneous Inversion of Rayleigh Phase Velocity and Attenuation for Near-Surface Site Characterization." Ph.D. Dissertation, School of Civil and Environmental Engineering, Georgia Institute of Technology, Atlanta, GA.

Maraschini, M. and Foti, S. (2010). "A Monte Carlo multimodal inversion of surface waves." Geophysical Journal International, Vol. 182(3), pp. 1557-1566.

Matasovic, N., and Hashash, Y. (2012) "NCHRP Synthesis 428: Practices and Procedures for Site-Specific Evaluations of Earthquake Ground Motions, A Synthesis of Highway Practice." National Cooperative Highway Research Program of the Transportation Research Board, Washington, D.C.

Molnar, S., Dosso, S. E., & Cassidy, J. F. (2010). "Bayesian inversion of microtremor array dispersion data in southwestern British Columbia." Geophysical Journal International, Vol. 183(2), pp. 923-940.

Park, C., Xia, J., and Miller, R. (1998). "Imaging dispersion curves of surface waves on multi-channel record." 68th Annual International Meeting of the Society of Exploration Geophysicists, Expanded Abstracts, pp. 1377-1380.

Poggi, V. and Fah, D. (2010). “Estimating Rayleigh wave particle motions from three-component array analysis of ambient vibrations.” Geophysical Journal International, Vol. 180, pp. 251-267.

Rathje, E.M., Kottke, A.R., and Trent, W.L. (2010). “Influence of Input Motion and Site Property Variabilities on Seismic Site Response Analysis.” Journal of Geotechnical and Geoenvironmental engineering, Vol. 136, No. 4, pp 607-619.

Rix, G.J., Hebeler, G.L., and Orozco, M.C. (2002). “Near-surface Vs Profiling in the New Madrid Seismic Zone Using Surface-save Methods”. Seismological Research Letters, Vol., 73, No., 3, pp. 380-392.

Rodriguez-Marek, A., Rathje, E.M., Bommer, J.J., Scherbaum, F., and Stafford, P.J. (2014). “Application of Single-Station Sigma and Site-Response Characterization in a Probabilistic Seismic-Hazard Analysis for a New Nuclear Site”. Bulletin of the Seismological Society of America, Vol. 104, No. 4.

Rothman, D. (1985). “Nonlinear inversion, statistical mechanics, and residual statics estimation.” Geophysics, Vol. 50, No. 12, pp. 2784-2796.

Socco, L. V. and D. Boiero. (2008). “Improved Monte Carlo inversion of surface wave data”. Geophysical Prospecting, 56, 357-371.

Socco., L., Foti, S., and Boiero, D. (2010). “Surface-wave analysis for building near-surface velocity models – Established approaches and new perspectives.” Geophysics, Vol. 75, No. 5, pp. 75A83-75A102.

Stokoe, K. H., II, Wright, S. G., Bay, J. A., and Roësset, J. M. (1994). "Characterization of geotechnical sites by SASW method." Geophysical Characterization of Sites, ed. R. D.Woods, Oxford & IBH Pub. Co., New Delhi, India, 15-25.

Thomson, W. T. (1950). “Transmission of elastic waves through a stratified solid medium.” Journal of Applied Physics, Vol. 21, pp. 89–93.

Toro, G. (1995) “Probabilistic models of the site velocity profiles for generic and site-specific ground-motion amplification studies.” Technical Report No. 779574, Brookhaven National Laboratory, Upton, N.Y. pp. 147.

Wathelet, M. (2005). “Array recordings of ambient vibrations”. Ph.D. thesis, The University of Leige, Leige, Wallonia, Belguim. pp. 144.

Wathelet, M. (2008). An improved neighborhood algorithm: parameter conditions and dynamic scaling. Geophysical Research Letters, Vol. 35, L09301.

Wood, C.M., Cox, B.R. (2012). “A Comparison of MASW Dispersion Uncertainty and Bias for Impact and Harmonic Sources,” ASCE Geo-Congress 2012: State of the Art and Practice in Geotechnical Engineering, Oakland, CA, 25-29 March 2012.

Wood, C.M., Ellis, T.B., Teague, D.P. and Cox, B.R. (2014). “Comprehensive Analysis of the UTexas1 Surface Wave Dataset Analyst I” https://nees.org/resources/13130, pp. 10.

Xia, J., R. D. Miller, and C. B. Park, (1999). Estimation of near-surface shear-wave velocity by inversion of Rayleigh waves, Geophysics, Vol. 64, No. 3, pp. 691-700.

Yamanaka, H. and H. Ishida (1996). “Application of generic algorithms to an inversion of surface-wave dispersion data.” Bulletin of Earthquake Engineering Vol. 86, No. 2, pp. 436–444.

Zywicki, D.J. (1999). Advanced signal processing methods applied to engineering analysis of seismic surface waves. Ph.D. Dissertation, School of Civil and Environmental Engineering, Georgia Institute of Technology, Atlanta, GA.

Chapter 4:

Mapping Dispersion Misfit and Uncertainty in Vs Profiles to Variability in Site Response Estimates

Shawn C. Griffiths [a], Brady R. Cox [a]*, Ellen M. Rathje [a], David P. Teague[a]

[a] Department of Civil, Architectural and Environmental Engineering, The University of Texas, 301 E Dean Keeton Stop C1792, Austin, TX, USA 78712
* Corresponding author. Tel.: 512 471 9162, *Email address:* brcox@utexas.edu

Abstract

Uncertainty in site response analyses can be attributed to a number of parameters, including, analysis methods, input ground motions, nonlinear dynamic soil properties, and shear wave velocity profiles. In this paper, several approaches commonly used to account for shear wave velocity (Vs) uncertainty in site response are investigated. Specifically, the Vs profiles considered are categorized into three groups: (1) Vs profiles determined directly from surface wave inversion, (2) simple statistical Vs profiles derived indirectly from the surface wave Vs profiles (including bounding-type, median, and other percentile Vs profiles), and (3) statistically-based, randomly-generated Vs profiles. A companion paper (Griffiths et al. 2015) discusses the development of these Vs profiles for two international blind-study sites and quantitatively evaluates the ability of each approach to realistically represent Vs uncertainty using the experimentally-measured surface wave dispersion data as a reference. Many of the Vs profiles generated statistically to account for Vs uncertainty were shown to have high dispersion misfit values. Meaning, they did not appropriately reflect the experimentally-measured site signature that indicates key characteristics of subsurface stiffness and wave propagation. In this paper, the effects of using each approach to account for Vs uncertainty in site response are investigated by linking the dispersion misfit values for each Vs profile to variability in equivalent linear site response estimates. Clear trends exist between variability in site response estimates and dispersion misfit values at both sites. Thus, the

experimental dispersion data can be used to help select suites of Vs profiles, generated either directly from inversion or through a randomization model, that account for uncertainty in a meaningful way without including unrealistic statistical profiles that result in too much site response variability.

4.1. INTRODUCTION

Uncertainty in site response analyses can be attributed to a number of parameters, including, analysis methods, input ground motions, nonlinear dynamic soil properties, and shear wave velocity profiles (Idriss 2004). Site response simulations using equivalent linear and nonlinear analyses have shown that the shear wave velocity (Vs) profile has a large influence on the amplitude and frequency content of predicted surface ground motions (e.g., Bazurro and Cornell 2004, Rathje et al. 2010, Barani et al. 2013). Hence, the development of appropriate Vs profiles for use in site response analyses is of paramount importance. Standard engineering design codes stress the importance of accounting for uncertainty in Vs when performing site-specific site response analyses (e.g., ASCE 2010, AASHTO 2011), yet no firm guidelines are provided regarding how to appropriately account for these uncertainties.

In a companion paper (Griffiths et al. 2015), the validity of a number of different methods that can be used to account for epistemic uncertainty and aleatory variability in Vs were quantitatively evaluated using a surface wave dispersion approach at two international blind-study sites. The two sites considered (Mirandola, Italy and Grenoble, France) were investigated as part of the Interpacific (Intercomparison of methods for site parameter and velocity profile characterization) project (Garafalo et al. 2016a and Garafalo et al. 2016b). The Vs profiles developed for each site by the authors of this paper can be categorized into three groups: (1) Vs profiles determined directly from surface wave inversion, (2) simple statistical Vs profiles derived indirectly from the surface wave Vs profiles (including bounding-type, median, and other percentile Vs profiles), and (3) statistically-based, randomly-generated Vs profiles developed using the

procedure proposed by Toro (1995). The Vs profiles developed for each site are shown in Figure 4.1 and include: 50 Vs profiles randomly selected from the 1000 "best" (i.e., lowest dispersion misfit) layered earth models obtained directly from inversion of surface wave data (referred to as the 50 Inversion profiles), the minimum misfit Vs profile obtained directly from inversion, the median Vs profile statistically derived from the 50 Inversion Vs profiles, the 5^{th} and 95^{th} percentile Vs profiles statistically derived from the 50 Inversion Vs profiles, the median +/- 20% Vs profiles, and 50 Vs profiles determined using the Toro (1995) randomization procedure (referred to as the 50 Toro profiles).

The dispersion misfit values (Wathelet 2005) between the experimentally measured dispersion data at each site and the theoretically calculated dispersion curves based on each Vs profile are provided in Table 4.1. Griffiths et al. (2015) concluded that the 50 Inversion Vs profiles at each site had low dispersion misfit values that matched the experimental dispersion data well and could be considered as viable options for realistically quantifying Vs uncertainty. The minimum misfit profile and the median Vs profile also provided low misfit values and matched the experimental dispersion data. The bounding-type Vs profiles developed from simple statistics (i.e., +/- 20% and 5^{th} and 95^{th} percentile Vs profiles) had high misfit values that did not match the experimental dispersion data well. As such, the use of such profiles to represent uncertainty in the subsurface stiffness characteristics was questioned. On the other hand, the 50 randomly-generated Toro Vs profiles were found to consist of some profiles that matched the experimental dispersion data well, reflected by the relatively lower misfit values ($< \sim 1.0$), and some profiles that poorly-matched the experimental data, reflected by high misfit values. In this paper, the effects of using each approach to account for Vs uncertainty in site response analyses are investigated by linking the dispersion misfit values for each Vs profile to variability in equivalent linear site response estimates.

Several previous research studies have focused on evaluating similarities and differences in site response estimates derived from suites of acceptable Vs profiles

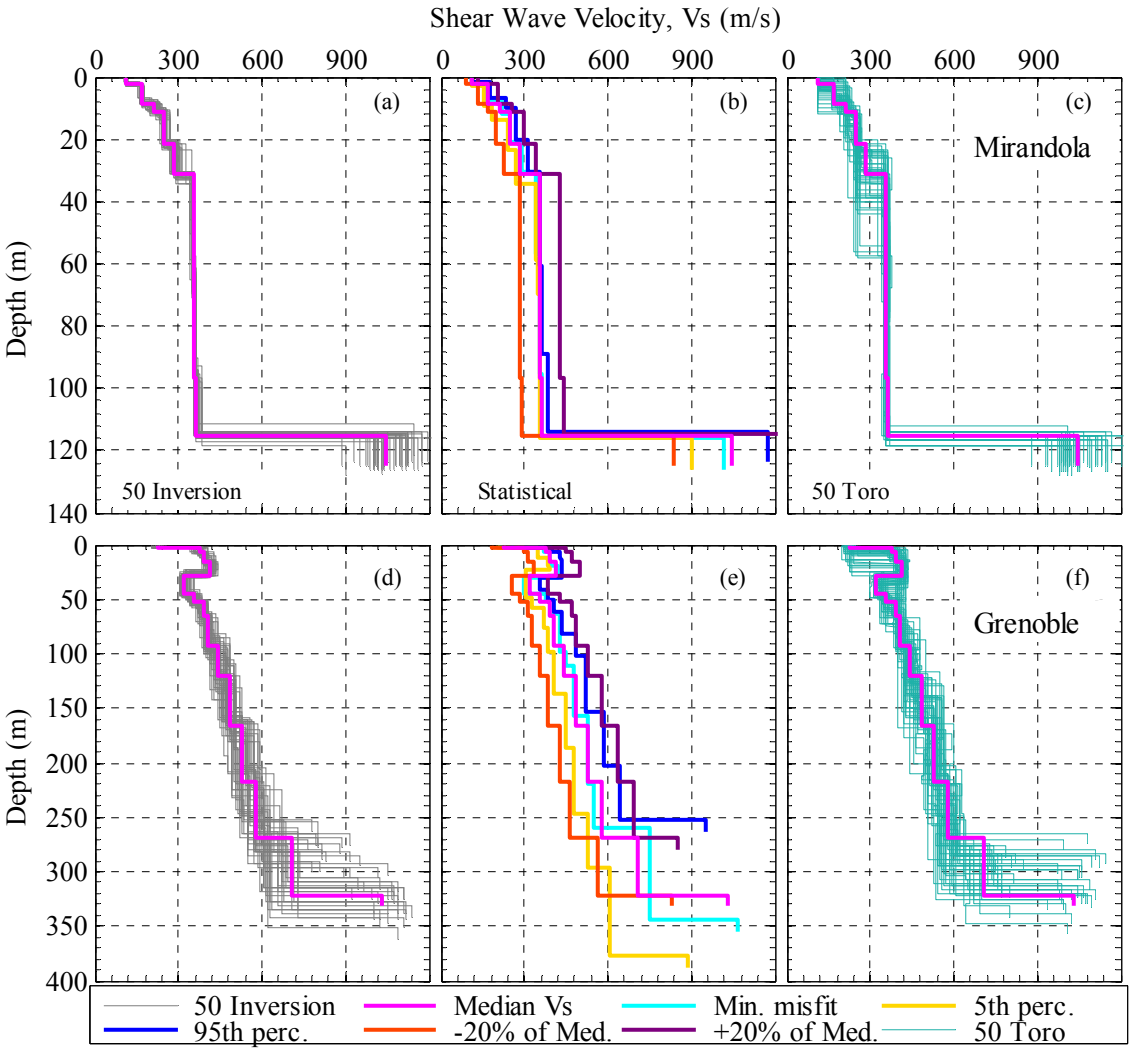

Figure 4.1. Suites of Vs profiles considered to represent the Vs uncertainty at Mirandola, Italy (top) and Grenoble, France (bottom).

Table 4.1. Dispersion misfit values for the Suites of Vs profiles at Mirandola and Grenoble

	50 Inversion	Median Vs/ Min. misfit	5th perc./ 95th perc.	-20% of Med. / +20% of Med.	50 Toro
Mirandola	0.32 - 0.45	0.35 / 0.29	2.41 / 1.96	5.66 / 3.38	0.7 - 9.24
Grenoble	0.19 - 0.33	0.27 / 0.17	1.85 / 1.95	2.76 / 3.18	0.43 - 4.08

determined from surface wave testing (e.g., Foti et al. 2009, Boaga et al. 2011, Jakka et al. 2014a). These studies have attempted to link uncertainty in Vs profiles to variability in site amplification. Findings from these studies have been somewhat conflicting. For example, Foti et al. (2009) found that when Vs profiles are equivalent with respect to Rayleigh wave dispersion (i.e., similar dispersion misfit values) they are also equivalent with respect to site amplification. However, Boaga et al. (2011) and Jakka et al. (2014a) found that profiles judged to be similar with respect to dispersion can, in some cases, be quite variable with respect to site amplification. Several follow-up discussions have resulted between these differing schools of thought (e.g., Comina and Foti 2014, Jakka et al. 2014b, Boaga et al. 2012, Socco et al. 2012), but no consensus has been reached. Regardless, we believe Vs profiles that fit the experimentally-measured dispersion data (i.e., the site signature) represent viable Vs profiles that can be used to help quantify Vs uncertainty in a meaningful way. Whether or not these Vs profiles produce similar or different site response estimates is less meaningful, so long as the variability (or lack thereof) is realistic. However, Vs profiles that do not fit the experimentally-measured site signature may not be appropriate for quantifying variability in site amplification in a meaningful way.

4.2. EQUIVALENT LINEAR SITE RESPONSE ANALYSES

The Vs profiles determined from surface wave inversion at Mirandola (Figure 4.1a) are normally dispersive (i.e., consistently increasing velocity with depth) and indicate that the bedrock depth ranges between approximately 110 and 120 m. The Vs of the rock varies from approximately 830 to 1,260 m/s, resulting in impedance ratios at the bedrock interface that vary between approximately 2.7 and 4.2. The Vs profiles determined from surface wave inversion at Grenoble (Figure 4.1d) exhibit a low velocity layer in the top 50 m, below which the Vs increases consistently with depth. The Vs profiles at Grenoble extend considerably deeper than those at Mirandola and do not reach a consistent, strong impedance contrast delineating bedrock. As such, for the site

response analyses, the Vs profiles were truncated at the first layer which exceeded 750 m/s. This termination criterion was selected to provide a consistent "soft rock" reference for use in subsequent site response analyses, resulting in half-space velocities ranging from just over 760 m/s to nearly 1100 m/s and depths ranging from about 250 m to 375 m.

The linear elastic and equivalent-linear (EQL) site response analyses were performed using a Matlab script developed at the University of Texas at Austin (George Zalachoris, personal communication, 2014). The script was modified to run analyses in a double batch mode were analyses looped through multiple Vs profiles and several input ground motions. The Matlab code included auto-discretization of the layered earth model, which subdivided the major layers into sub-layers so that numerical filtering below 50 Hz would not be problematic. The Matlab script was verified by comparing the predicted amplification factors and pseudo-acceleration response spectra with those computed using DEEPSOIL v5.1 (Hashash et al. 2012). The two programs yielded nearly identical response spectra and amplification factors for the soil models considered.

The nonlinear shear stress-shear strain soil response was modeled using the modulus reduction (G/G_{max}) and damping (D) relationship developed by Darendeli (2001). This relationship was used to assign the G/G_{max} and D curves for every sub-layer, which varied as a function of depth/confining pressure. No attempt was made to vary dynamic soil properties based on the exact soil type (i.e., clay vs. sand vs. gravel) for each layer. Rather, the cohesionless soil model (i.e., PI = 0) was used in the Darendeli (2001) relationship for all layers. While this is clearly a simplification of the true subsurface conditions at each site, this simplification is justified in the present research because the focus is on quantifying similarities and differences in site response due to uncertainties associated with the Vs profiles, not the nonlinear soil properties. Meaning, absolute/true site response estimates for each site are not important to the current study, while relative similarities/differences based on Vs are.

The importance of selecting and appropriately scaling input ground motions for site response analyses has been well documented (Bazzurro and Cornell 2004, De Luca et al. 2009, Rathje et al. 2010, Barani et al. 2013). However, once again, this issue is most important for studies that are focused on back-analyses aimed at replicating a measured surface response, or forward-analyses used for design purposes at a particular site, which is not the case for this study. Nonetheless, it is important to select input ground motions that reflect appropriate bedrock conditions and frequency content. Thus, a target spectrum for the selection of input motions was determined from the ground motion prediction equation of Boore and Atkinson (2008), assuming; a magnitude (Mw) 7.5 earthquake, a Joyner-Boore distance of 15 km, and an average Vs in the top 30 m (Vs_{30}) of 750 m/s. This target spectrum is shown in Figure 4.2.

The PEER (2011) strong motion database was used to develop a library of 80 time histories recorded at sites with Vs_{30} between 500 m/s and 1500 m/s, distances between 5 km and 80 km, and Mw between 7.0 and 8.0. Using the library of 80 motions, the computer program SigmaSpectra (Kottke and Rathje 2008, Kottke and Rathje 2013) was used to select and scale eight time histories that, on average, reasonably matched the shape of the target response spectrum (Figure 4.2). To investigate how different input motion intensities affect the nonlinear response of the Vs profiles, the eight input time histories were each scaled to peak ground accelerations (PGA) of 0.1 and 0.5 g. It should also be noted that eight additional input ground motions were selected to fit a target spectrum for a Mw = 6.0 event in order to investigate the impact of frequency content on the site response estimates. However, only results using the Mw = 7.5 ground motions scaled to a PGA of 0.5 g are provided below, because the results for other scenarios had similar trends.

4.3. INFLUENCE OF VS PROFILES ON SITE RESPONSE RESULTS

To isolate the effects of the Vs profiles and minimize the effects of the input motion variability on site response results, a median acceleration response spectrum is

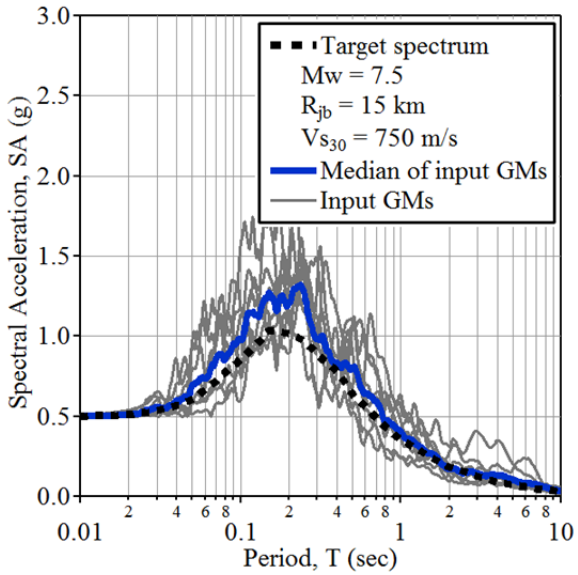

Figure 4.2. Eight input time histories representing a Mw 7.5 earthquake scaled to a PGA of 0.5 g along with the target spectrum and the median of the eight input time histories.

calculated for each Vs profile using the individual response spectra resulting from the eight input time histories, as shown in Figure 4.3a. A reference response spectrum (Reference SA) was determined by computing the median of the 50 median response spectra associated with the 50 Inversion Vs profiles (i.e., a median of medians), as shown in Figure 4.3b. It is important to point out that the Reference SA in Figure 4.3b is not associated with a specific Vs profile. Rather, it is the median of the site response results obtained from all 50 Vs profiles determined directly from surface wave inversion. This response estimate is used as a reference to compare the response spectra obtained from other statistical Vs profiles at a given site. The Reference SA should not be confused with the response spectrum obtained from the Median Vs profile that was determined statistically from the 50 Inversion Vs profiles.

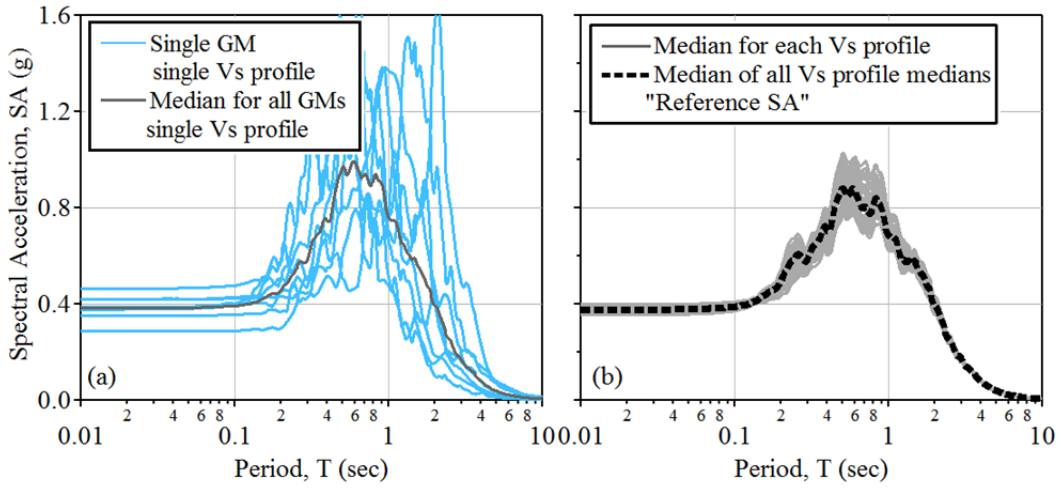

Figure 4.3. Schematic showing (a) the median surface response spectrum for a single Vs profile obtained from eight input ground motions, and (b) the Reference SA calculated from the median response spectrum from each of the 50 Inversion Vs profiles.

4.3.1 Linear Elastic Response

Linear elastic analyses do not incorporate the effects of soil nonlinearity on the predicted surface response, and thus offer insights into differences in surface response due only to variations in the Vs profiles. Figure 4.4 presents the linear elastic acceleration response spectra (SA) and amplification factors (AF $=SA_{surface}/SA_{rock}$) at Mirandola using the Mw 7.5 input motions scaled to a PGA of 0.5 g. Included in each panel of Figure 4.4 for comparison purposes is the Reference SA, or Reference AF, determined from the 50 Inversion Vs profiles, as described above.

Figures 4.4 a, b, and c present the response spectra associated with all of the Vs profiles at the Mirandola site, while Figures 4.4 d, e, and f present the AF for each of the Vs profiles. It is readily apparent that the response spectra and amplification factors for the 50 Inversion Vs profiles exhibit much less variability than those for the 50 Toro Vs profiles at all periods less than 1.0 second. This is not surprising given the much larger range of dispersion misfit values for the 50 Toro profiles (refer to Table 4.1). To more

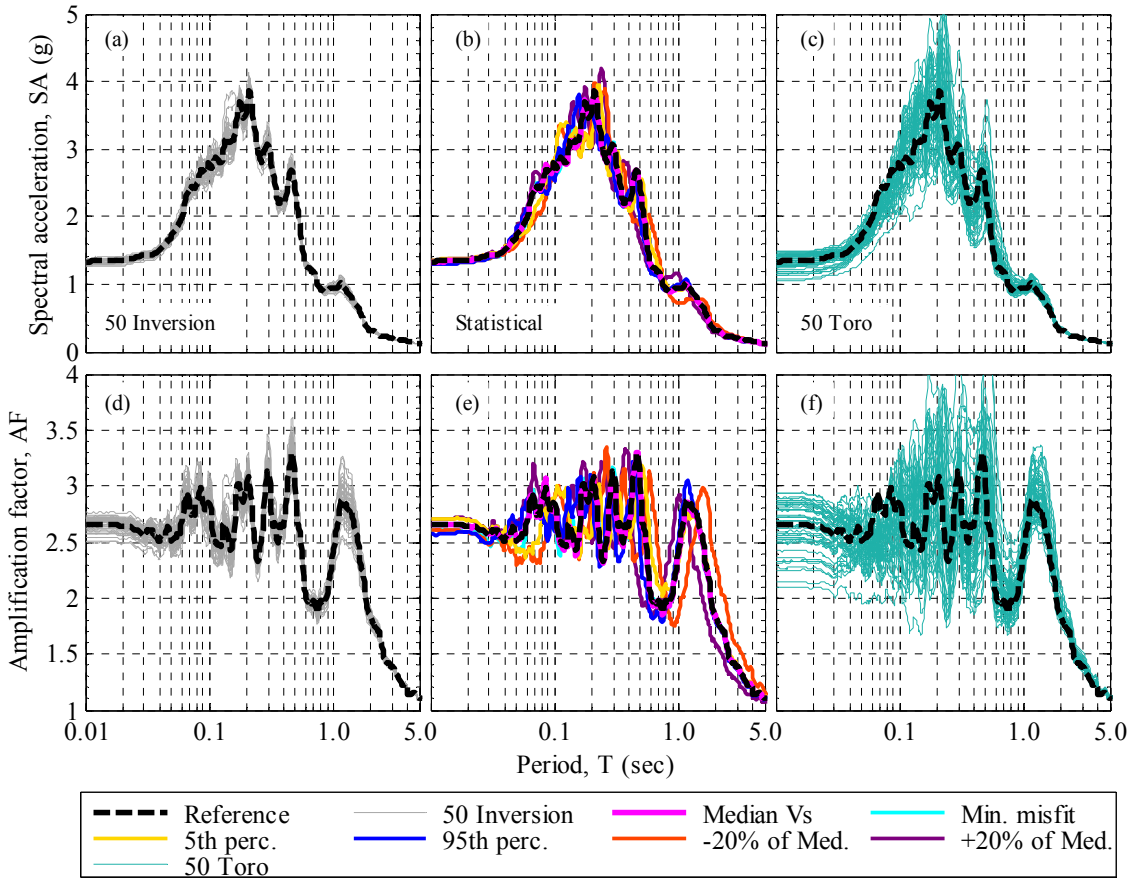

Figure 4.4. Linear elastic response spectra (top) and amplification factors (bottom) for each Vs profile at Mirandola.

quantitatively compare the site response results obtained from different Vs profiles, the following parameters are considered: the maximum spectral acceleration (SA_{max}), the predominant period (T_P), defined as the period associated with SA_{max}, the AF at the fundamental site period (AF_0), and the fundamental site period (T_0).

At Mirandola, the SA_{max} values from the 50 Inversion Vs profiles and the simple statistical Vs profiles range from approximately 3.6 to 4.2 g, while the SA_{max} values from the 50 Toro Vs profiles are more variable, ranging from approximately 3.0 - 5.1 g. The T_P values of the response spectra from the 50 Toro profiles are similar to the T_P values

from the simple statistical profiles, with only minor variability, ranging from approximately 0.15 to 0.25 sec. The T_P

values from the 50 Inversion profiles show almost no variability, at just over 0.2 sec. The small variability in T_P for all of these Vs profiles are a result of modeling the soil as linear-elastic, in which case the peak in the surface response spectrum occurs at a similar period to the input ground motion response spectrum (or in this case the median of the eight input response spectra, refer to Figure 4.2). The AF_0 values at Mirandola are quite similar for the 50 Inversion Vs profiles and the 50 Toro profiles, ranging from about 2.6 - 3.3. The AF_0 values for the statistical profiles only range from approximately 2.9 – 3.1. However, the T_0 values for the statistical profiles range from 1.0 to 1.6 sec, driven by the +/- 20% Vs profiles, respectively. This range of T_0 values is significantly greater than that exhibited by the 50 Toro profiles, which only vary from 1.2 - 1.4 sec, and the 50 Inversion profiles, which all have at T_0 of approximately 1.2 sec.

Figures 4.5 presents the linear elastic response spectra and amplification factors associated with all of the Vs profiles at the Grenoble site. Similar to the results for Mirandola, the SA and AF values for the 50 Inversion Vs profiles exhibit much less variability than those for the 50 Toro Vs profiles, reflecting well the trends observed in the dispersion misfit values. While the simple statistical profiles appear to have less variability with respect to SA, there is clearly more variability when viewed in terms of AF. Specifically, the relatively stiffer statistical Vs profiles (i.e., +20% and 95th percentile) yield noticeably smaller T_0 values (approximately 1.5 sec), while the softer Vs profiles (i.e., -20% and 5th percentile) yield noticeably larger T_0 values (approximately 2.7 sec). This significant variation in T_0 values from the bounding-type statistical profiles was also noted at Mirandola, however, the relative range between the smallest and largest AF_0 values is greater at Grenoble than Mirandola. Interestingly, at period less than 1.0 sec, many of the SA and AF values from the 50 Toro profiles are greater (consistently biased higher) than the Reference values. After scrutinizing these results, it was found that the Toro Vs profiles that have the largest SA_{max} values also have a soft surface layer that is between approximately 8 - 20 m thick. The linear elastic transfer functions for these profiles (not shown) have large amplitudes

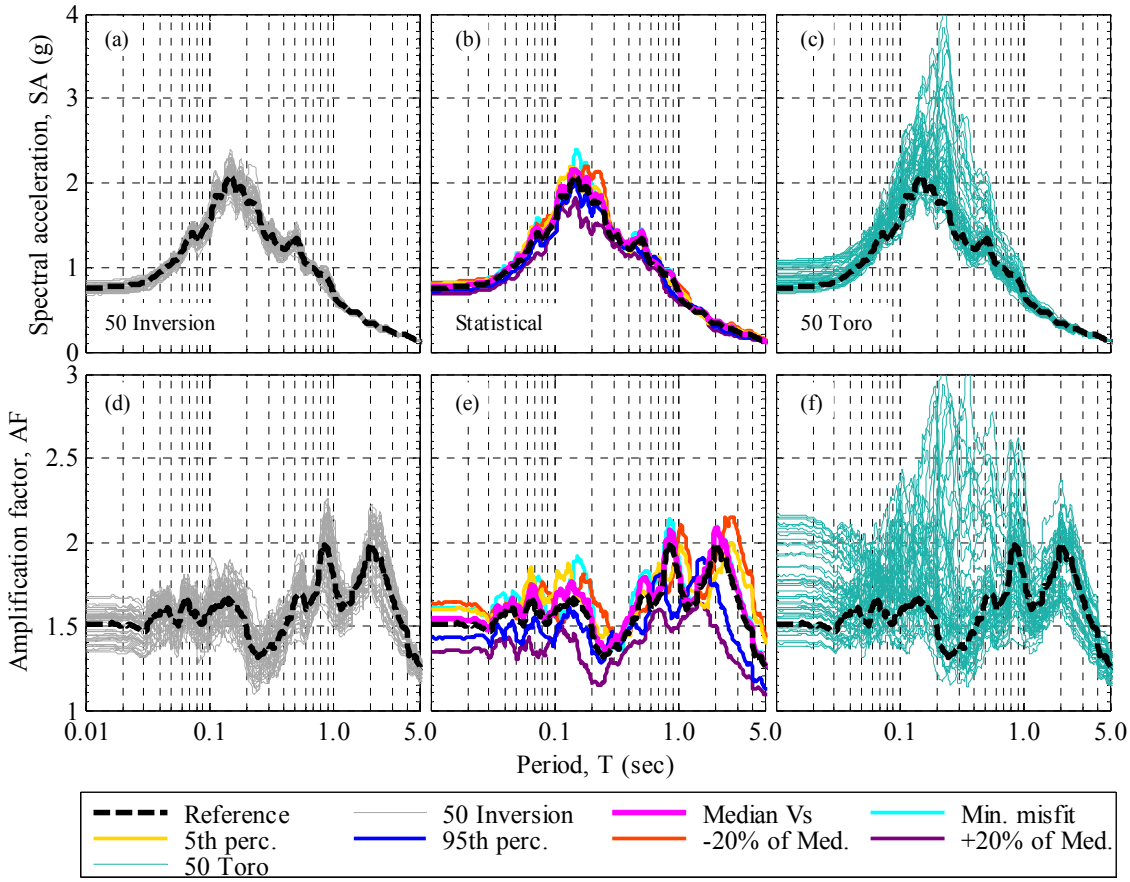

Figure 4.5. Linear elastic response spectra (top) and amplification factors (bottom) for each Vs profile at Grenoble.

(2 - 4) in the period range between 0.1 - 0.3 seconds, which is the same period range of the largest spectral accelerations in the input ground motions. Although, thick, soft surface layers present in the 50 Toro Vs profiles were generally noted by Griffiths et al. (2015) as the primary cause for high dispersion misfit values, only the Vs profiles with soft surface layers between approximately 8-20 m thick (not necessarily the thickest layers, which caused the worst dispersion misfit values) were found to yield the greatest linear elastic SA and AF values for Grenoble. Additional links between dispersion misfit values and site response estimates are discussed in more detail later in the paper.

Linear elastic analyses performed at Mirandola and Grenoble revealed that, for both sites, the variability in the SA and AF values for the 50 Toro profiles was significantly greater than for the 50 Inversion profiles. Also, in general, the bounding-type Vs profiles (i.e., +/- 20% and 5^{th} and 95^{th} percentile profiles) exhibited significantly greater variability in terms of AF than the 50 Inversion profiles.

4.3.2 Equivalent Linear Response

The equivalent linear (EQL) SA and AF values for Mirandola are presented in Figure 4.6. Due to the effects of soil nonlinearity and high-intensity input ground motions, the EQL SA values are much less than the linear elastic SA values presented in Figure 4.4. Once again, the variability in the SA and AF values associated with the 50 Toro Vs profiles is quite a bit greater than the variability from the 50 Inversion profiles. However, while the simple statistical profiles showed minor variability in terms of SA for the linear elastic case, they show significant variability in terms of SA for the EQL analyses. Specifically, the stiffer +20% profile exhibits a much shorter T_P and higher SA_{max} (by a factor of two or more) than the softer -20% profile. This is the result of lower strain levels/less non-linear behavior in the stiffer Vs profiles, thus resulting in higher transfer of seismic energy to the ground surface. In terms of AF, the 50 Inversion Vs profiles all yield very similar results, with T_0 ranging only from 2.0 – 2.2 and AF_0 ranging from 2.75 – 3.15. The simple statistical profiles and 50 Toro profiles exhibit much greater variability in terms of T_0 and AF_0. Furthermore, at periods less than 2.0 sec, the SA and AF for most of the 50 Toro profiles are significantly less than the Reference values. This is caused by the soft, thick, surface layers present in many of the Toro profiles, which result in higher shear strains, greater damping, and period elongation. Once again, these near-surface layers were identified by Griffiths et al. (2015) as significant contributors to the poor dispersion misfit in some of the Toro models for the Mirandola site.

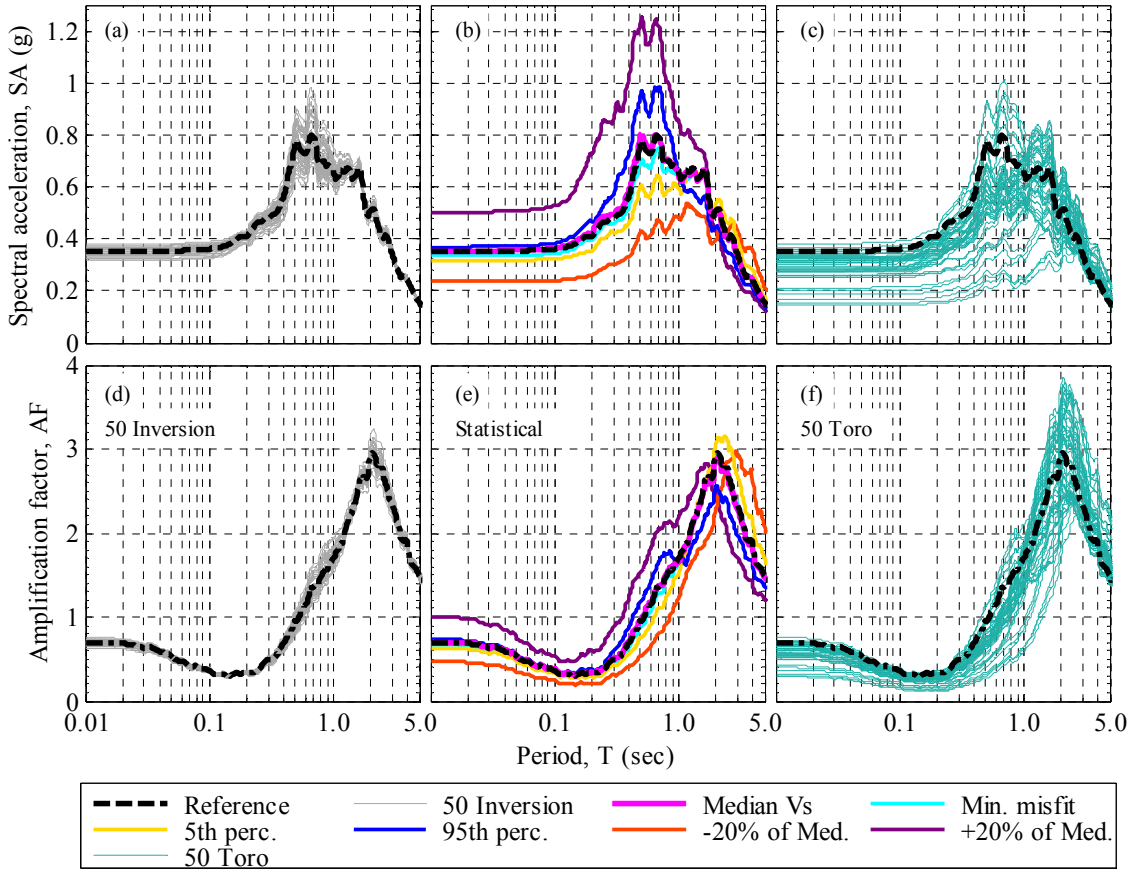

Figure 4.6. Equivalent linear response spectra (top) and amplification factors (bottom) for each Vs profile at Mirandola.

The equivalent linear SA and AF values for Grenoble are presented in Figure 4.7. Similar trends are noted for the variability in site response at Grenoble as those discussed above for Mirandola. However, at Grenoble, the SA and AF values associated with the Toro profiles are generally greater than the Reference values at periods less than 1.0 sec, which is opposite the trend for Mirandola. In this case, the greatest SA and AF values at Grenoble resulted from Toro Vs profiles that do not include some sort of low velocity layer (i.e., soft layer under a stiff layer) between depths of 30 - 50 m. A low velocity layer was present in all of the Inversion Vs profiles because it was required to fit the dispersion data (refer to Figure 1; see Griffiths et al. 2015 for more details). However,

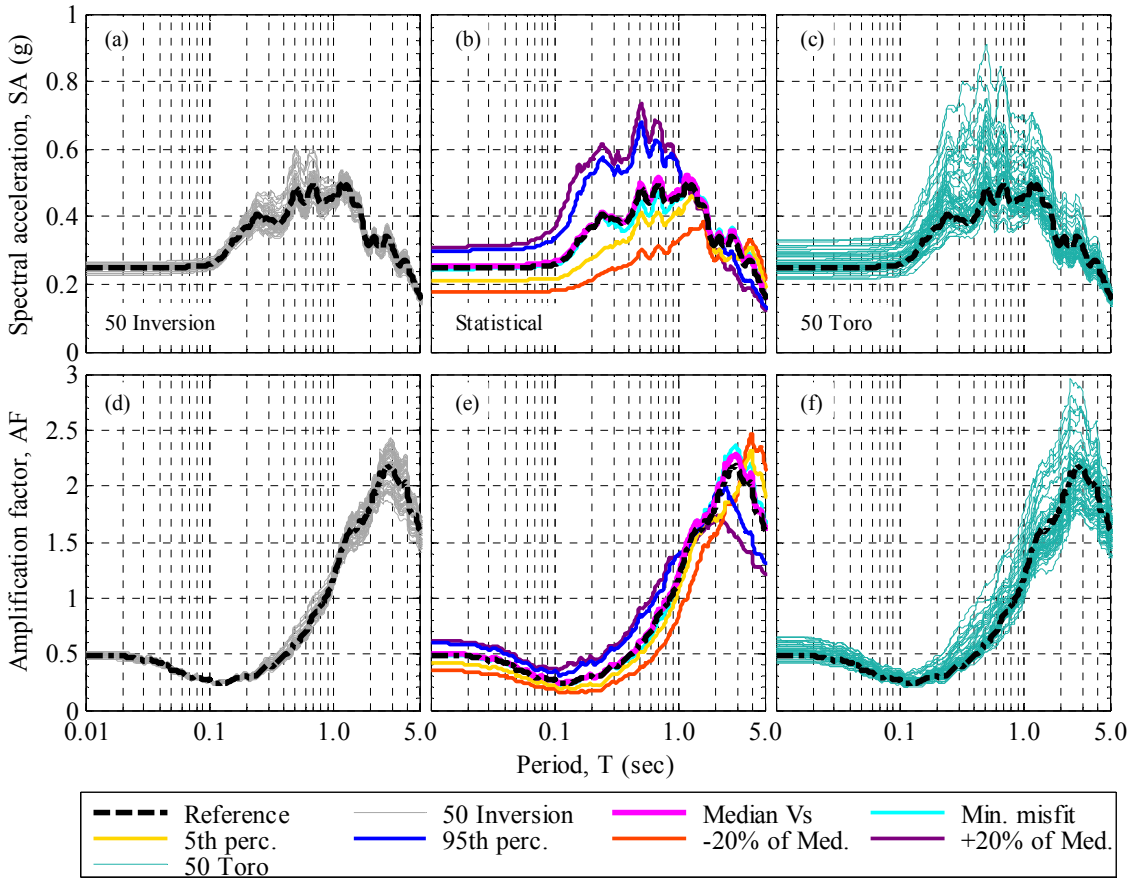

Figure 4.7. Equivalent linear response spectra (top) and amplification factors (bottom) for each Vs profile at Grenoble.

only some of the randomly-generated Toro Vs profiles included a low velocity layer between depth of 30 - 50 m. The profiles with low velocity layers at depth strained significantly, resulting in lower surface response, which can be attributed to increased modulus nonlinearity and increased damping at the depths corresponding to the low velocity layer. The absolute location and thickness of this layer seemed to be less important than its presence and, when absent, the surface response for the high-intensity EQL analyses was significantly amplified. Like Mirandola, the soft, thick, surface layers at Grenoble also resulted in higher shear strains, greater damping, and lower SA than the

same profiles in the linear elastic analyses. However, the SA values did not become lower than the Reference SA and, in fact, ended up matching it quite well at most periods

4.4. RELATIONSHIP BETWEEN RESPONSE SPECTRA DEVIATIONS AND DISPERSION MISFIT

To further investigate a potential relationship between variability in site response estimates and the dispersion misfit values, a single, qualitative measure of the deviation for a single acceleration response spectrum relative to the Reference SA was calculated. The root-mean-square-difference (RMSD) between SA obtained from an individual Vs profile and the Reference SA can be calculated as follows:

$$RMSD = \sqrt{\frac{1}{N_p}\sum_{i=1}^{N_p}\left(\ln SA_i - \ln SA_{ref,i}\right)^2} \qquad \text{(Eq.4.2)}$$

where Np is the number of discrete periods in the response spectrum. All the response spectra in this study have 512 periods equally spaced on a logarithmic scale between 0.01 - 10.0 sec.

We recognize that a single RMSD value cannot be used to distinguish between variability in SA caused by differences in period, differences in amplitude, or some combination of both. Nevertheless, the RMSD provides a single, qualitative value that can be used to evaluate general variability in SA resulting from various Vs profiles. Similar to the dispersion misfit, the RMSD is always a positive number with smaller values corresponding to a better match between the Reference SA and the SA obtained from an individual Vs profile. Box plots of the RMSD values obtained from the EQL results for the Mirandola and Grenoble sites are presented in Figure 4.8. These box plots represent the counted 16th percentile, median (50th percentile) and 84th percentile values of the data, with the whisker lines extending to the 5th and 95th percentile values. Data points outside the 5th and 95th percentile values are shown as red symbols (outliers). Box plots are only shown for the 50 Inversion and 50 Toro profiles because they each

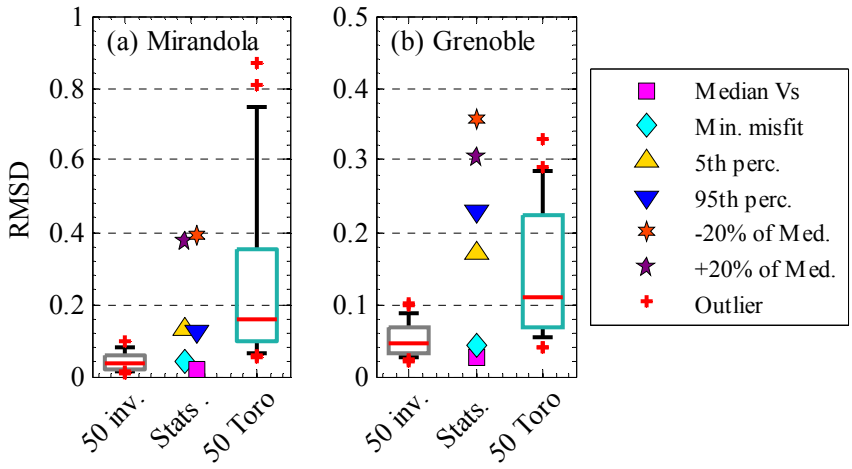

Figure 4.8. Box plots depicting the distribution of the RMSD values of the median response spectra obtained from the Vs profiles for a) Mirandola, and b) Grenoble.

represent a statistical sample. The results from the simple statistical Vs profiles are shown as individual symbols instead of box plots.

At both sites, the ranges in RMSD values are substantially greater for the 50 Toro Vs profiles than the 50 Inversion Vs profiles. However, this is not unexpected because the Reference SA used in the RMSD calculation was obtained from the median response spectra of the 50 Inversion profiles. Nonetheless, the large RMSD values for some of the Toro Vs profiles are significant. For both sites, the RMSD values of the median Vs profile and minimum misfit profile are similar to the RMSD values from the 50 Inversion profiles. However, the RMSD values from the bounding-type statistical Vs profiles (i.e., +/- 20% and 5^{th} and 95^{th} percentile Vs profiles) are significantly greater than the range of RMSD values from the 50 Inversion profiles. These trends seem to mimic the trends in dispersion misfit data reported in Table 4.1.

To further investigate the potential relationship between RMSD and dispersion misfit values, RMSD is plotted as a function of dispersion misfit for the simple statistical Vs profiles and the 50 Toro Vs profiles at Mirandola in Figure 9a. A positive trend depicting greater RMSD with greater misfit is clearly observed. This trend indicates that

if a Vs profile has a high dispersion misfit value, indicating a poor fit to the experimental dispersion data, it is likely to produce a response spectra that is an outlier in terms of RMSD. A better understanding of the relationship between the theoretical dispersion curves, Vs profiles, and acceleration response spectra has been investigated by selecting the "best" and "worst" Vs profiles from the 50 Toro profiles, as shown in Figure 4.9 b, c, and d. The best and worst Vs profiles were selected using the lowest and highest dispersion misfit values, respectively. The theoretical dispersion curve of the best Vs profile matches the experimental dispersion curve at all frequencies (refer to Figure 4.9b), while the worst profile results in a theoretical dispersion curve that has a lower phase velocity (V_R) than the experimental dispersion curve at frequencies greater than 2 Hz. The poor fit with the experimental dispersion curve for the worst profile is due to the thick, soft, surface layer in the Vs profile, which is apparent in Figure 4.9c. This thick near surface layer was generated within the Toro (1995) randomization model despite using site-specific layering model parameters that were more restrictive than the default layering model parameters (Griffiths et al. 2015). The response spectrum from the best Vs profile (Figure 9d) matches the response spectrum from the median Vs profile at most periods, while the response spectrum from the worst Vs profile does not match well at periods less than 2.0 sec.

A plot of RMSD versus dispersion misfit for the simple statistical Vs profiles and the 50 Toro Vs profiles at Grenoble is presented in Figure 4.10a. A positive trend depicting greater RMSD with greater misfit values is also observed, although the trend is not as consistent for Grenoble as for Mirandola. Because of this, the "worst RMSD" profile is investigated along with the "best misfit" and "worst misfit" profiles from the 50 Toro Vs profiles. The best misfit and worst misfit profiles were determined in terms of the lowest and highest dispersion misfit values, respectively, while the worst RMSD profile was determined from the highest RSMD value. The theoretical dispersion curve

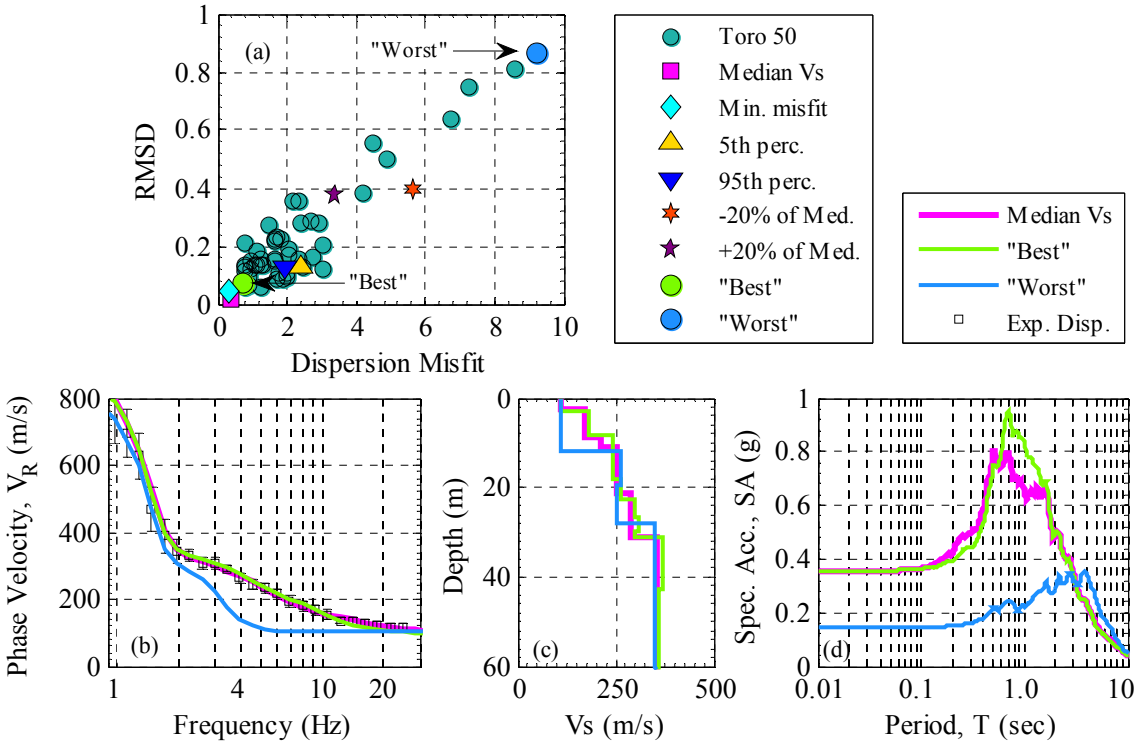

Figure 4.9. Summary plot investigating the best and worst Toro Vs profiles in terms of dispersion misfit for Mirandola, including; a) relationship between the RMSD and the dispersion misfit, b) dispersion curves, c) Vs profiles, and d) response spectra.

of the best misfit Vs profile matches the experimental dispersion curve at all frequencies, while the worst misfit and worst RMSD Vs profiles exhibit theoretical dispersion curves that are lower than the experimental dispersion curve at high frequencies (Figure 4.10b). The worst RMSD Vs profile does not correctly model a low velocity layer somewhere in the top 30 to 50 m (Figure 10c), resulting in a response spectrum that is much greater than the response spectrum predicted from the Median Vs profile obtained from surface wave inversion. Despite the worst misfit Vs profile including a thick, soft, surface layer, similar to the worst misfit Vs profile at Mirandola, the response spectrum from the worst misfit profile is similar to the response spectrum from the Median Vs profile from inversion. Upon further investigation, it was found that some of the Toro Vs profiles

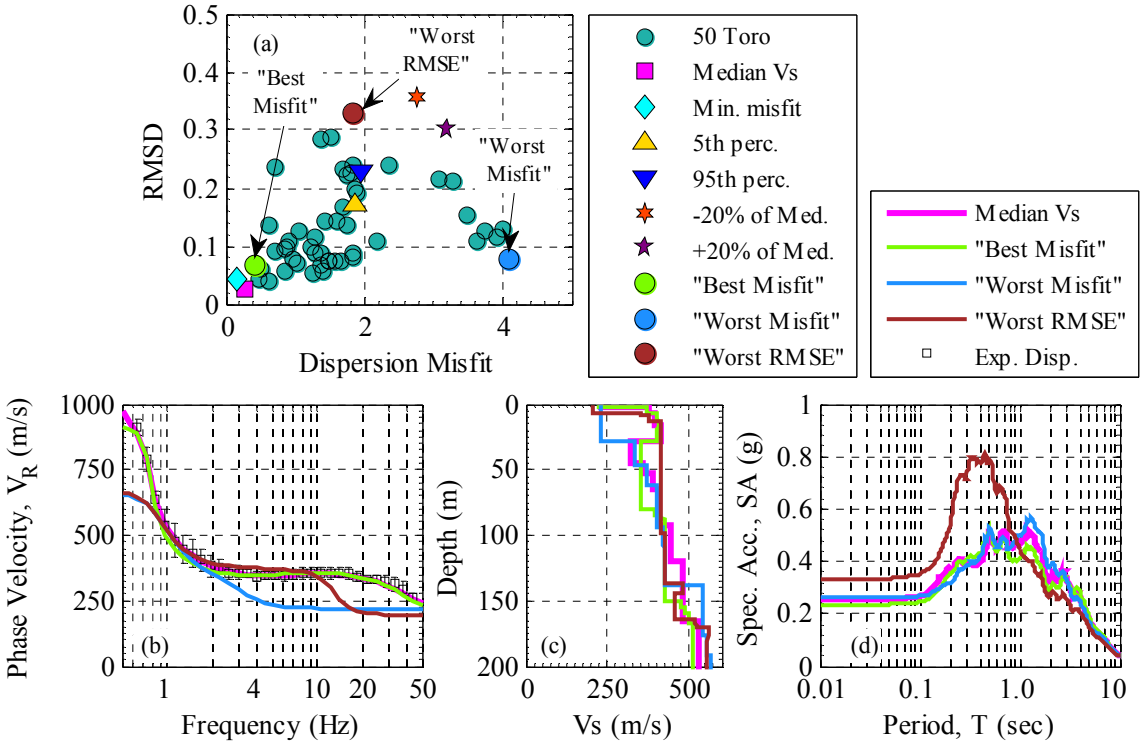

Figure 4.10. Summary plot investigating the best and worst Toro Vs profiles in terms of dispersion misfit and worst RMSD for Grenoble, including; a) relationship between the RMSD and the dispersion misfit, b) dispersion curves, c) Vs profiles, and d) response spectra.

with soft, thick, surface layers resulted in similar SA values as the Median Vs profile. In fact, a progression from high SA values towards the Reference SA obtained from surface wave Vs profiles was evident as the thickness of the soft layer increased from about 20 m to nearly 30 m, despite the fact that none of the surface wave Vs profiles have thick, soft surface layers. When nonlinear soil properties are accounted for in EQL site response analyses with high-intensity input ground motions, high shear strains will develop in any thick, soft layer (whether at depth or at the surface). These high shear strains and the associated softening/high damping result in a decrease in the SA values at most periods and a shift to longer predominant periods. At Grenoble, the thick, soft surface layer associated with the worst misfit Toro Vs profile serendipitously resulted in shifting and

decreasing the SA such that it reasonably matched the SA from the surface wave inversion Vs profiles, which have low velocity layers at depth. Thus, complex interactions between layers in dynamic site response will likely prevent a perfect trend between site response variability and dispersion misfit, particularly at geologically-complicated sites.

4.5. VARIABILITY IN RESPONSE SPECTRA AFTER CULLING VS PROFILES

Griffiths et al. (2015) recommended comparing the theoretical dispersion curves from potential Vs profiles with the experimentally measured surface wave data prior to use in site response analyses. However, the impact of this suggestion was not demonstrated. Their recommendation was simply made from the assumption that theoretical dispersion curves which are within the uncertainty bounds of the measured surface wave data have Vs profiles that more accurately reflect the site stiffness. In order to explore how only using Vs profiles that reasonably match the experimental dispersion data affect the variability in site response, a subset of the 50 Toro Vs profiles has been obtained by culling-out the Vs profiles that do not fit within the uncertainty bounds of the experimentally-measured dispersion data.

At Mirandola, a subset of 15 profiles were found to have theoretical dispersion curves that visually fit within the measured experimental uncertainty. The theoretical dispersion curves and corresponding Vs profiles for Mirandola are presented in Figure 4.11 for both the original 50 Toro profiles and the subset of Toro profiles. The misfit values of the Toro subset are between 0.7 and 1.26 (as indicated inside brackets in the figure legend). As expected, the Vs profiles for the Toro subset exhibit significantly less variability, particularly in the near-surface layers, than the original 50 Toro Vs profiles. Similarly, the dispersion curves and Vs profiles for Grenoble are presented in Figure 4.12. For this site, only eight Vs profiles were found to have theoretical dispersion curves that visibly fit within the uncertainty bounds at most frequencies of the experimental dispersion data. The misfit values of the subset are between 0.43 and 1.39.

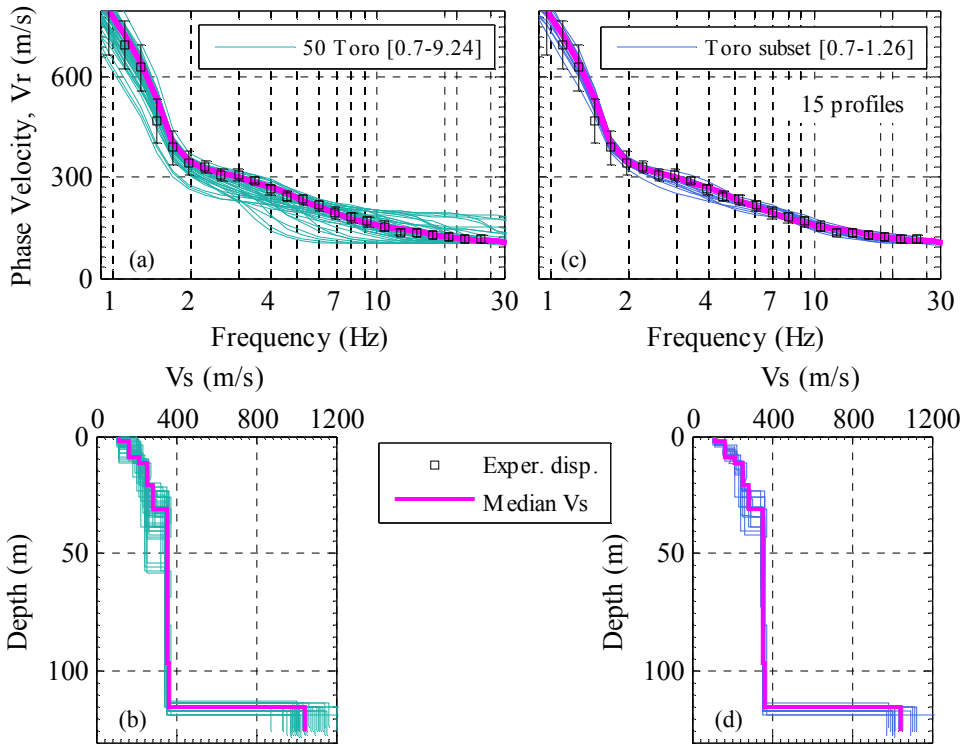

Figure 4.11. Theoretical dispersion curves and Vs profiles at Mirandola for the original 50 Toro profiles (a,b) and the subset of the 50 Toro profiles that fit the experimental dispersion data (c,d).

At both sites, the near surface Vs layering for the Toro subset profiles are clearly more similar to the median Vs profile, which was used as the input Vs profile for the Toro (1995) randomization procedure (Griffiths et al. 2015).

In particular, the top-most layers show significantly less variability and clearly match the experimental dispersion data much better at higher frequencies. Furthermore, at Grenoble, the Vs profiles from the Toro subset also contain low velocity/inverse layers in the depth range of 30 – 50 m, which is important for matching the site signature.

Figures 4.13 and 4.14 present the SA and AF at Mirandola and Grenoble, respectively, for the 50 Inversion Vs profiles, the Toro subset profiles, and the 50 Toro profiles. At Mirandola, the variability exhibited in the SA and AF from the Toro subset profiles is greater than the 50 Inversion profiles, but much less than the original 50 Toro

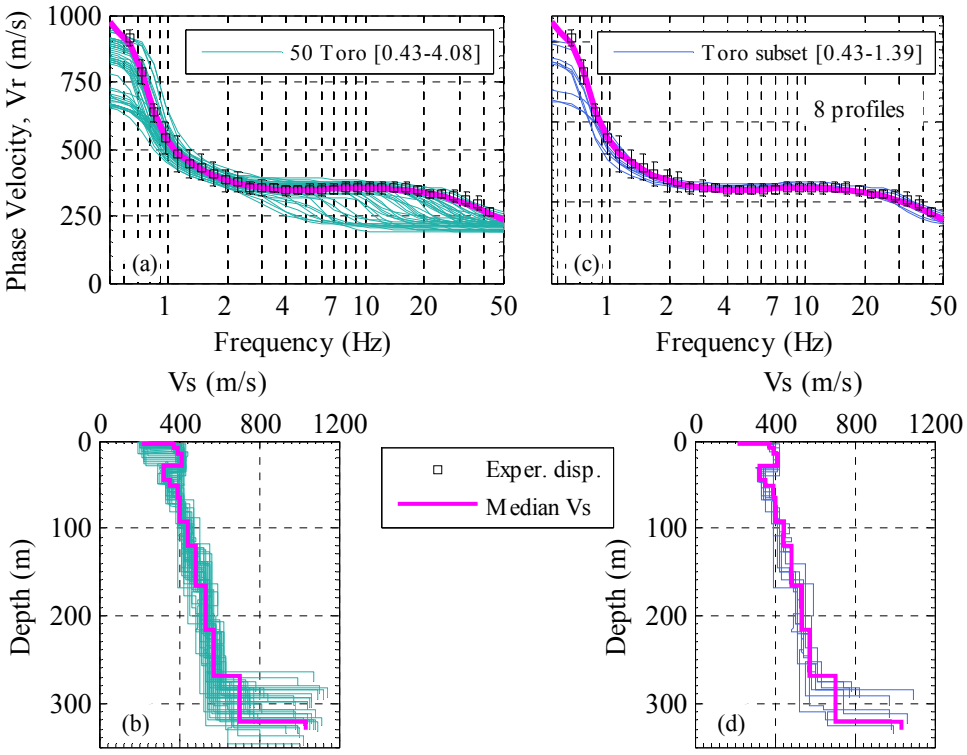

Figure 4.12. Theoretical dispersion curves and Vs profiles at Grenoble for the original 50 Toro profiles (a,b) and the subset of the 50 Toro profiles that fit the experimental dispersion data (c,d).

profiles. The same trend is visible for Grenoble. We believe that the variability exhibited in the SA estimates obtained from the subsets of the 50 Toro profiles, which more closely match the experimental dispersion data, are much more realistic/representative of the expected variability in site response estimates than the SA values from the original/un-culled 50 Toro profiles.

4.6. CONCLUSION

Shear wave velocity profile characterization plays a critical role in site response analyses and realistic methods to account for uncertainty in Vs are needed. In a companion paper, experimentally-measured dispersion data was used to investigate common methods of accounting for uncertainty in Vs profiles at two sites in Mirandola,

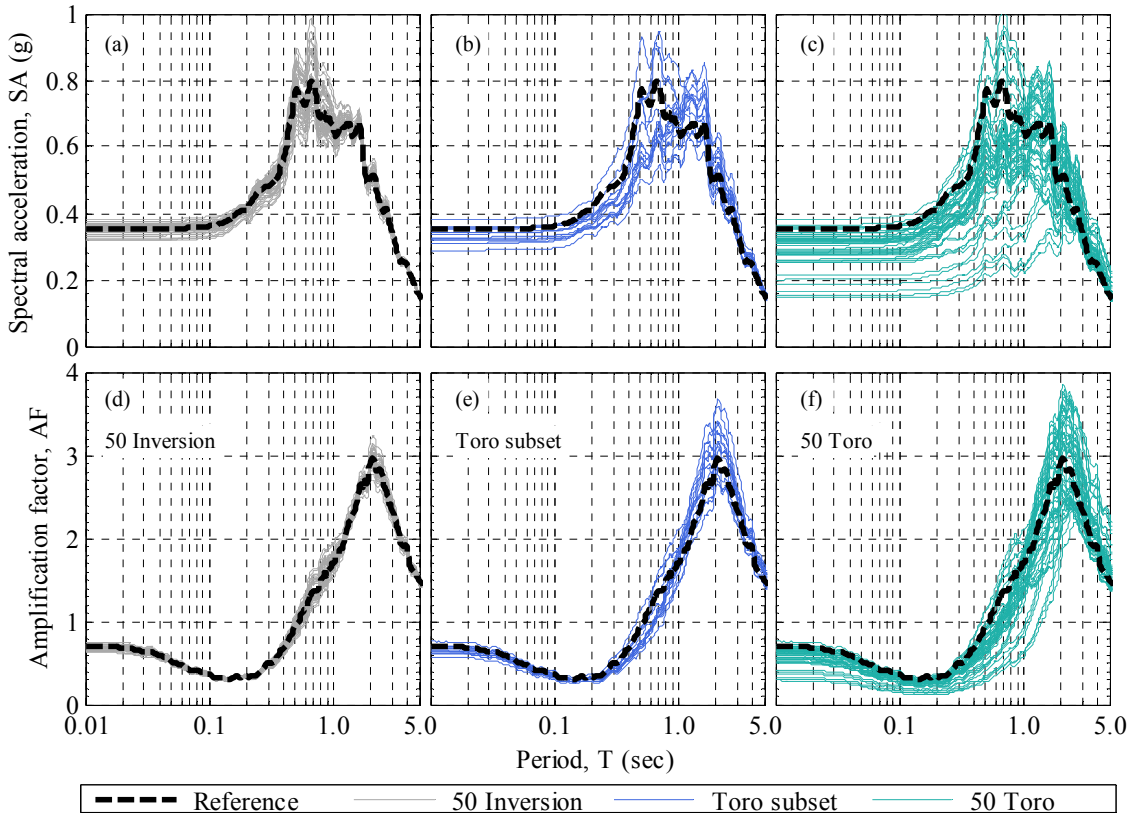

Figure 4.13. Equivalent linear response spectra (top) and amplification factors (bottom) at Mirandola for the 50 Inversion profiles, Toro subset profiles, and 50 Toro profiles.

Italy and Grenoble, France (Griffiths et al, 2015). At these two sites, three sets of Vs profiles were determined, including: (1) Vs profiles determined directly from surface wave inversion, (2) simple statistical Vs profiles derived indirectly from the surface wave Vs profiles (including bounding-type, median, and other percentile Vs profiles), and (3) statistically-based, randomly-generated Vs profiles developed using the procedure proposed by Toro (1995). In this paper, the three sets of Vs profiles at both sites were used to perform linear elastic and equivalent linear site response analyses as a means to investigate variability in ground motion prediction based on common methods used to account for uncertainty in Vs.

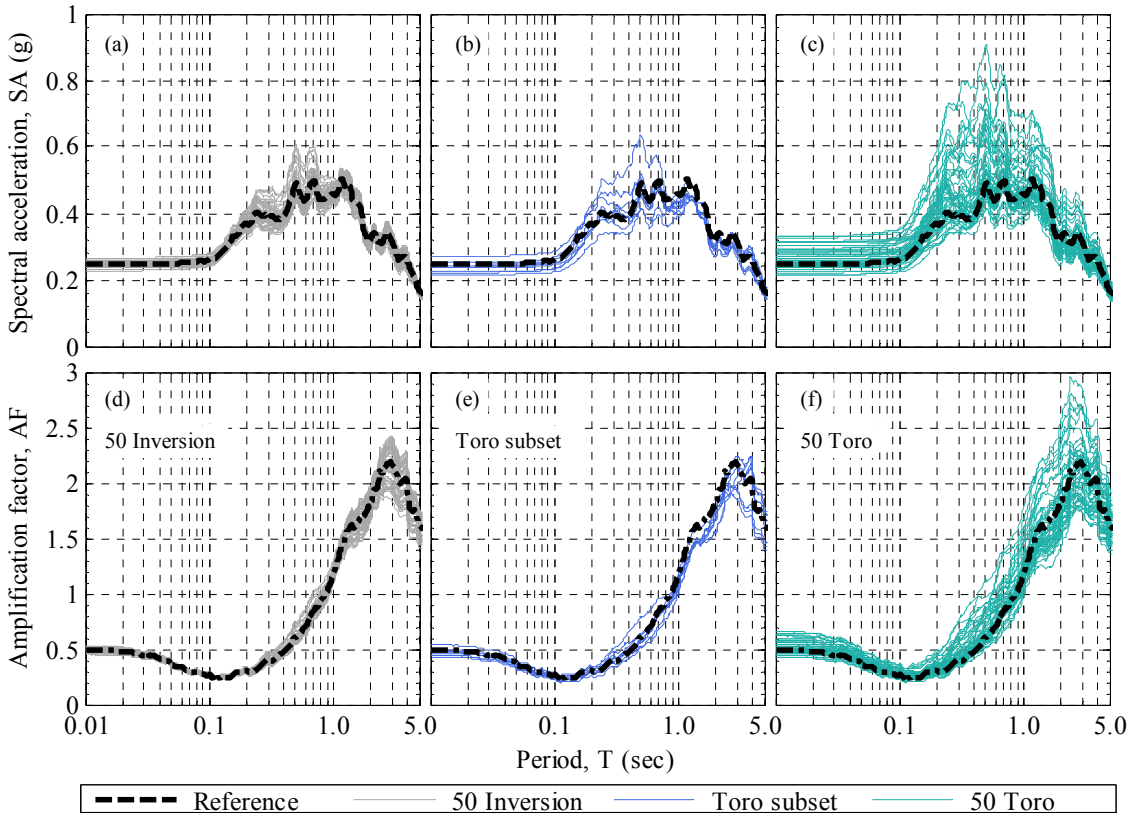

Figure 4.14. Equivalent linear response spectra (top) and amplification factors (bottom) at Greoble for the 50 Inversion profiles, Toro subset profiles, and 50 Toro profiles.

In general, the response spectra and amplification factors obtained from the Vs profiles determined directly from surface wave inversion resulted in much less variability than either the simple statistical Vs profiles or the randomly-generated Vs profiles. General trends between variability in site response and dispersion misfit were observed To further investigate the potential relationship between variability in site response estimates and the dispersion misfit values, a single, qualitative measure of the deviation in acceleration response spectral estimates, called the root-mean-square-difference (RMSD), was calculated. A strong, but not perfect, trend was noted between increasing RMSD values and increasing dispersion misfit values. In particular, the statistical bounding-type Vs profiles (i.e., +/- 20% and 5th and 95th percentile Vs profiles) that are

commonly used to account for epistemic uncertainty in site response yielded large dispersion misfit values and large RMSD values. Thus, these types of profiles were not just outliers in terms of dispersion, but also in terms of site response. The Vs profiles derived from the Toro (1995) randomization model resulted in a very wide range of dispersion misfit and RMSD values (some good/acceptable and some bad/unacceptable). As a result, the Toro profiles were examined in more detail by selecting only the Vs profiles that had theoretical dispersion curves that matched the experimentally measured dispersion data. This culling of Toro Vs profiles based on dispersion misfit resulted in a subset of 15 Vs profiles for Mirandola and 8 Vs profiles for Grenoble. The variability in the site response estimates from the subsets of Toro Vs profiles was much less than the variability from the un-culled, original Toro Vs profiles. Therefore, Vs profiles that result in theoretical dispersion curves which fit within the uncertainty bounds of the experimentally-measured dispersion data appeared to be more representative of subsurface stiffness conditions and, hence, more reasonable when attempting to account for variability in site response due to Vs uncertainty.

4.7. ACKNOWLEDGMENTS

This work was supported primarily by U.S. National Science Foundation (NSF) grant CMMI-1261775. However, any opinions, findings, and conclusions or recommendations expressed in this material are those of the authors and do not necessarily reflect the views of NSF. The authors gratefully acknowledge George Zalachoris for sharing his Matlab code for equivalent linear and linear elastic site response. The authors would also like to acknowledge and thank the organizing committee of the InterPacific project, which was formed under the Research & Development Program SIGMA, funded by EDF, AEREVA, CEA, ENEL, and the CASHIMA project, funded by CEA, ILL and IITER Organization.

4.8. REFERENCES

American Association of State Highway and Transportation Officials (AASHTO). Guide Specifications for LRFD Seismic Bridge Design 2011. 2nd ed., AASHTO Washington, D.C.

American Society of Civil Engineers (ASCE). Minimum design loads for buildings and other structures, ASCE Standard ASCE/SEI 7-10, published by ASCE, Reston, Virginia.

Barani, S., Ferrari, R.D., and Ferretti, G. (2013) "Influence of Soil Modeling Uncertainties on Site Response." Earthquake Spectra, Vol. 29, No. 3, pp 705-732.

Bazzuro,P., and Cornell, C. (2004). "Ground-Motion Amplification in Nonlinear Soil Sites with Uncertain Properties". Bulletin of the Seismological Society of America, Vol. 94, No. 6, pp. 2090-2109.

Boaga, J., Vignoli, G., and Cassiani, G. (2011) "Shear wave profiles from surface inversion: the impact of uncertainty on seismic site response analysis". Journal of Geophysics and Engineering. Vol. 8, pp. 162-174.

Boaga, J., Vignoli, G., and Cassiani, G. (2012) "Reply to comment on Shear wave profiles from surface inversion: the impact of uncertainty on seismic site response analysis". Journal of Geophysics and Engineering. Vol. 9, pp. 244-246.

Boore, D., and G. Atkinson (2008). "Ground-motion Prediction Equations for the Average Horizontal Component of PGA, PGV, and the 5%-damped PSA at spectral periods between 0.01 s and 10.0 s". Earthquake Spectra, Vol. 24, pp. 99-138.

Comina, C., and Foti, S. (2014). Discussion on "Implications of Surface Save Data Measurement Uncertainty on Seismic Ground Response Analysis" by Jakka et al. Soil Dynamics and Earthquake Engineering.

Darendeli, M.B. (2001). "Development of A New Family of Normalized Modulus Reduction and Material Damping Curves." Ph.D. Dissertation, School of Civil, Architectural and Environmental Engineering, The University of Texas at Austin, Austin, TX.

De Luca, F., Iervolino, I., and Cosenza, E. (2009). "Unscaled, scaled, and artificial spectral matching accelerograms: Displacement- and energy-based assessment." in Proceedings, XIII ANIDIS Condference, Bologna, Italy.

Foti, S., Comina,C., Boiero, D., and Socco, L.V. (2009). "Non-uniqueness in surface-wave inversion and consequences on seismic site response analyses." Soil Dynamics and Earthquake Engineering, Vol. 29, pp. 982-993.

Garofalo, F., Foti, S., Hollender, F., Bard, P.-Y., Cornou, C., Cox, B.R., Ohrnberger, M., Sicilia, D., Asten, M., Di Giulio, G., Forbriger, T., Guiller, B., Hayashi, K., Martin, A., Matsushima, S., Mercerat, D., Poggi, V., Yamanaka, H. (2016a). "InterPACIFIC Project: Comparison of Invasive and Non-Invasive Methods for Seismic Site Characterization Part I: Intra-Comparison of Surface Wave Methods," Soil Dynamics and Earthquake Engineering, (submitted).

Garofalo, F., Foti, S., Hollender, F., Bard, P.-Y., Cornou, C., Cox, B.R., Dechamp, A., Ohrnberger, M., Sicilia, D., Vergniault, C. (2016b). "InterPACIFIC Project: Comparison of Invasive and Non-Invasive Methods for Seismic Site Characterization Part II: Inter-Comparison Between Surface Wave and Borehole Methods," Soil Dynamics and Earthquake Engineering, (submitted).

Hashash, Y.M.A., Groholski, D.R., Phillips, C.A., Park, D, and Musgrove, M. (2012) "DEEPSOIL 5.1, User Manual and Tutorial." pp. 107.

Idriss, I.M. (20014). "Evolution of the State of Practice." International Workshop on the Uncertainties in Nonlinear Soil Properties and Their Impact on Modeling Dynamic Soil Response, Pacific Earthquake Engineering Research Center, Richmond, CA.

Jakka, R.S., and Roy, N., and Wason, H.R. (2014a). "Implications of Surface Save Data Measurement Uncertainty on Seismic Ground Response Analysis" Soil Dynamics and Earthquake Engineering, Vol. 61-62, pp. 239-245.

Jakka, R.S., and Roy, N., and Wason, H.R. (2014b). Reply on "Implications of Surface Save Data Measurement Uncertainty on Seismic Ground Response Analysis" Soil Dynamics and Earthquake Engineering.

Kottke, A., and Rathje, E. (2009). "Technical Manual for Strata." Report No. 2008/10, Pacific Earthquake Engineering Research Center, Berkeley, California.

Kottke, A. and Rathje, E. (2008). "A Semi-Automated Procedure for Selection and Scaling of Recorded Earthquake Motions for Dynamic Analysis" Earthquake Spectra, Earthquake Engineering Research Institute, Vol. 24, No. 4, pp. 911-932.

Kottke, A. and Rathje, E. (2013). "SigmaSpectra," <http://nees.org/resources/sigmaspectra>.

Matasovic, N., and Hashash, Y. (2012) "NCHRP Synthesis 428: Practices and Procedures for Site-Specific Evaluations of Earthquake Ground Motions, A Synthesis of Highway Practice." National Cooperative Highway Research Program of the Transportation Research Board, Washington, D.C.

Pacific Earthquake Engineering Research Center, PEER (2011). "Users Manual for the PEER Ground Motions Database Web Application" The PEER Center, University of California, Berkeley, CA. http://peer.berkeley.edu/peer_ground_motion_database/site.

Rathje, E.M., Kottke, A.R., and Trent, W.L. (2010). "Influence of Input Motion and Site Property Variabilities on Seismic Site Response Analysis." Journal of Geotechnical and Geoenvironmental engineering, Vol. 136, No. 4, pp 607-619.

Socco, L.V., Foti, S., and Comina, C. (2012) "Comment on Shear wave profiles from surface inversion: the impact of uncertainty on seismic site response analysis". Journal of Geophysics and Engineering. Vol. 9, pp. 241-243.

Toro, G. (1995) "Probabilistic models of the site velocity profiles for generic and site-specific ground-motion amplification studies." Technical Report No. 779574, Brookhaven National Laboratory, Upton, N.Y. pp. 147.

Wathelet, M. (2005). "Array recordings of ambient vibrations". Ph.D. thesis, The University of Leige, Leige, Wallonia, Belguim. pp. 144.

Chapter 5:

Conclusion

5.1. Major Findings, Recommendations and Future Work

Although the major findings and recommendations for each chapter are included at the end of each chapter, a brief summary is also included here.

5.1.1. Modeling Large Shear Strains in Site Response Analyses of Soft Soils

Nonlinear and equivalent linear site response analyses often result in large induced shear strains (3-10%) at soft soil sites subject to high-intensity input ground motions. However, dynamic soil properties typically used in these site response analyses were generally developed from minimal data at shear strains greater than 0.1-0.3%. Therefore, modulus reduction and damping curves must be extended to greater shear strains with care, such that they provide realistic estimates of soil strength, stiffness, and damping. Site response analyses performed at Treasure Island, a well-known soft soil site near several major active faults, demonstrated the challenges associated with accurately modeling large shear strains and developing realistic surface ground motions.

The Treasure Island analyses were performed using input ground motions scaled to a target uniform hazard spectrum, which was developed using a 2% probability of exceedance in 50 years. Both equivalent linear (EQL) and nonlinear (NL) site response analyses, with identical shear wave velocity profiles and nonlinear shear modulus reduction (G/G_{max}) and damping curves, were performed. G/G_{max} curves at large shear strains were strength corrected to better match the estimated static shear strength of the soil according to the method proposed by Hashash et al. (2010). Additionally, damping at large shear strains was capped at 15%. Modifying G/G_{max} in the layers with the greatest predicted shear strains had a more significant impact on the amplitude and shape of the surface time histories and response spectra than any further modifications to G/G_{max} or damping. Nonetheless, modifications to the modulus reduction and damping curves for

all layers within a soft soil model should be investigated to ensure that realistic shear strengths are modeled and excessive damping values are not utilized.

Even after fully-modifying dynamic soil properties in all layers, the site response results at Treasure Island qualitatively appear to be uncharacteristic relative to typical high-intensity surface ground motions recorded at soft soil sites. This is true for both EQL and NL analyses. Specifically, the spectral shapes of surface ground motions predicted by EQL analyses appear to have unrealistically high kappa values, while those predicted by NL analyses do not resemble a typical kappa relationship. Therefore, future work should focus on improvements to current of EQL and NL site response models to better predict the high frequency characteristics of earthquake shaking for soft soil sites subject to high intensity input motions and to preserve realistic acceleration time histories.

Although it is commonly believed that NL site response analyses provide more realistic estimates of site response at large strains, and in particular predict larger amplification at short periods, this study shows that predicted short period amplification from EQL analyses can be larger than from NL analyses. In fact, EQL analyses actually produced spectral accelerations that were approximately twice as large as the NL values across all periods at the Treasure Island site. Therefore, until the issues associated with modeling large shear strains are resolved, caution should be exercised in simply assuming that NL analyses will provide the most conservative estimates of site response at soft soil sites.

5.1.2. A Surface Wave Dispersion Approach for Evaluating Statistical Models that Account for Shear Wave Velocity Uncertainty

Surface wave data collected as part of the InterPacific project (Garofalo et al. 2016a and Garafalo et a. 2016b) at Mirandola, Italy and Grenoble, France sites, was used to determine a suite of 50 Vs profiles. The suite of Vs profiles generated directly from inversion analyses capture realistic subsurface uncertainty/variability, yet still fit the

experimental dispersion data very well. The theoretical dispersion curves associated with the median of the 50 inversion Vs profiles fit the experimental data well at both sites. In fact, the median of the 50 inversion Vs profiles exhibited a lower misfit than many of the profiles that came directly from the inversion analyses. Therefore, the median profile is considered a good, simple statistical profile that can be used to reasonably represent the site stiffness. Conversely, the theoretical dispersion curves associated with the bounding-type 5^{th} and 95^{th} percentile, and the +/- 20% Vs profiles do not fit the experimental dispersion data well at either site. As such, these Vs profiles do not appropriately capture the experimentally-measured site signature and should not be used to reflect Vs uncertainty at a site where dispersion data have been collected.

Based on the findings presented in Chapter 3, a few suggestions regarding dispersion-based options for realistically accounting for Vs profile uncertainty include:

1) At sites where high-quality surface wave dispersion data is available, use multiple Vs profiles resulting directly from inversion in subsequent analyses. These profiles should all fit the experimental data and its associated uncertainties, which are inherently a combination of epistemic uncertainty and aleatory variability. If Vs randomization is still desired to further account for aleatory variability, Toro-type models or Monte Carlo simulations can be used, provided the resulting profiles are checked by comparing the theoretical dispersion curves with the experimental data. This will ensure that only profiles that fit the experimentally-measured site signature are used in subsequent analyses. Blindly using relatively stiff and soft bounding-type Vs profiles (e.g., +/- 20%) to account for epistemic uncertainty at sites where dispersion measurements are available is not appropriate and should not be done.
2) At sites where only borehole data is available, a theoretical dispersion curve could be calculated from the borehole Vs and Vp data. Realistic Uncertainty bounds could then be added to the theoretical dispersion curve in order to create a pseudo-experimental target curve. Since borehole measurements represent a point

measurement and can deviate from the experimental dispersion curve obtained from surface wave methods, the uncertainty bounds may need to exceed the 5 - 10% that is often associated with surface wave data. Nonetheless, this pesuedo-experimental dispersion target curve could then form the basis for evaluating the validity of randomly generated Vs profiles meant to account for aleatory variability. If multiple boreholes are available, the data from each one could be used as a starting model for this randomization.

These are currently only suggestions for readers to consider when attempting to account for realistic Vs uncertainty in site response analyses. Additional research is needed in order to truly account for epistemic uncertainty and aleatory variability in a meaningful way. However, some current methodologies may not be appropriate and may actually result in unintended consequences when attempting to predict site response.

5.1.3. Mapping Dispersion Misfit and Uncertainty in Vs Profiles to Variability in Site Response Estimates

Shear wave velocity profile characterization plays a critical role in site response analyses and realistic methods to account for uncertainty in Vs are needed. In Chapter 4, the three sets of Vs profiles at both sites were used to perform linear elastic and equivalent linear site response analyses as a means to investigate variability in ground motion prediction based on common methods used to account for uncertainty in Vs.

In general, the response spectra and amplification factors obtained from the Vs profiles determined directly from surface wave inversion resulted in much less variability than either the simple statistical Vs profiles or the randomly-generated Vs profiles. General trends between variability in site response and dispersion misfit were observed To further investigate the potential relationship between variability in site response estimates and the dispersion misfit values, a single, qualitative measure of the deviation in acceleration response spectral estimates, called the root mean square difference (RMSD), was calculated. A strong, but not perfect, trend was noted between increasing

RMSD values and increasing dispersion misfit values. In particular, the statistical bounding-type Vs profiles (i.e., +/- 20% and 5th and 95th percentile Vs profiles) that are commonly used to account for epistemic uncertainty in site response yielded large dispersion misfit values and large RMSD values. Thus, these types of profiles were not just outliers in terms of dispersion, but also in terms of site response. The Vs profiles derived from the Toro (1995) randomization model resulted in a very wide range of dispersion misfit and RMSD values (some good/acceptable and some bad/unacceptable). As a result, the Toro profiles were examined in more detail by selecting only the Vs profiles that had theoretical dispersion curves that matched the experimentally measured dispersion data. This culling of Toro Vs profiles based on dispersion misfit resulted in a subset of 15 Vs profiles for Mirandola and 8 Vs profiles for Grenoble. The variability in the site response estimates from the subsets of Toro Vs profiles was much less than the variability from the un-culled, original Toro Vs profiles. Therefore, Vs profiles that result in theoretical dispersion curves which fit within the uncertainty bounds of the experimentally-measured dispersion data appeared to be more representative of subsurface stiffness conditions and, hence, more reasonable when attempting to account for variability in site response due to Vs uncertainty.

References

Aki, K., (1957). "Space and time spectra of stationary stochastic waves, with special reference to microtremors". Bulletin of Earthquake Research Institute, 35, 415–457

American Association of State Highway and Transportation Officials (AASHTO). Guide Specifications for LRFD Seismic Bridge Design 2011. 2nd ed., AASHTO Washington, D.C.

American Society of Civil Engineers (ASCE). Minimum design loads for buildings and other structures, ASCE Standard ASCE/SEI 7-10, published by ASCE, Reston, Virginia.

Anderson, J.G., and Hough, S.E. (1984). "A Model for the Shape of the Fourier Amplitude Spectrum of Acceleration at High Frequencies." Bulletin of the Seismological Society of America. Vol., 74, No. 5, pp. 1969-1993.

Barani, S., Ferrari, R.D., and Ferretti, G. (2013) "Influence of Soil Modeling Uncertainties on Site Response." Earthquake Spectra, Vol. 29, No. 3, pp 705-732.

Bazzuro,P., and Cornell, C. (2004). "Ground-Motion Amplification in Nonlinear Soil Sites with Uncertain Properties". Bulletin of the Seismological Society of America, Vol. 94, No. 6, pp. 2090-2109.

Bettig, B., Bard, P.Y., Scherbaum, F., Riepl, J., Cotton, F., Cornou, C., and Hatzfeild, D. (2001). "Analysis of dense array noise measurements using the modified spatial auto correlation method (SPAC): application to the Grenoble area." Bollettino de Geofisica Teoria e Applicata, 42(3-4), 281-304.

Boaga, J., Vignoli, G., and Cassiani, G. (2011) "Shear wave profiles from surface inversion: the impact of uncertainty on seismic site response analysis". Journal of Geophysics and Engineering. Vol. 8, pp. 162-174.

Boaga, J., Vignoli, G., and Cassiani, G. (2012) "Reply to comment on Shear wave profiles from surface inversion: the impact of uncertainty on seismic site response analysis". Journal of Geophysics and Engineering. Vol. 9, pp. 244-246.

Boore, D., and G. Atkinson (2008). "Ground-motion Prediction Equations for the Average Horizontal Component of PGA, PGV, and the 5%-damped PSA at spectral periods between 0.01 s and 10.0 s". Earthquake Spectra, Vol. 24, pp. 99-138.

Campbell, K.W. (2003). "Prediction of Strong Ground Motion Using the Hybrid Empirical Method and Its Use in the Development of the Ground-Motion (Attenuation) Relations in Eastern North America". Bulletin of the Seismological Society of America, Vol., 93, No. 3, pp. 1012-1033.

Campbell, K.W. (2009). "Estimates of Shear-Wave Q and κ_o for Unconsolidated and Semiconsolidated Sediments in Eastern North America". Bulletin of the Seismological Society of America, Vol., 99, No. 4, pp. 2365-2392.

Capon, J. (1969). "High Resolution Frequency-Wavenumber Spectrum Analysis." Proceedings of the IEEE, Vol. 57, Issue 8, pp. 1408–1418.

Chiu, P., Pradel, D.E., Kwok, A.O., Stewart, J.P. (2008). "Seismic Response Analyses for the Silicon Valley Rapid Transit Project." Proc., ASCE conference of Geotechnical Earthquake Engineering and Soil Dynamics IV, Geotechnical Special Publication 181, ASCE, Sacramento, CA.

Comina C., Foti S., Boiero D., Socco L.V. (2011). "Reliability of VS,30 Evaluation from Surface-Wave Tests." Journal of Geotechnical and Geoenvironmental Engineering, Vol. 137, pp. 579–86.

Comina, C., and Foti, S. (2014). Discussion on "Implications of Surface Save Data Measurement Uncertainty on Seismic Ground Response Analysis" by Jakka et al. Soil Dynamics and Earthquake Engineering.

Cornou, C., Ohrnberger, M., Boore, D.M., Kudo K., and Bard P-Y (2006). "Derivation of Structural Models from Ambient Vibration Array Tecordings: Results from an International Blind Test" In: Bard P-Y, Chaljub E, Cornou C, Cotton F, Gueguen P (eds) Third International symposium on the effects of surface geology on seismic motion, vol. 2. Grenoble, 1127–1219.

Cox, B.R., Wood, C.M. and Teague, D.P. (2014) " Synthesis of the UTexas1 Surface Wave Dataset Blind-Analysis Study: Inter-Analyst Dispersion and Shear Wave Velocity Uncertainty" Proceedings of the 2014 Geo-Congress Technical Papers, pp. 850-859.

Darendeli, M.B. (2001). "Development of A New Family of Normalized Modulus Reduction and Material Damping Curves." Ph.D. Dissertation, School of Civil, Architectural and Environmental Engineering, The University of Texas at Austin, Austin, TX.

De Luca, F., Iervolino, I., and Cosenza, E. (2009). "Unscaled, scaled, and artificial spectral matching accelerograms: Displacement- and energy-based assessment." in Proceedings, XIII ANIDIS Condference, Bologna, Italy.

Dickenson, S.E. (1994). "Dynamic Response of Soft and Deep Cohesive Soils During the Loma Prieta Earthquake of October 14, 1989". Ph.D. thesis, University of California, Berkeley, p. 331.

Dou, S. and Ajo-Franklin, J.B. (2014). "Full-waveform inversion of surface waves for mapping embedded low-velocity zones in permafrost." Geophysics, Vol. 79, No. 6, pp. EN107–EN124.

Dunkin J.W. (1965). "Computation of modal solutions in layered, elastic media at high frequencies." Bulletin of the Seismological Society of America, Vol. 55, pp. 335–358.

Electric Power Research Institute, EPRI (1993). "Guidelines for Determining Design Basis Ground Motions". Report No. EPRI TR-102293, Palo Alto, CA.

Electric Power Research Institute (EPRI) "Seismic Evaluation Guidance: Screening, Prioritization and Implementation Details (SPID) for the Resolution of Fukushima Near-Term Task Force Recommendation 2.1: Seismic" Eletric Power Research Institute, Palo Alto, CA: 2012, Report 1025287, pp. 206.

Fah, D., Stamm, G., Havenith, H.B. (2008). "Analysis of three-component ambient vibration array measurements." Geophysical Journal International, 172, 199-213.

Foti, S., Comina,C., Boiero, D., and Socco, L.V. (2009). "Non-uniqueness in surface-wave inversion and consequences on seismic site response analyses." Soil Dynamics and Earthquake Engineering, Vol. 29, pp. 982-993.

Foti, S., Lai, C., Rix, G., and Strobbia, C. (2014). "Surface Wave Methods for Near-Surface Characterization." CRC Press, Boca Raton, Florida, pp. 4.

Foti, S., Parolai, S., Albarello, D., and Picozzi, M. (2011). "Application of Surface-wave methods for seismic site characterization." Surveys in Geophysics, Vol. 32, Issue. 6, pp. 777-825.

Garofalo, F., Foti, S., Hollender, F., Bard, P.-Y., Cornou, C., Cox, B.R., Ohrnberger, M., Sicilia, D., Asten, M., Di Giulio, G., Forbriger, T., Guiller, B., Hayashi, K., Martin, A., Matsushima, S., Mercerat, D., Poggi, V., Yamanaka, H. (2016a). "InterPACIFIC Project: Comparison of Invasive and Non-Invasive Methods for Seismic Site Characterization Part I: Intra-Comparison of Surface Wave Methods," Soil Dynamics and Earthquake Engineering, (submitted).

Garofalo, F., Foti, S., Hollender, F., Bard, P.-Y., Cornou, C., Cox, B.R., Dechamp, A., Ohrnberger, M., Sicilia, D., Vergniault, C. (2016b). "InterPACIFIC Project: Comparison of Invasive and Non-Invasive Methods for Seismic Site Characterization Part II: Inter-Comparison Between Surface Wave and Borehole Methods," Soil Dynamics and Earthquake Engineering, (submitted).

Hardin, B.O., and Drnevich, V.P. (1972). "Shear Modulus and Damping in Soils: Measurement and Parameter Effects". Journal of the Soil Mechanics and Foundations Division, Proceedings of the American Society of Civil Engineers, Vol. 98, No. SM6, pp. 603-624.

Hashash, Y.M.A., Groholski, D.R., Phillips, C.A., Park, D, and Musgrove, M. (2012) "DEEPSOIL 5.1, User Manual and Tutorial." pp. 107.

Hashash, Y.M.A., Phillips, C., and Groholski., D.R. (2010). "Recent Advances in Non-linear Site Response Analysis." Proc., 5th International Conf. on Recent Advances in Geotechnical Earthquake Engineering and Soil Dynamics, NEES, San Diego, CA.

Haskell, N. A. (1953). "The dispersion of surface waves on multilayered media." Bulletin of Seismological Society of America, Vol. 43, pp. 17–34.

Herrmann, R. B. (1987). "Surface wave inversion. Computer program in seismology." Vol. 4, Saint Louis University.

Hobiger, M., Le Bihan, N., Cornou, C., and Bard, P.Y. (2012). "Multicomponent Signal Processing for Rayleigh Wave Ellipicity Estimation." IEEE Signal Processing Magazine, pp. 29–39.

Idriss, I.M. (20014). "Evolution of the State of Practice." International Workshop on the Uncertainties in Nonlinear Soil Properties and Their Impact on Modeling Dynamic Soil Response, Pacific Earthquake Engineering Research Center, Richmond, CA.

Jakka, R.S., and Roy, N., and Wason, H.R. (2014a). "Implications of Surface Save Data Measurement Uncertainty on Seismic Ground Response Analysis" Soil Dynamics and Earthquake Engineering, Vol. 61-62, pp. 239-245.

Jakka, R.S., and Roy, N., and Wason, H.R. (2014b). Reply on "Implications of Surface Save Data Measurement Uncertainty on Seismic Ground Response Analysis" Soil Dynamics and Earthquake Engineering.

Kaklamanos, J., Bradley, B.A., Thompson, E.M., and Baise, L.G. (2013) "Critical Parameters Affecting Bias and Variability in Site-Response Analyses Using Kik-net Downhole Array Data". Bulletin of the Seismological Society of America, Vol. 103, No. 3. pp. 1733-1749.

Kilb, D., Biasi, G., Anderson, J., Brune, J., Peng, Z., and Vernon, F. (2012). "A Comparison of the Spectral Parameter Kappa from Small and Moderate Earthquakes Using Southern California ANZA Seismic Network Data." Bulletin of the Seismological Society of America. Vol., 102, No. 1, pp. 284-300.

Knopoff L. (1964). "A matrix method for elastic wave problems." Bulletin of the Seismological Society of America, Vol. 54, pp. 431–438.

Kottke, A., and Rathje, E. (2009). "Technical Manual for Strata." Report No. 2008/10, Pacific Earthquake Engineering Research Center, Berkeley, California.

Kottke, A. and Rathje, E. (2008). "A Semi-Automated Procedure for Selection and Scaling of Recorded Earthquake Motions for Dynamic Analysis" Earthquake Spectra, Earthquake Engineering Research Institute, Vol. 24, No. 4, pp. 911-932.

Kottke, A. and Rathje, E. (2013). "SigmaSpectra," <http://nees.org/resources/sigmaspectra>.

Kramer, S. (1996). "Geotechnical Earthquake Engineering," Prentice Hall, Upper Saddle River, New Jersey, pp. 653.

Lai, C. G. (1998). "Simultaneous Inversion of Rayleigh Phase Velocity and Attenuation for Near-Surface Site Characterization." Ph.D. Dissertation, School of Civil and Environmental Engineering, Georgia Institute of Technology, Atlanta, GA.

Maraschini, M. and Foti, S. (2010). "A Monte Carlo multimodal inversion of surface waves." Geophysical Journal International, Vol. 182(3), pp. 1557-1566.

Matasovic, N., and Hashash, Y. (2012) "NCHRP Synthesis 428: Practices and Procedures for Site-Specific Evaluations of Earthquake Ground Motions, A Synthesis of Highway Practice." National Cooperative Highway Research Program of the Transportation Research Board, Washington, D.C.

Menq, F. Y. (2003) "Dynamic Properties of Sandy and Gravelly Soils," Ph.D. Dissertation, University of Texas at Austin. Austin, TX.

Molnar, S., Dosso, S. E., & Cassidy, J. F. (2010). "Bayesian inversion of microtremor array dispersion data in southwestern British Columbia." Geophysical Journal International, Vol. 183(2), pp. 923-940.

Pacific Earthquake Engineering Research Center, PEER (2011). "Users Manual for the PEER Ground Motions Database Web Application" The PEER Center, University of California, Berkeley, CA. http://peer.berkeley.edu/peer_ground_motion_database/site.

Park, C., Xia, J., and Miller, R. (1998). "Imaging dispersion curves of surface waves on multi-channel record." 68th Annual International Meeting of the Society of Exploration Geophysicists, Expanded Abstracts, pp. 1377-1380.

Pass, D.E. (1994). "Soil Characterization of the Deep Accelerometer Site at Treasure Island, SanFrancisco, California". M.S. thesis, University of New Hampshire, Durham, NH.

Phillips, C., and Hashash, Y.M.A. (2009). "Damping Formulation for Non-linear Site Response Analyses." Soil Dynamics and Earthquake Engineering. Vol., 29, pp. 1143-1158.

Poggi, V. and Fah, D. (2010). "Estimating Rayleigh wave particle motions from three-component array analysis of ambient vibrations." Geophysical Journal International, Vol. 180, pp. 251-267.

Rathje, E.M., Kottke, A.R., and Trent, W.L. (2010). "Influence of Input Motion and Site Property Variabilities on Seismic Site Response Analysis." Journal of Geotechnical and Geoenvironmental engineering, Vol. 136, No. 4, pp 607-619.

Rix, G.J., Hebeler, G.L., and Orozco, M.C. (2002). "Near-surface Vs Profiling in the New Madrid Seismic Zone Using Surface-save Methods". Seismological Research Letters, Vol., 73, No., 3, pp. 380-392.

Rodriguez-Marek, A., Rathje, E.M., Bommer, J.J., Scherbaum, F., and Stafford, P.J. (2014). "Application of Single-Station Sigma and Site-Response Characterization in a Probabilistic Seismic-Hazard Analysis for a New Nuclear Site". Bulletin of the Seismological Society of America, Vol. 104, No. 4.

Rothman, D. (1985). "Nonlinear inversion, statistical mechanics, and residual statics estimation." Geophysics, Vol. 50, No. 12, pp. 2784-2796.

Seed, H. and Idriss, I. (1970). "Soil Moduli and Damping Factors for Dynamic Response Analyses," *Report No. EERC-70-10*, Earthquake Engineering Research Center, University of California, Berkeley, CA.

Socco, L. V. and D. Boiero. (2008). “Improved Monte Carlo inversion of surface wave data”. Geophysical Prospecting, 56, 357-371.

Socco., L., Foti, S., and Boiero, D. (2010). “Surface-wave analysis for building near-surface velocity models – Established approaches and new perspectives.” Geophysics, Vol. 75, No. 5, pp. 75A83-75A102.

Socco, L.V., Foti, S., and Comina, C. (2012) “Comment on Shear wave profiles from surface inversion: the impact of uncertainty on seismic site response analysis”. Journal of Geophysics and Engineering. Vol. 9, pp. 241-243.

Stewart, J.P., and Kwok, A.O.L. (2008). “Nonlinear Seismic Ground Response Analysis: Code Usage Protocols and Verification against Vertical Array Data.” Proc., ASCE conference of Geotechnical Earthquake Engineering and Soil Dynamics IV, Geotechnical Special Publication 181, ASCE, Sacramento, CA.

Stokoe, K. H., II, Wright, S. G., Bay, J. A., and Roësset, J. M. (1994). "Characterization of geotechnical sites by SASW method." Geophysical Characterization of Sites, ed. R. D.Woods, Oxford & IBH Pub. Co., New Delhi, India, 15-25.

Thomson, W. T. (1950). “Transmission of elastic waves through a stratified solid medium.” Journal of Applied Physics, Vol. 21, pp. 89–93.

Toro, G. (1995) “Probabilistic models of the site velocity profiles for generic and site-specific ground-motion amplification studies.” Technical Report No. 779574, Brookhaven National Laboratory, Upton, N.Y. pp. 147.

United States Geological Survey (USGS), (2008). “National Seismic Hazard Maps: Documentation,” USGS Open File Report 2008-1128.

United Sates Geological Survey (USGS), (2008). 2008 Interactive Deaggregations, <http://geohazards.usgs.gov/deaggint/2008/>, (Jan 9, 2013).

Van Houtte, C., Drouet, S., and Cotton, G. (2011) “Analysis of the Origins of κ (Kappa) to Compute Hard Rock to Rock Adjustment Factors for GMPEs”. Bulletin of the Seismological Society of America, Vol., 101, No. 6, pp. 2926-2941.

Vucetic, M., and Dobry, R. (1991). “Effect of Soil Plasticity on Cyclic Response”. Journal of Geotechnical Engineering, Vol. 117, No. 1, pp. 89-107.

Wathelet, M. (2005). “Array recordings of ambient vibrations”. Ph.D. thesis, The University of Leige, Leige, Wallonia, Belguim. pp. 144.

Wathelet, M. (2008). An improved neighborhood algorithm: parameter conditions and dynamic scaling. Geophysical Research Letters, Vol. 35, L09301.

Wood, C.M., Cox, B.R. (2012). "A Comparison of MASW Dispersion Uncertainty and Bias for Impact and Harmonic Sources," ASCE Geo-Congress 2012: State of the Art and Practice in Geotechnical Engineering, Oakland, CA, 25-29 March 2012.

Wood, C.M., Ellis, T.B., Teague, D.P. and Cox, B.R. (2014). "Comprehensive Analysis of the UTexas1 Surface Wave Dataset Analyst I" https://nees.org/resources/13130, pp. 10.

Xia, J., R. D. Miller, and C. B. Park, (1999). Estimation of near-surface shear-wave velocity by inversion of Rayleigh waves, Geophysics, Vol. 64, No. 3, pp. 691-700.

Yamanaka, H. and H. Ishida (1996). "Application of generic algorithms to an inversion of surface-wave dispersion data." Bulletin of Earthquake Engineering Vol. 86, No. 2, pp. 436–444.

Zywicki, D.J. (1999). Advanced signal processing methods applied to engineering analysis of seismic surface waves. Ph.D. Dissertation, School of Civil and Environmental Engineering, Georgia Institute of Technology, Atlanta, GA.